Fragmentation of carbon ions in particle therapy: secondary particle characterization and Monte Carlo validation

L. Gesson, J. Gross, C. Mozzi, C. Reibel, Ch. Finck, S. Higueret, T.D. Lê, A. Sécher, M. Pullia, N. Arbor, M. Vanstalle

IPHC Institut Pluridisciplinaire Hubert CURIEN STRASBOURG
CNRS

61st International Winter Meeting on Nuclear Physics Bormio 2025

01. Secondary particles in heavy ion therapy

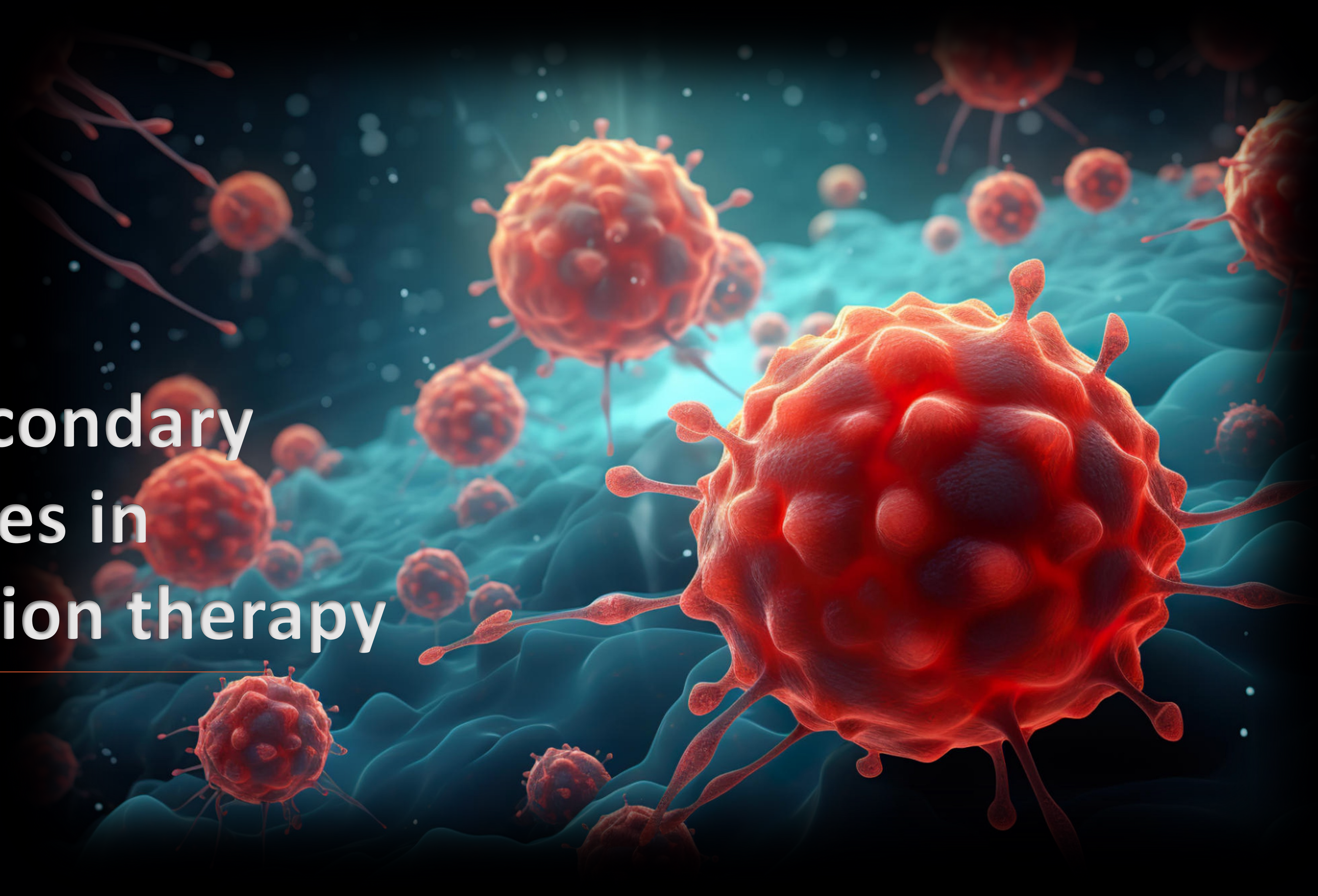

Secondary particles in heavy ion therapy

Cancer treatments

- First cause of death in Europe and North America

Secondary particles in heavy ion therapy
Cancer treatments

- First cause of death in Europe and North America

Secondary particles in heavy ion therapy
Cancer treatments

- First cause of death in Europe and North America

X-rays therapy
Ion beam therapy

Secondary particles in heavy ion therapy

Cancer treatments

- First cause of death in Europe and North America

Secondary particles in heavy ion therapy

Cancer treatments

- First cause of death in Europe and North America

Radiation therapy →
- **X-rays therapy**
- **Ion beam therapy**
  - **Carbon 120 – 400 MeV/u**
  - **Proton 70 – 250 MeV**

Secondary particles in heavy ion therapy

Charged particles effects

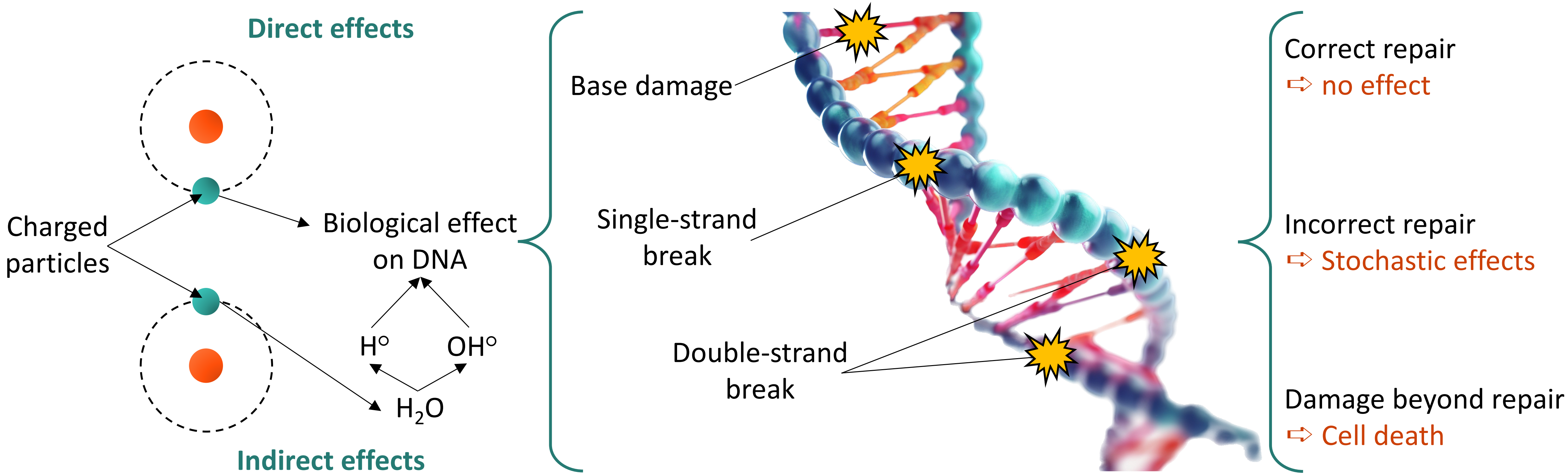

Secondary particles in heavy ion therapy

Charged particles interactions

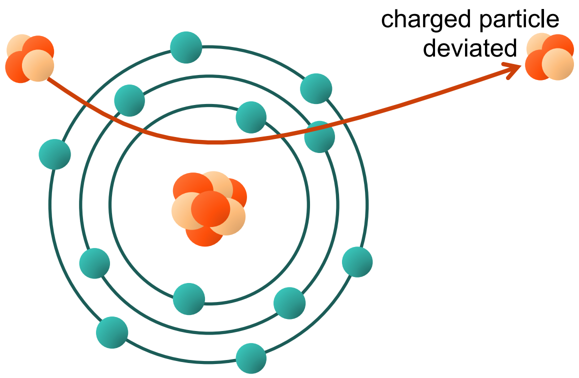

Elastic diffusion

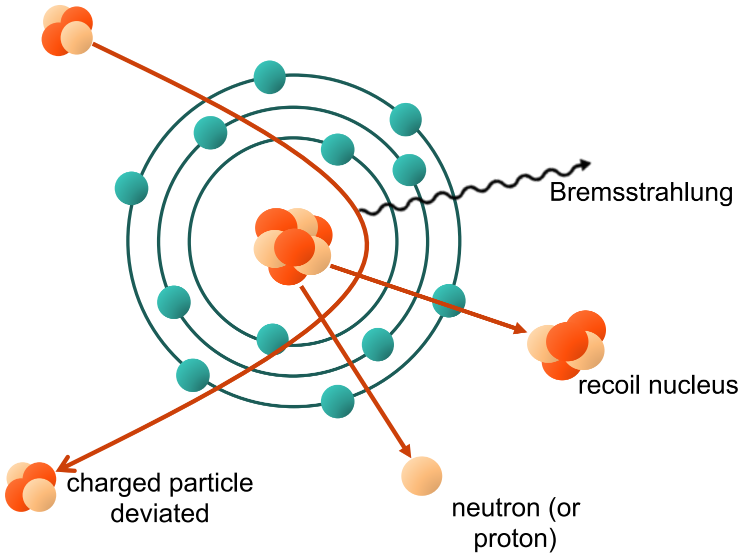

Inelastic diffusion

Stopping power

→ Slowing process dominated by inelastic collisions with target e$^-$

→ $$\frac{dE}{dx} = \frac{4\pi e^4 z_t z_p^2}{m_e v^2}\left[ln\frac{2m_e v^2}{< I >} - \ln(1-\beta^2) - \beta^2 - \frac{c}{z_t} - \frac{\delta}{2}\right]$$

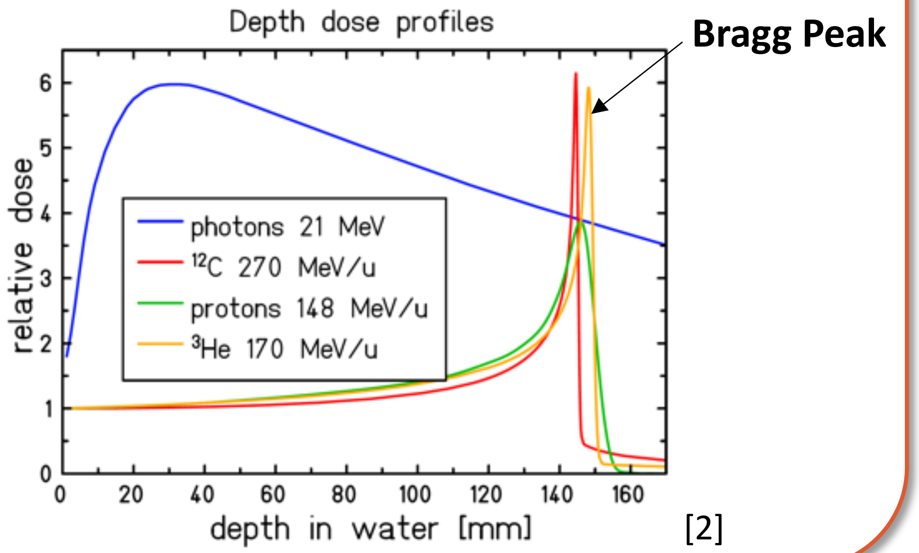

[2]

Secondary particles in heavy ion therapy

Charged particles interactions

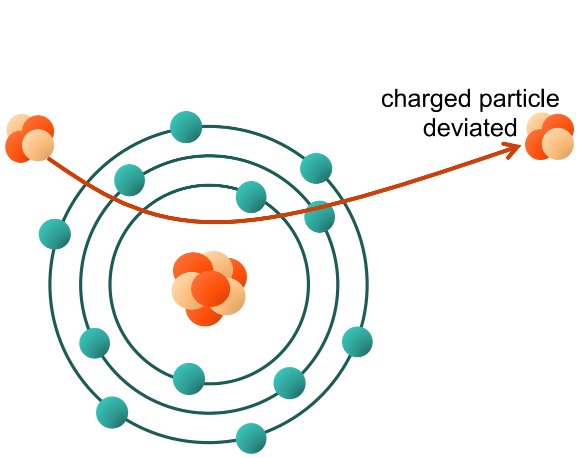

Elastic diffusion

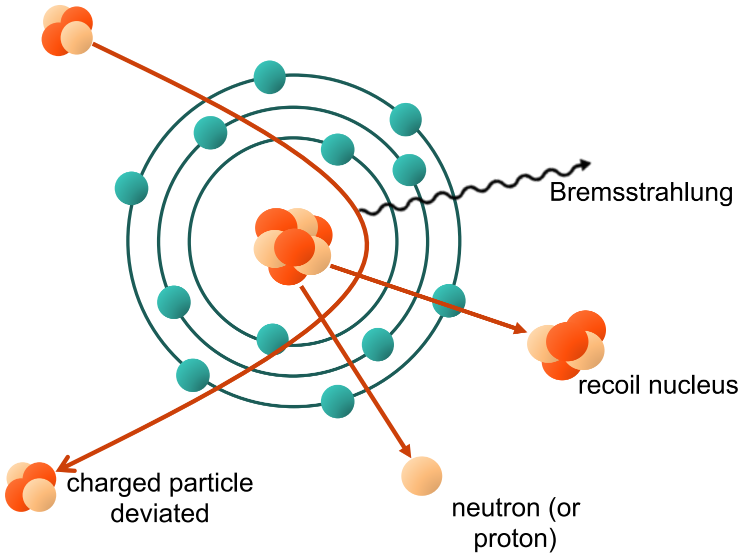

Inelastic diffusion

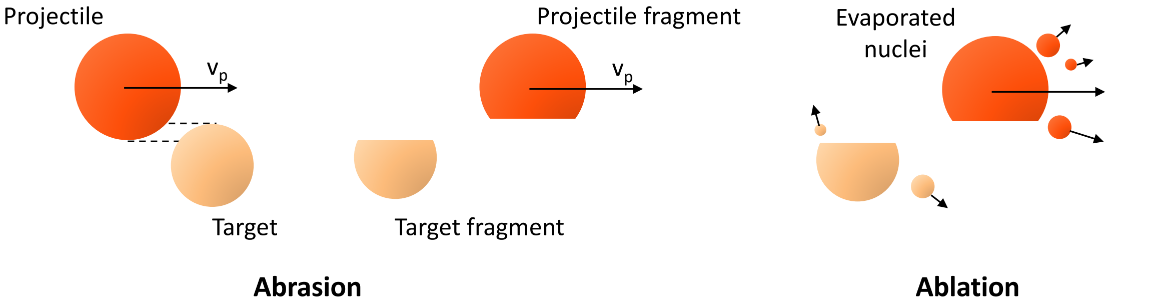

Fragmentation

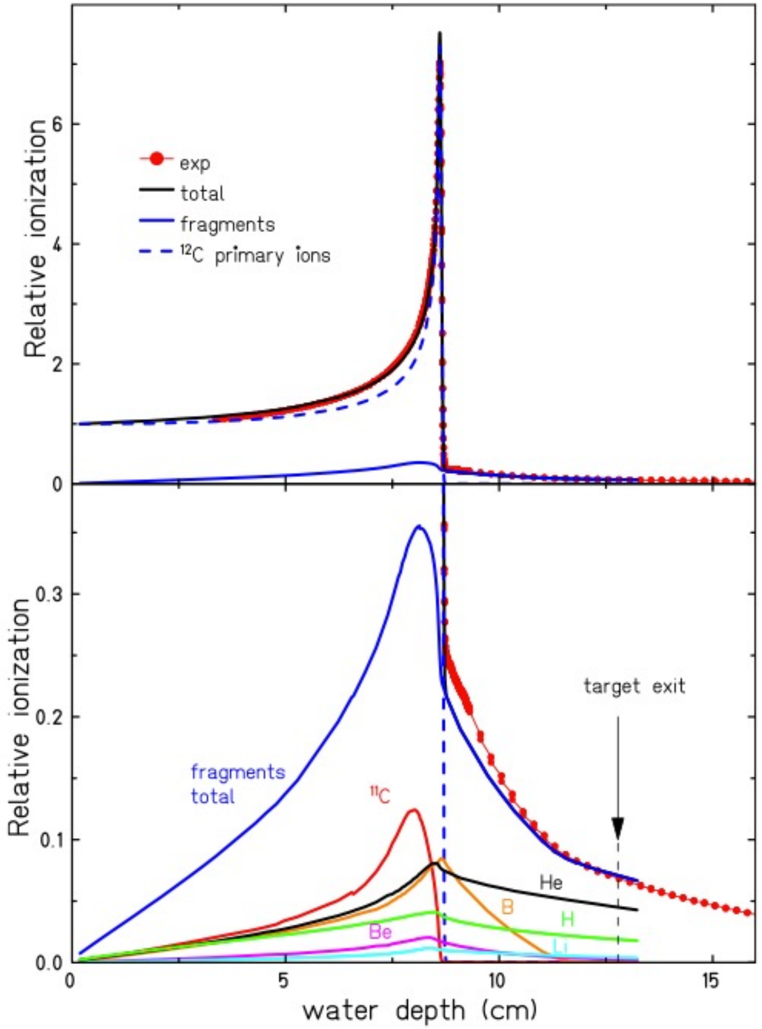

Figure - Bragg curve of a 200 MeV/u ^{12}C ion beam in water with the Monte-Carlo code PHITS [1]

Secondary particles in heavy ion therapy
Uncertainties

Secondary particles dose distribution not taken into account

- ~ 5% of total dose in Bragg peak (BP)
- dose tail after BP
- higher Linear Energy Transfer
- interact outside tumor → healthy tissues irradiation

Secondary particles in heavy ion therapy

Uncertainties

Secondary particles dose distribution not taken into account

- ~ 5% of total dose in Bragg peak (BP)
- dose tail after BP
- higher Linear Energy Transfer
- interact outside tumor → healthy tissues irradiation

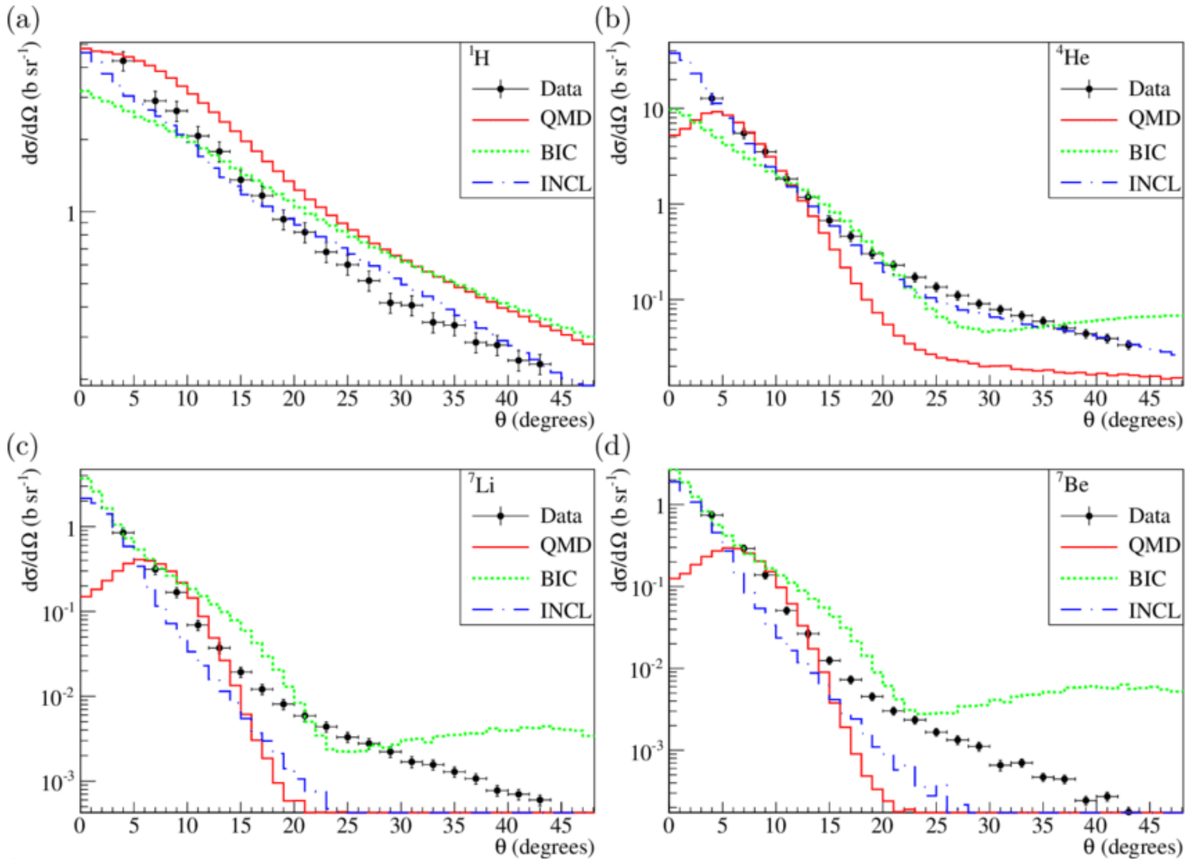

Figure - Absolute differential angular cross-sections of protons, ^{4}He, ^{6}Li, ^{7}Be, obtained for the carbon target. [7]

Secondary particles in heavy ion therapy

Uncertainties

Secondary particles dose distribution not taken into account

- ~ 5% of total dose in Bragg peak (BP)
- dose tail after BP
- higher Linear Energy Transfer
- interact outside tumor → healthy tissues irradiation

- Incomplete cross-section data
- Discrepancies between | hadronic models in MC
  | MC and experiment

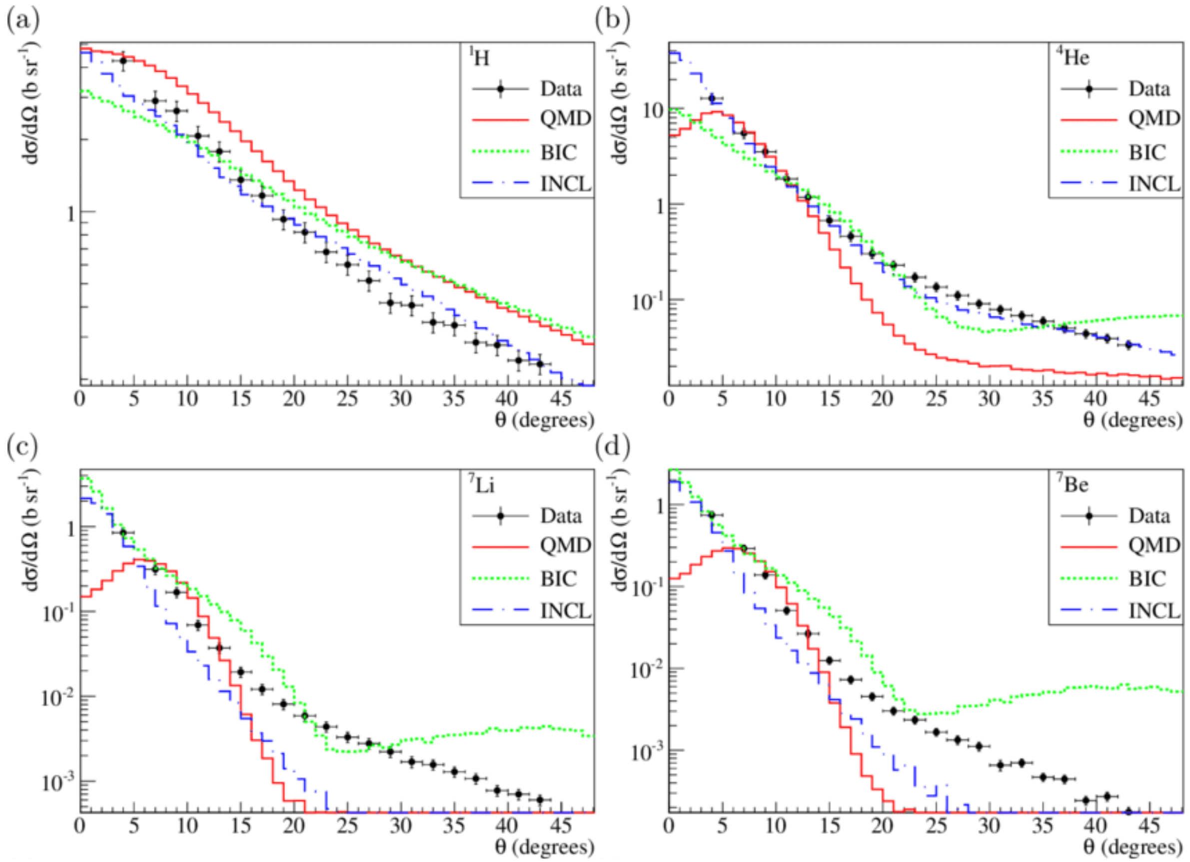

Figure - Absolute differential angular cross-sections of protons, ^{4}He, ^{6}Li, ^{7}Be, obtained for the carbon target. [7]

Secondary particles in heavy ion therapy

Uncertainties

Secondary particles dose distribution not taken into account

- ~ 5% of total dose in Bragg peak (BP)
- dose tail after BP
- higher Linear Energy Transfer
- interact outside tumor → healthy tissues irradiation

- Incomplete cross-section data
- Discrepancies between | hadronic models in MC
  | MC and experiment

Enhance nuclear reaction models to better understand secondary particles production

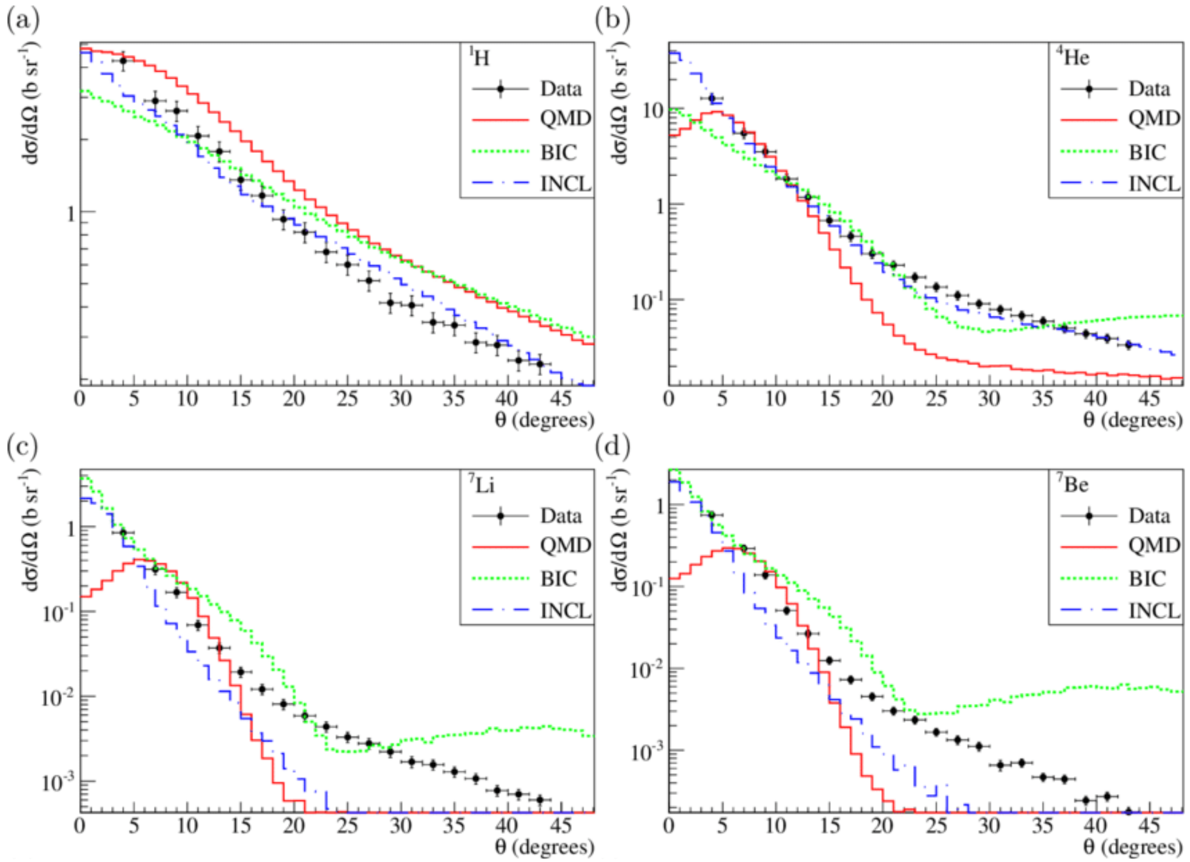

Figure - Absolute differential angular cross-sections of protons, ^{4}He, ^{6}Li, ^{7}Be, obtained for the carbon target. [7]

Secondary particles in heavy ion therapy

Uncertainties

Enhance nuclear reaction models to better understand secondary particles production

- Cross-sections experimental measurements (ex. FOOT collaboration experiments)
- Hadronic models theory improvement (ex. DINo deep learning algorithm)
- More “simpler” and “direct” measurements (statistics, energies, angular distribution)

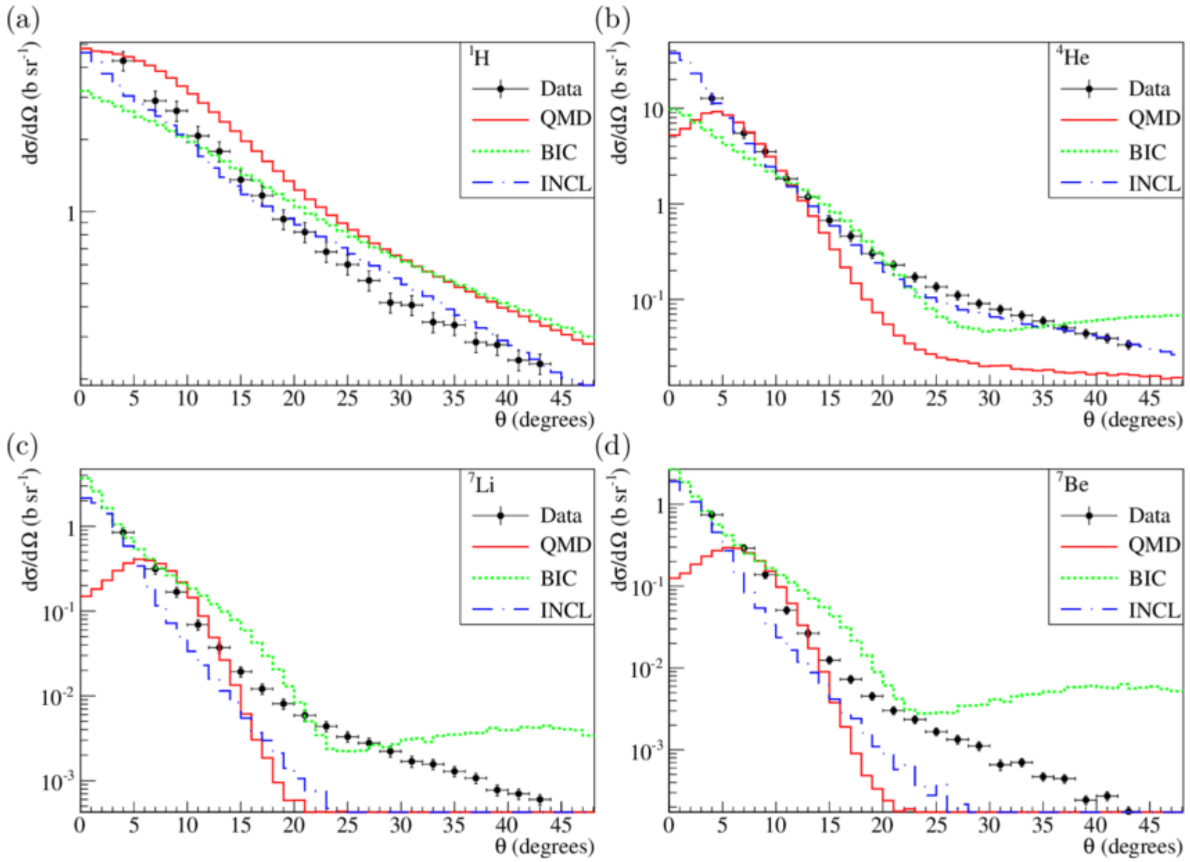

Figure - Absolute differential angular cross-sections of protons, ^{4}He, ^{6}Li, ^{7}Be, obtained for the carbon target. [7]

02. CLINM – Secondary particles measurements

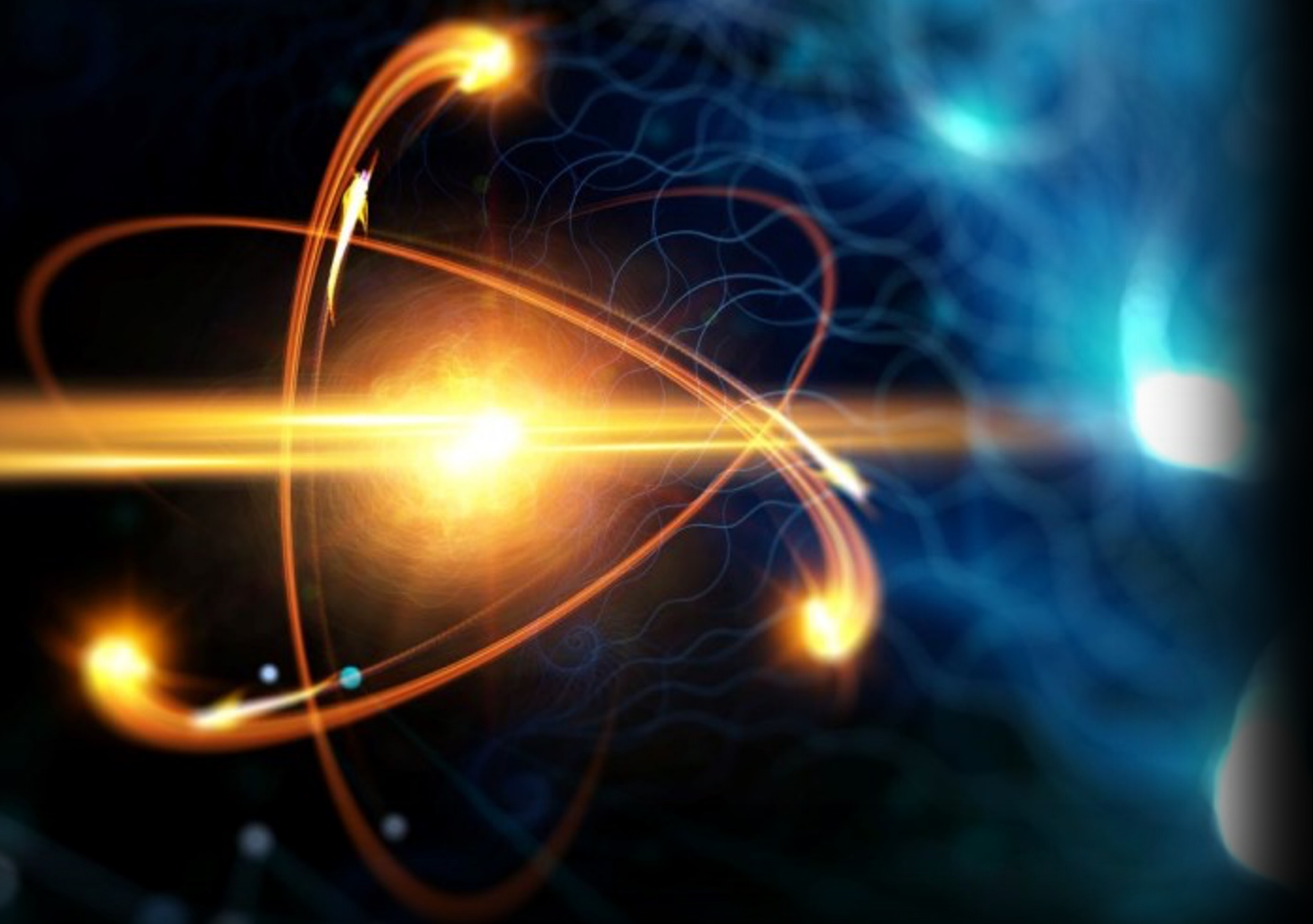

Secondary particles measurement
CLINM project

CLINM – Cross-Sections of Light Ion and Neutron Measurements

- Combined measurement of secondary particles and radiolysis effectiveness with radiochemistry team (IPHC)
- Secondary charged particle identification + γ + neutrons of high energy measurement

Secondary particles measurement

CLINM project

CLINM – Cross-Sections of Light Ion and Neutron Measurements

- Combined measurement of secondary particles and radiolysis effectiveness with radiochemistry team (IPHC)
- Secondary charged particle identification + γ + neutrons of high energy measurement

Secondary particles measurement
CLINM project

CLINM – Cross-Sections of Light Ion and Neutron Measurements

- Combined measurement of secondary particles and radiolysis effectiveness with radiochemistry team (IPHC)
- Secondary charged particle identification + γ + neutrons of high energy measurement

ΔE-E telescope

$CeBr_3$ crystal scintillator + plastic scintillator

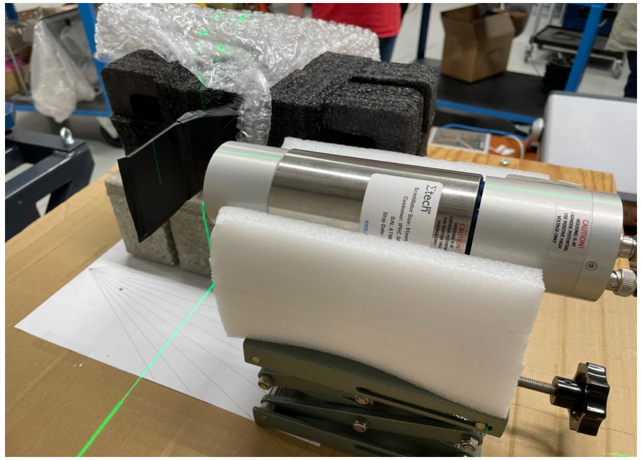

Facility	Ion type	Energy
GSI - Darmstadt	^{12}C	110 - 180 MeV/u
CNAO - Pavia	^{12}C	120 - 200 MeV/u
	^{1}H	80 – 200 MeV/u

Secondary particles measurement

Experiment at CNAO

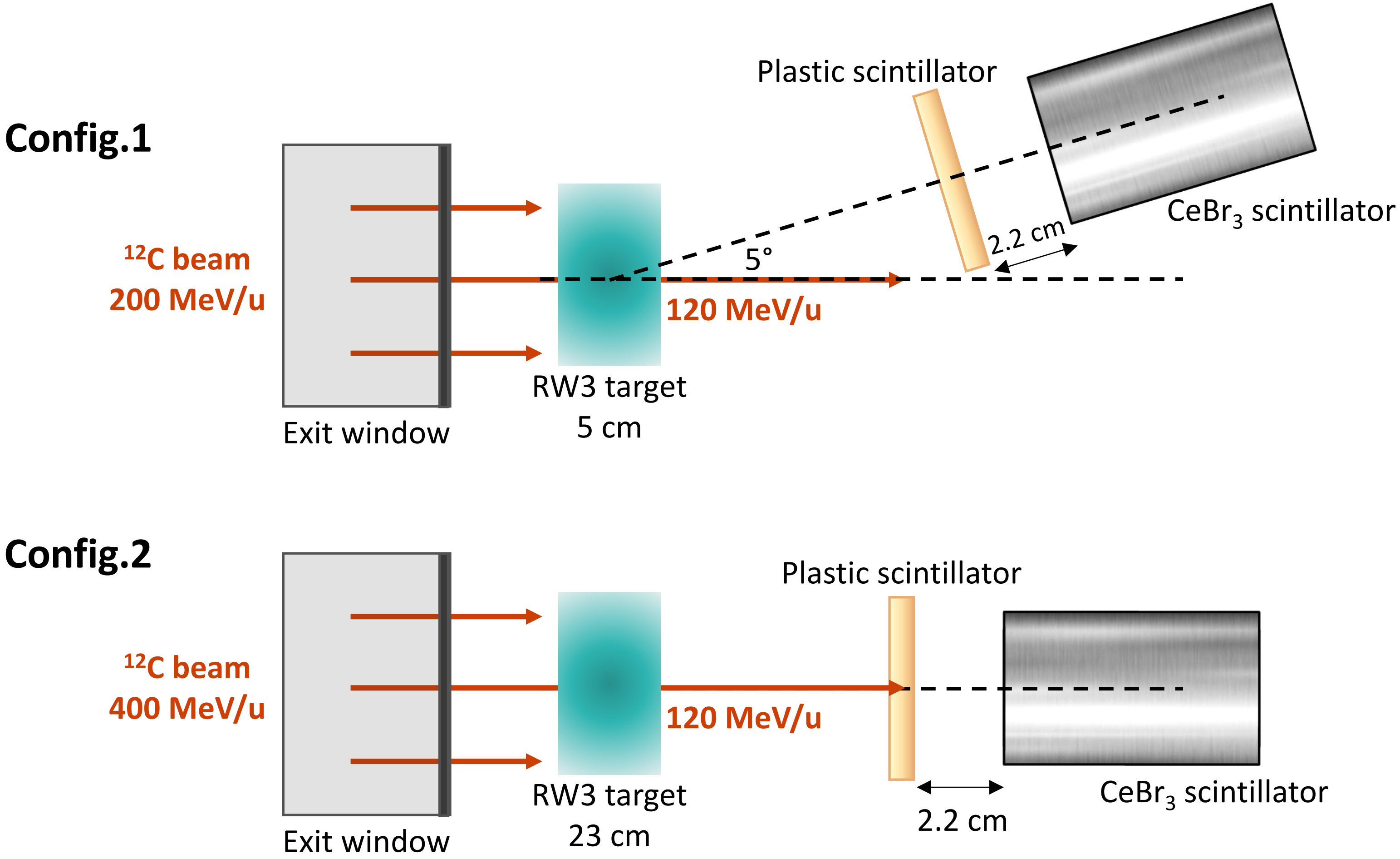

Secondary particles measurement
Experiment at CNAO

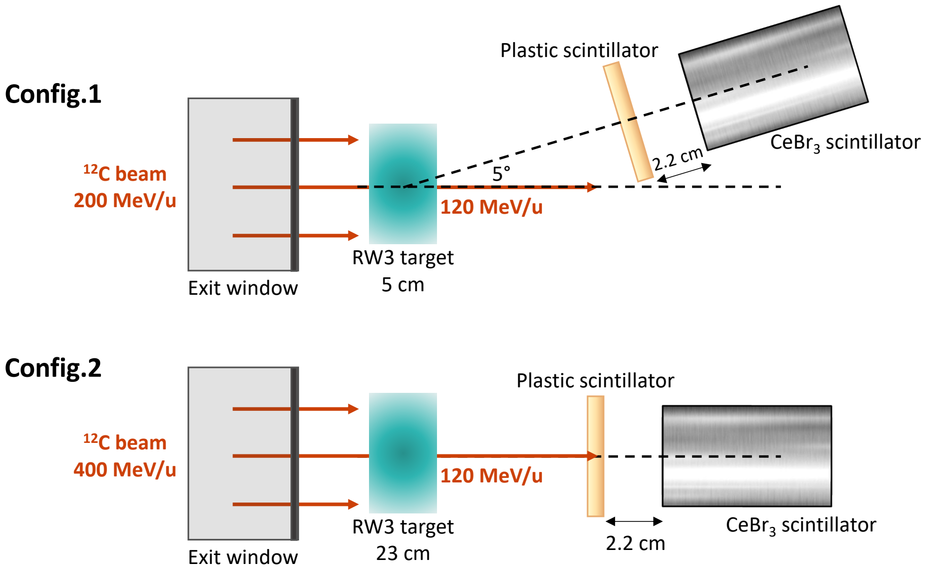

MC Geant4 10.07 simulation

- INCL++ physic list
- Experimental setup materials, geometry detector resolutions
- Number of events : 200 000 000
- Gaussian beam energy
- Particle cuts

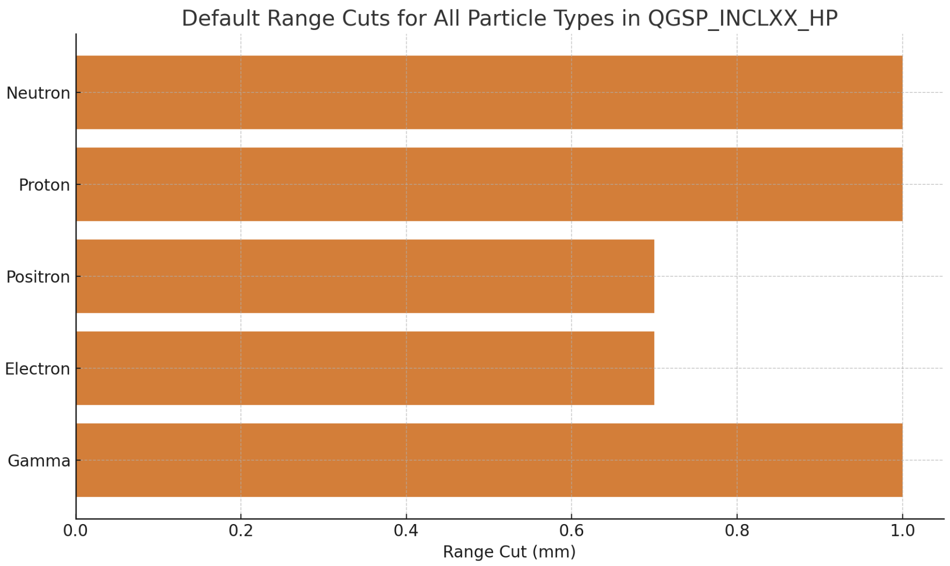

Secondary particles measurement

Experiment at CNAO

Config.1

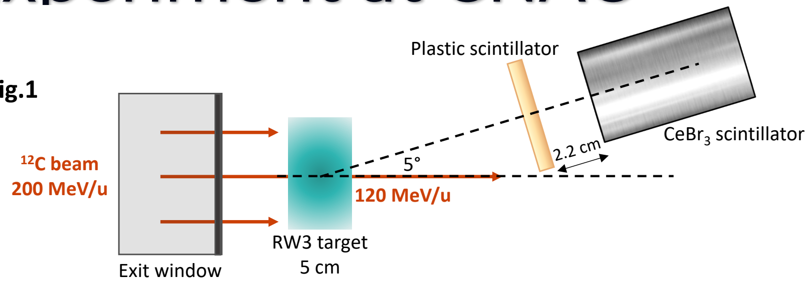

Experimental data

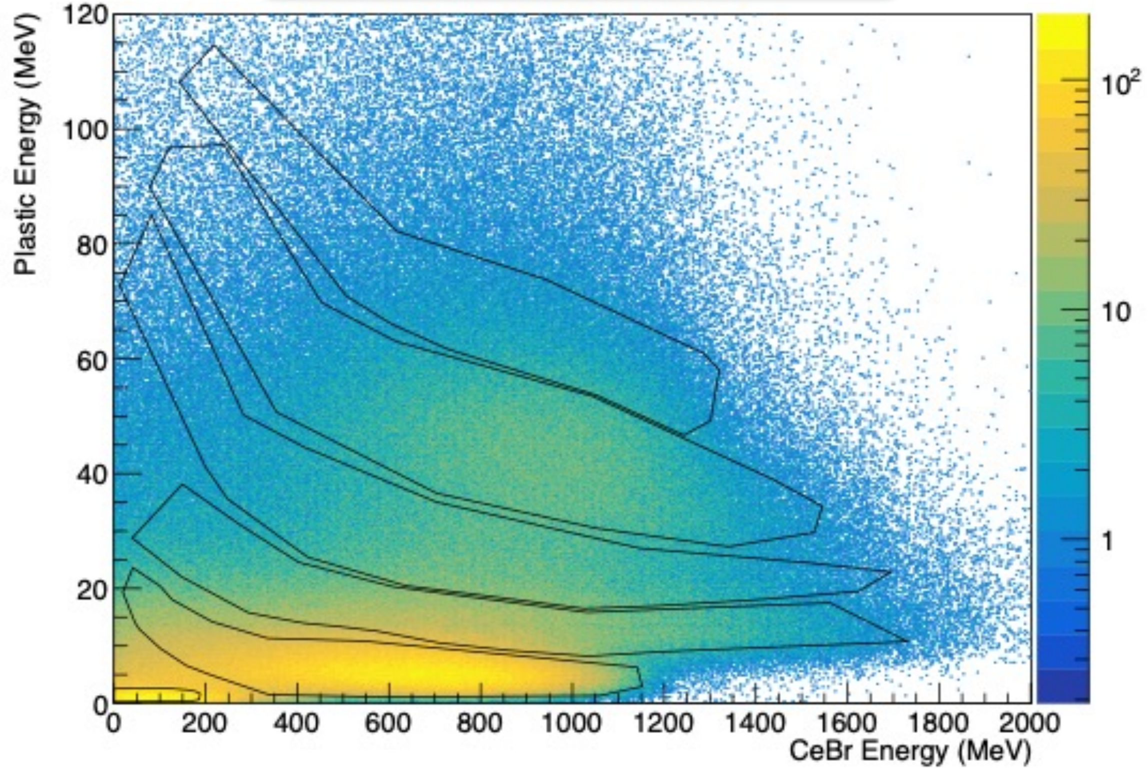

Geant 4 simulation

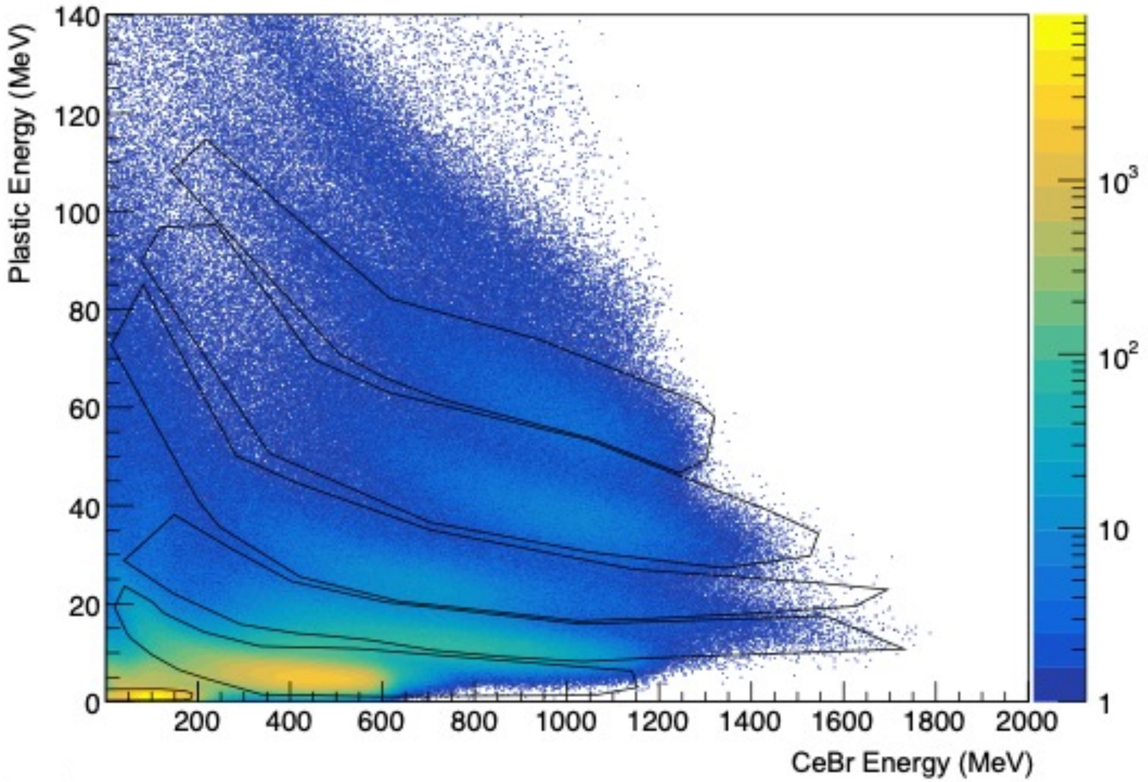

Secondary particles measurement

Experiment at CNAO

Config.1

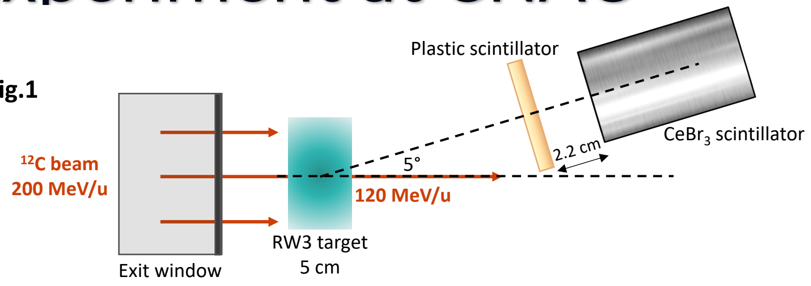

Experimental data

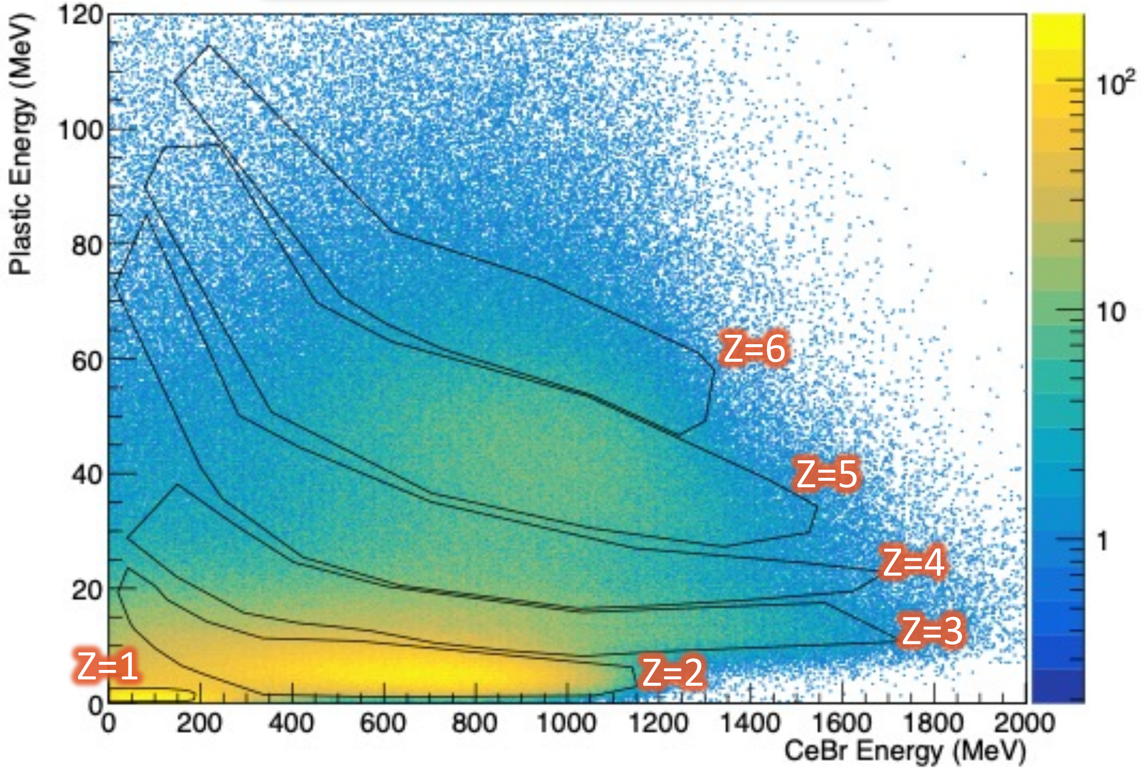

Geant 4 simulation

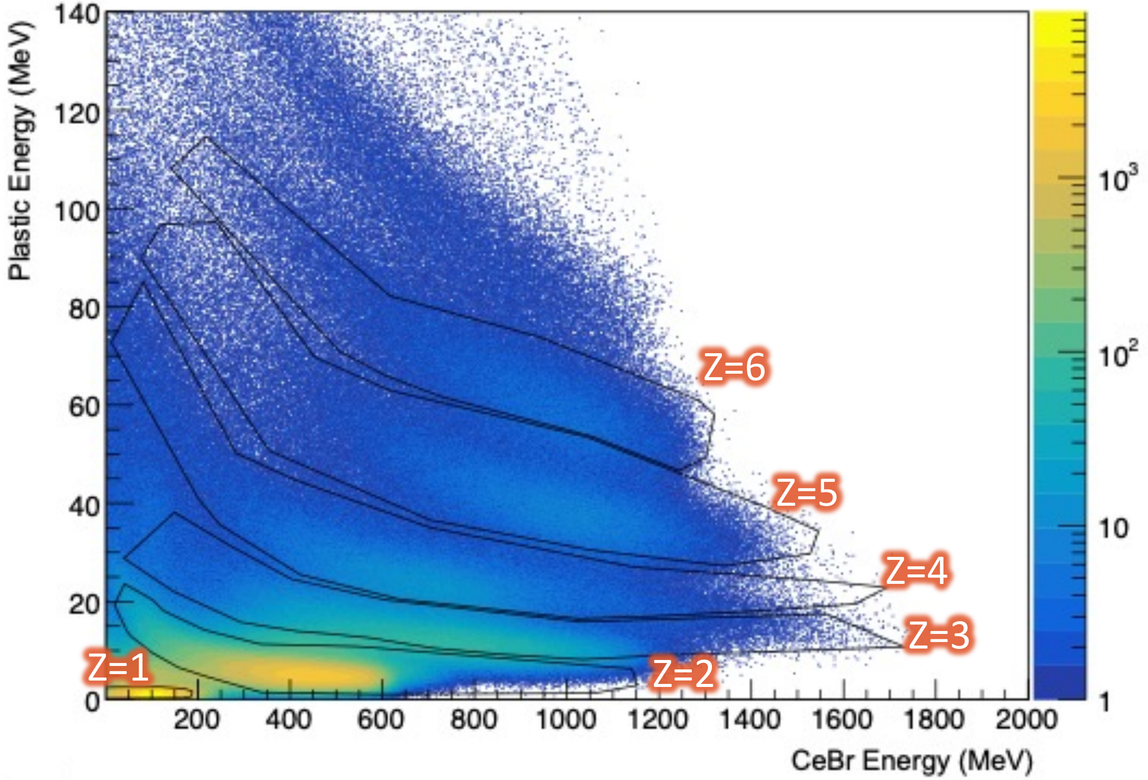

Secondary particles measurement

Experiment at CNAO

Config.2

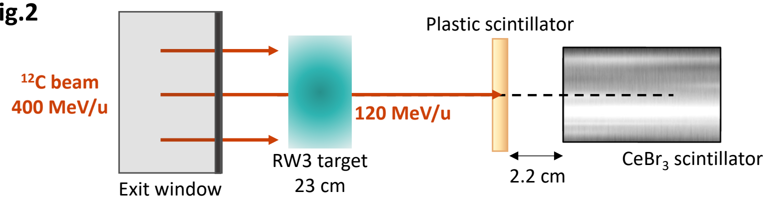

Experimental data

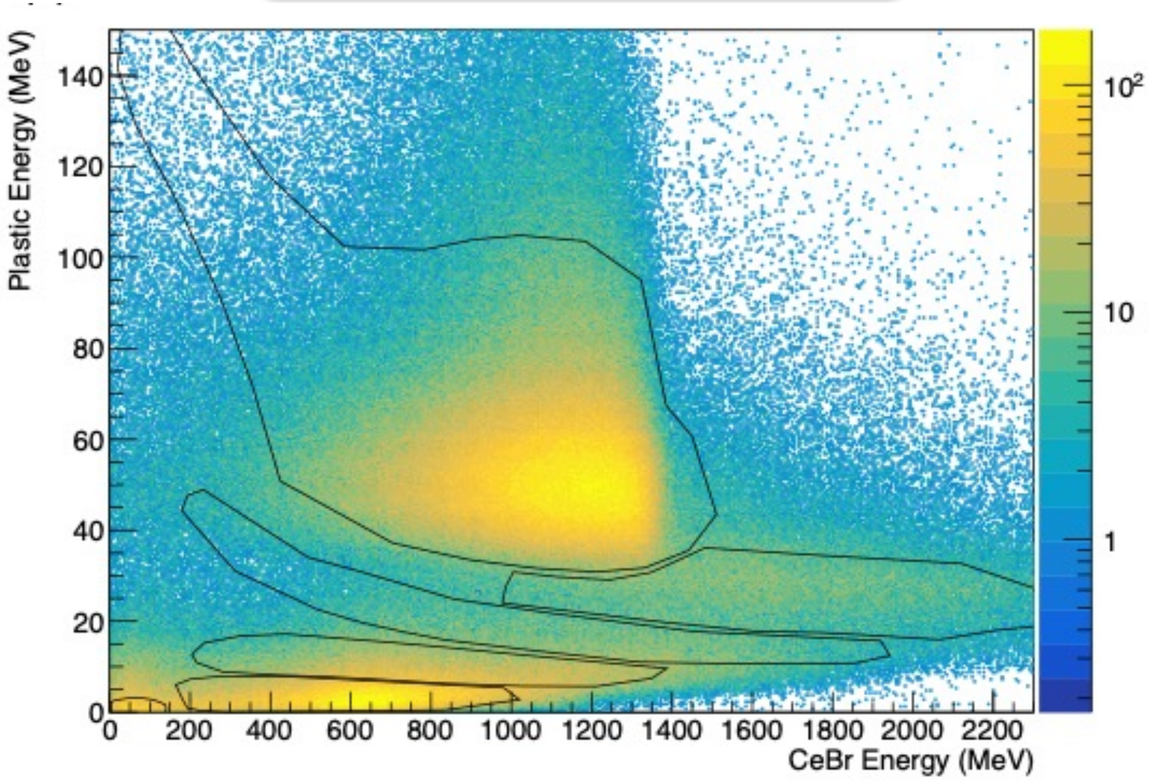

Geant 4 simulation

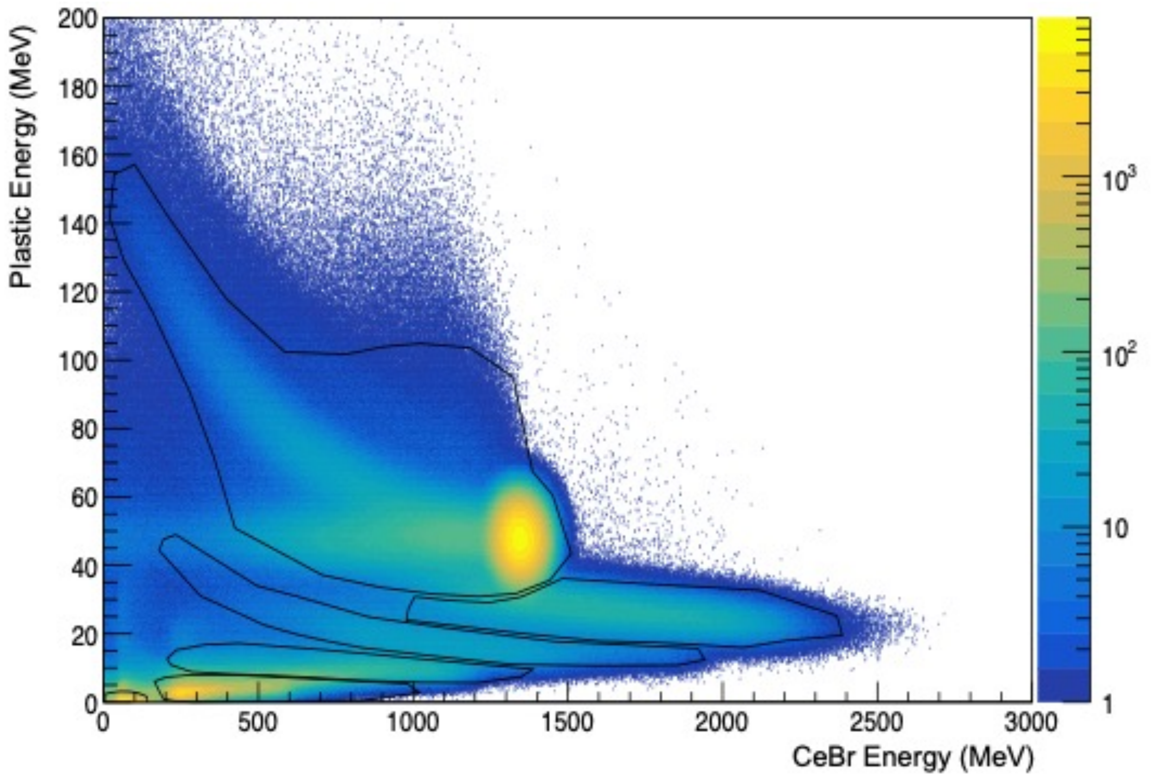

Secondary particles measurement

Experiment at CNAO

Config.2

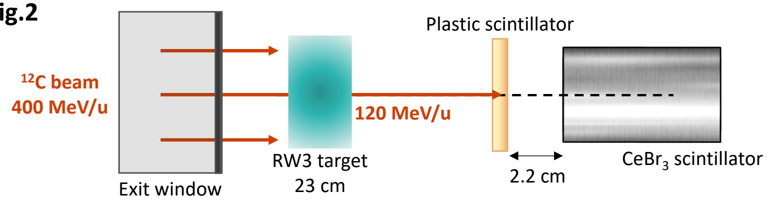

Experimental data

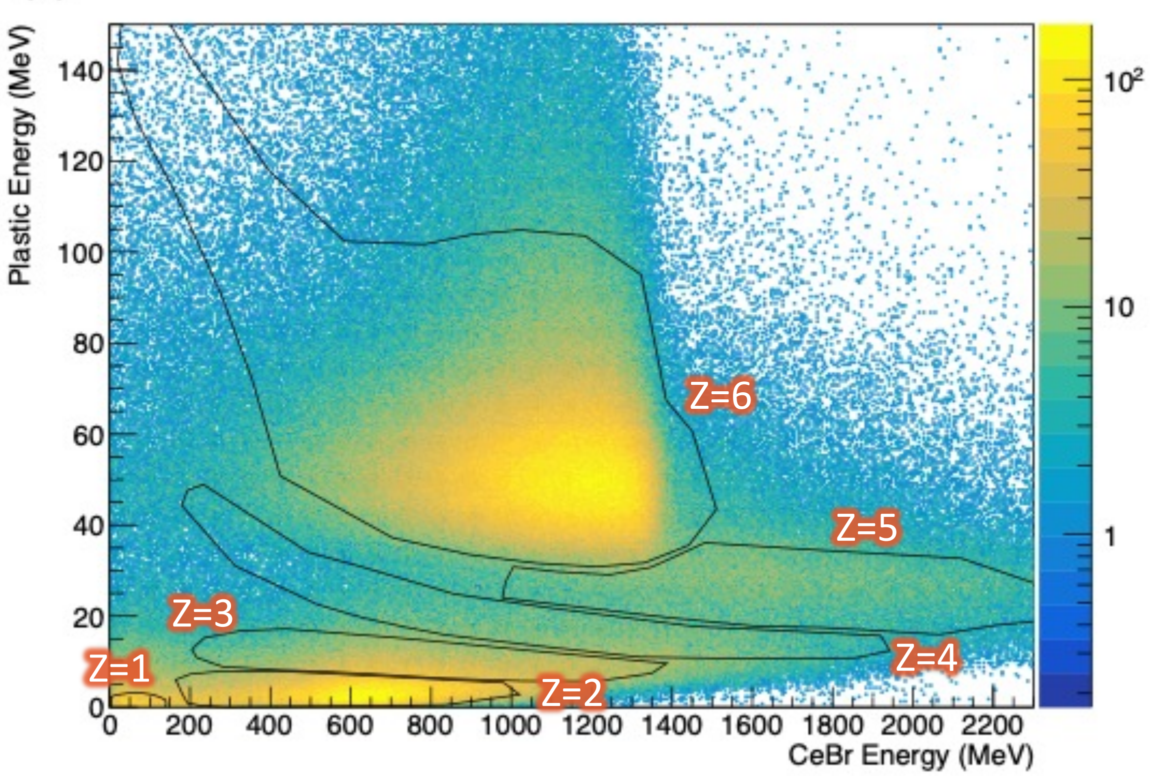

Geant 4 simulation

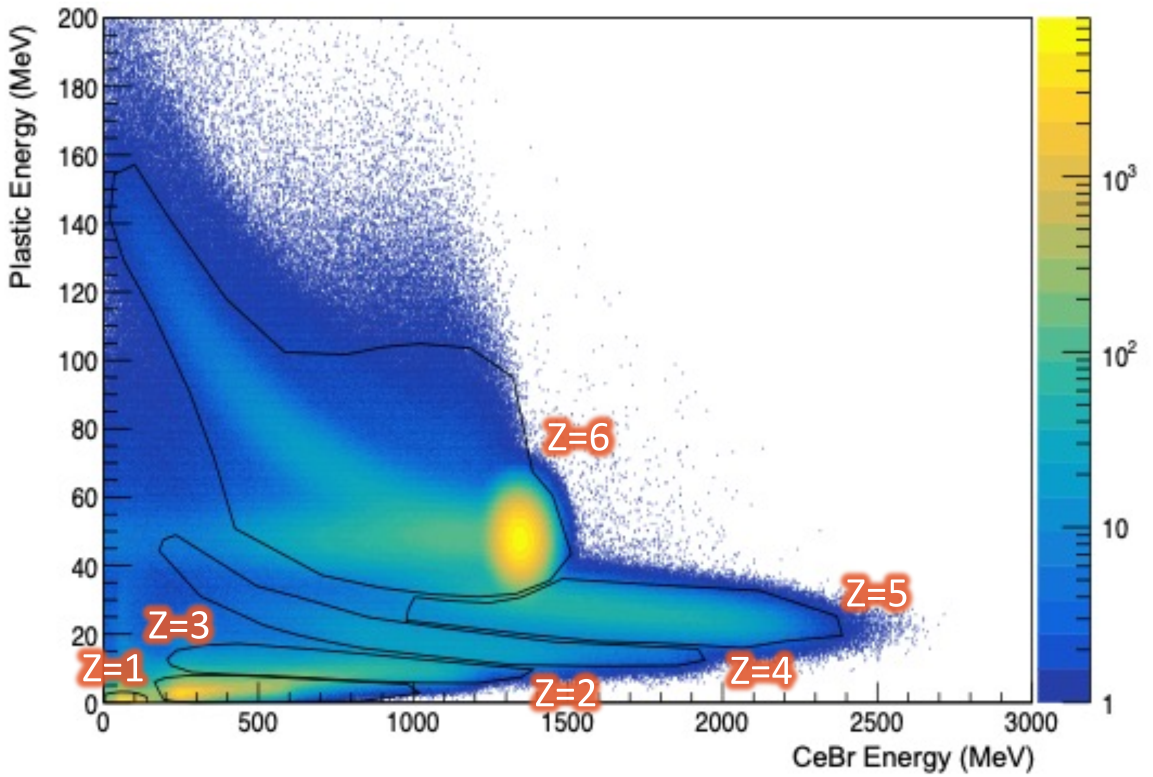

Secondary particles measurement

Experiment at CNAO

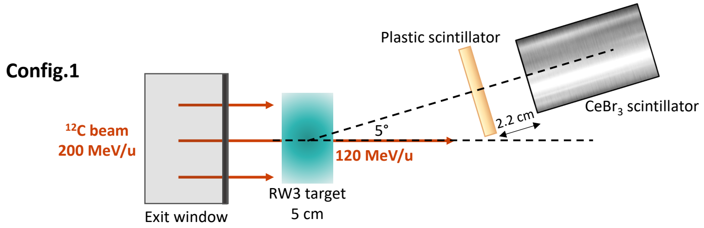

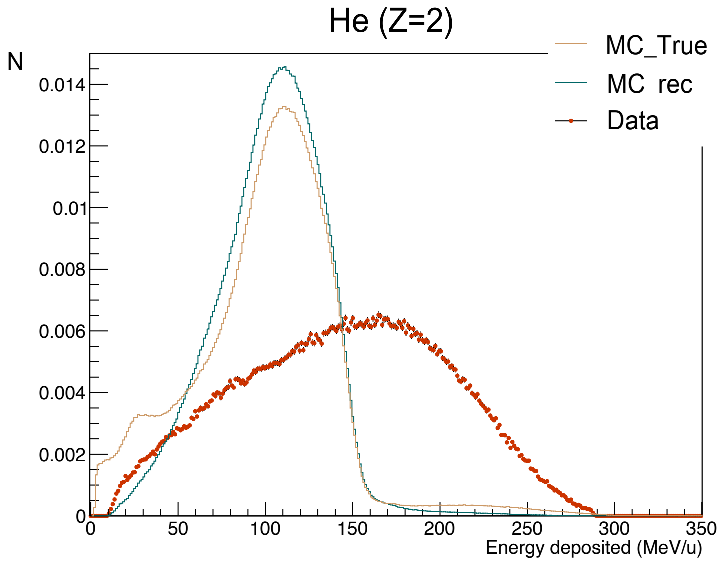

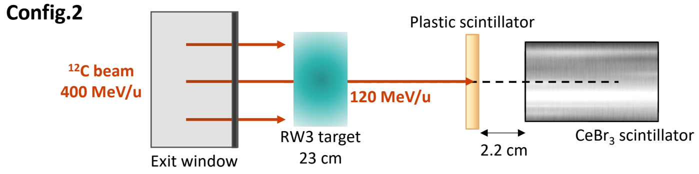

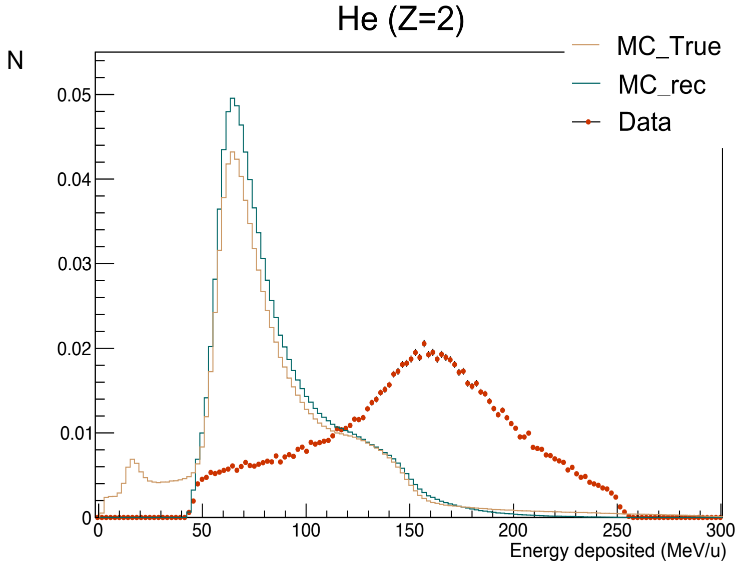

Secondary particles measurement

Experiment at CNAO

Config.1

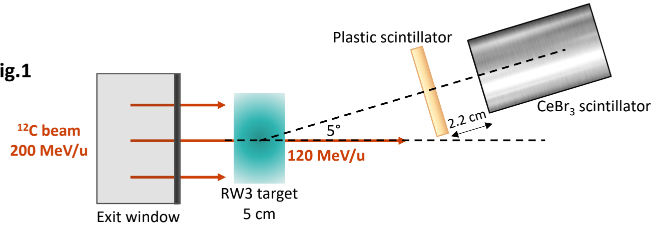

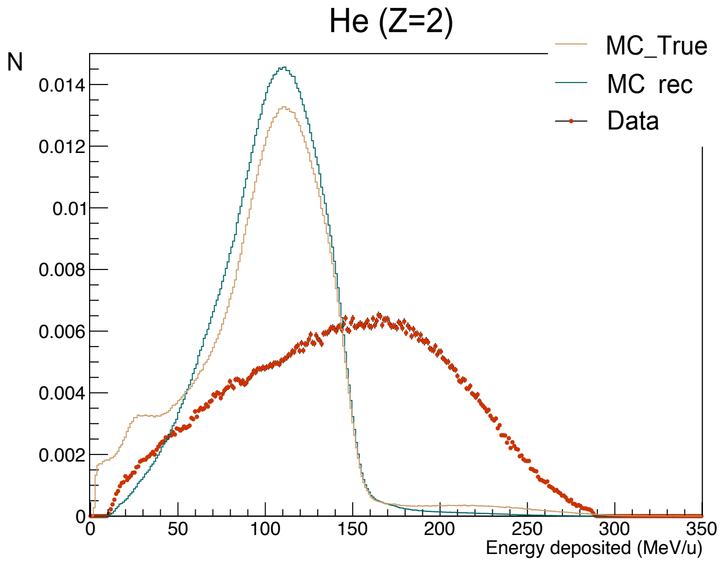

Z=2 Helium

- Inability of Geant4 to model carbon break-up

$^{12}C \rightarrow 3\alpha$

$^{12}C \rightarrow 2\alpha$ + residuals (light nuclei)

- α Pile-up in detectors

Config.2

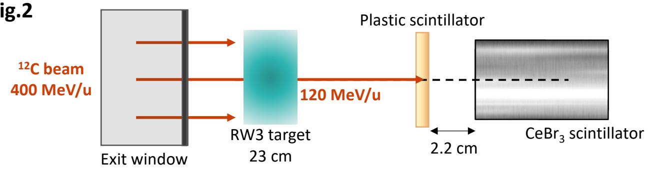

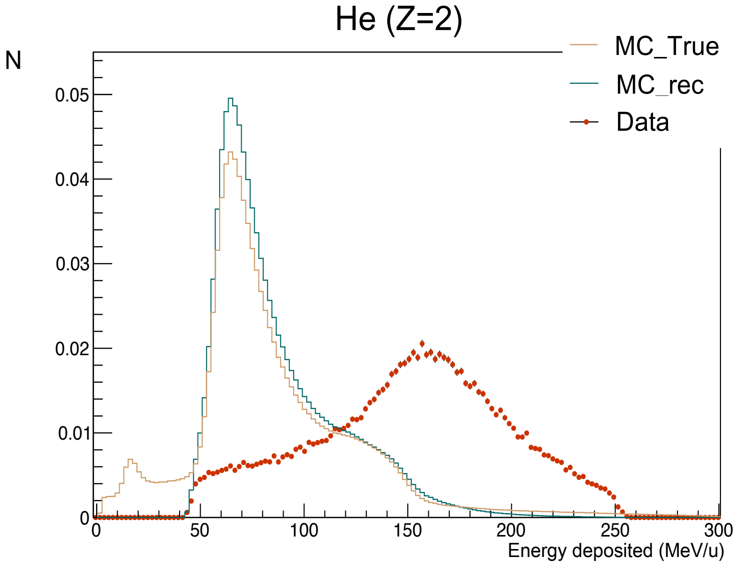

Secondary particles measurement

Experiment at CNAO

Config.1

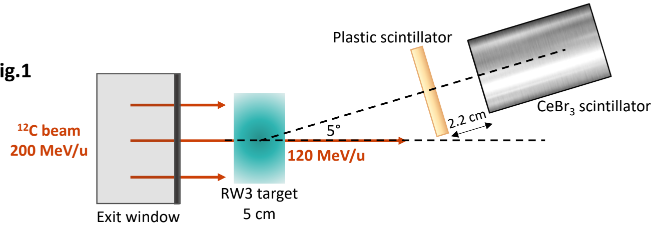

Config.2

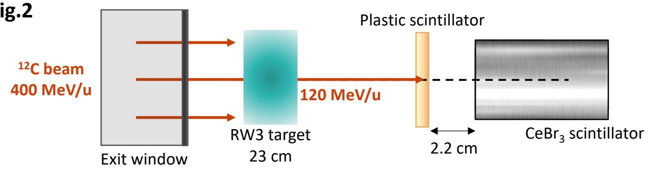

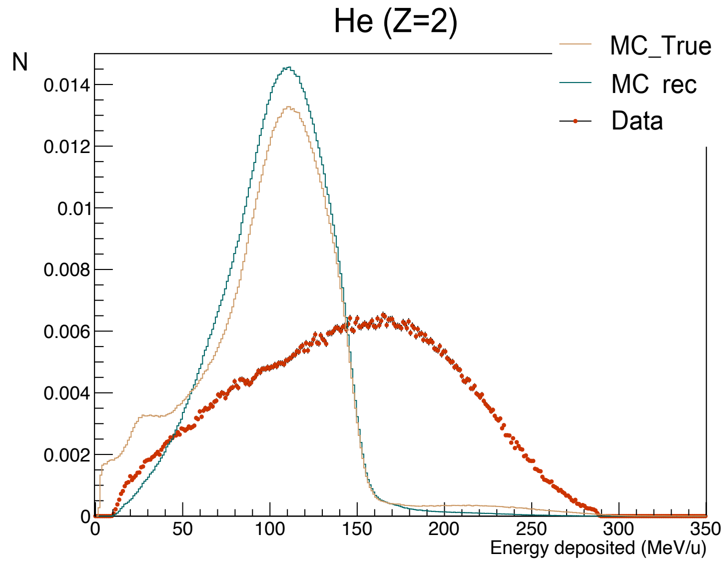

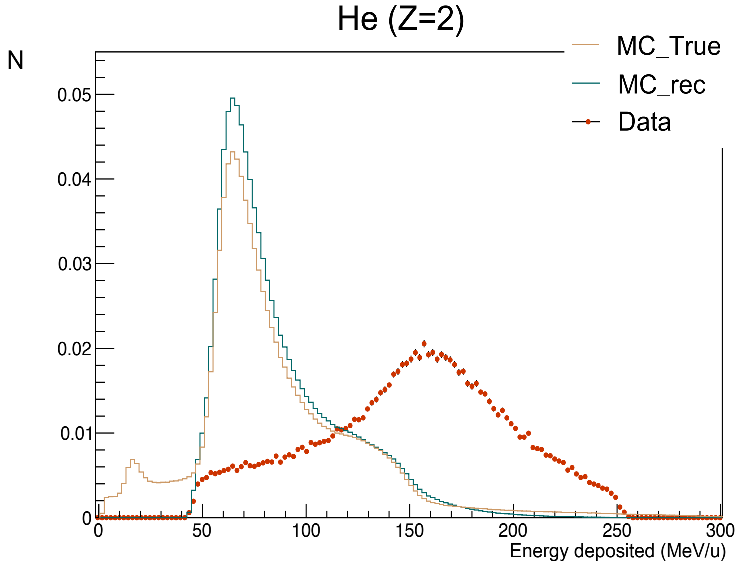

Z=2 Helium

- Inability of Geant4 to model carbon break-up

$$^{12}C \rightarrow 3\alpha$$

$$^{12}C \rightarrow 2\alpha + \text{residuals (light nuclei)}$$

- α Pile-up in detectors

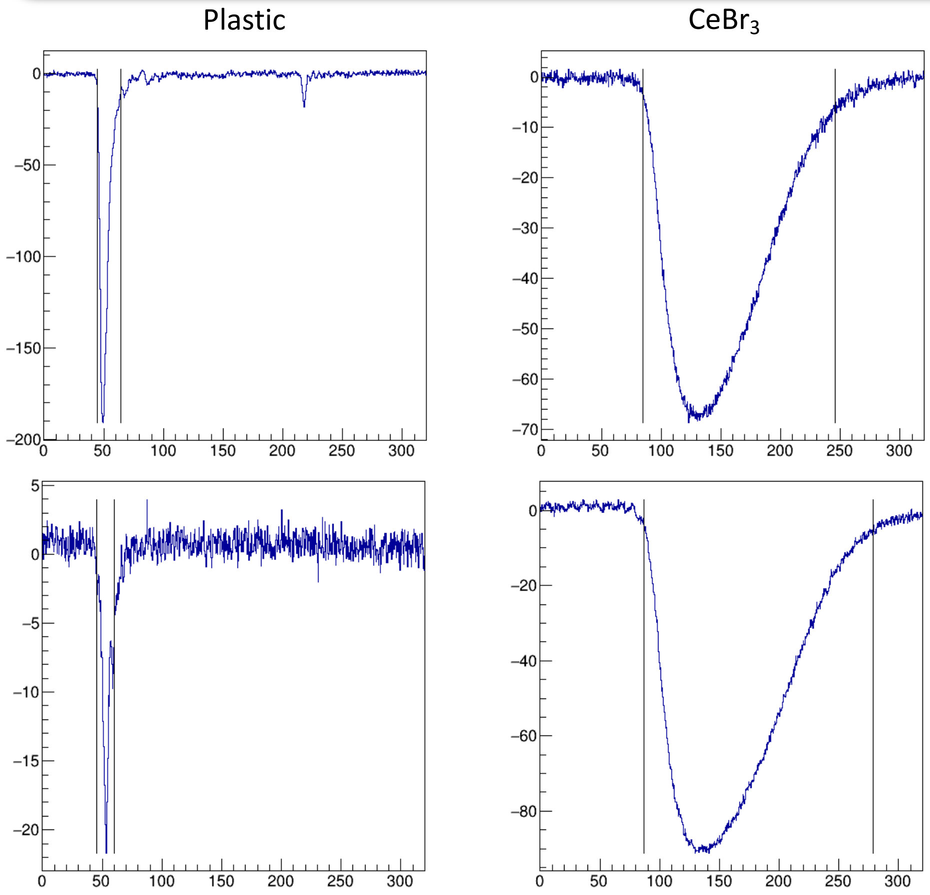

Secondary particles measurement

Experiment at CNAO

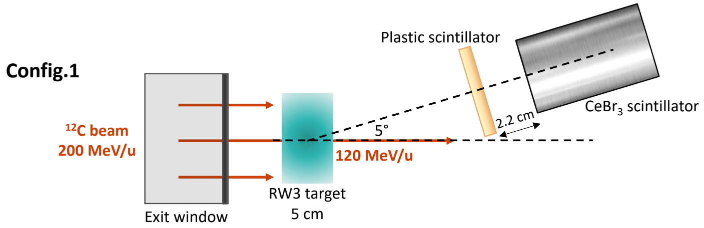

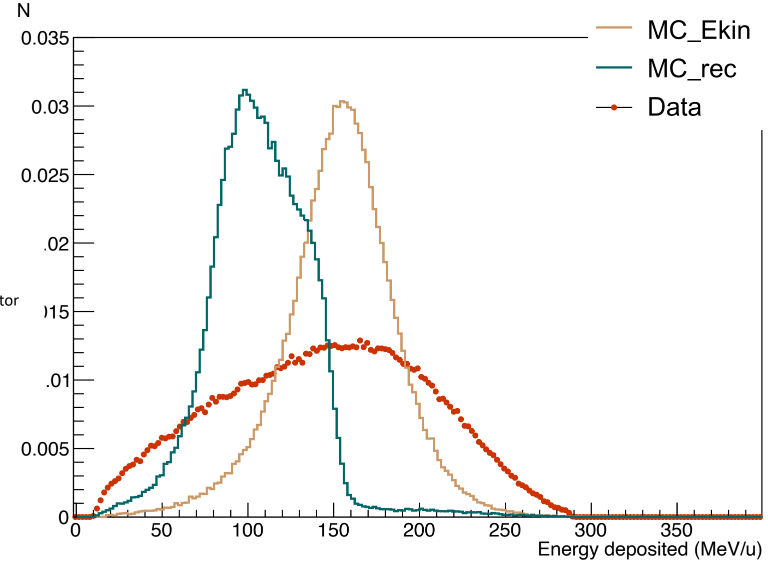

Z=2 Helium

- Inability of Geant4 to model carbon break-up

$$^{12}C \rightarrow 3\alpha$$

$$^{12}C \rightarrow 2\alpha + \text{residuals (light nuclei)}$$

- α Pile-up in detectors

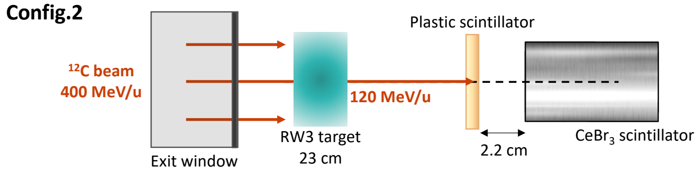

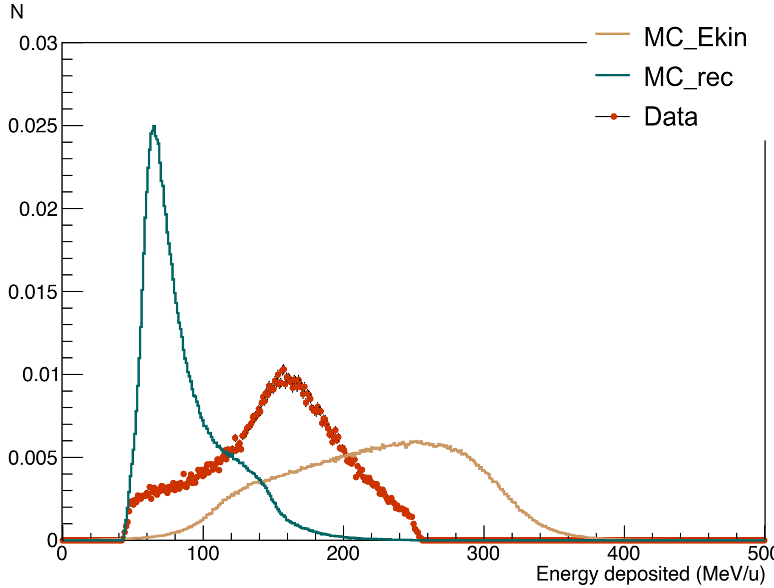

	Config. 1	Config. 2
He energy after target	130 MeV/u	260 MeV/u
He initial energy	200 MeV/u	400 MeV/u

- Each α should have half or third of initial energy
- Show the simulation inability to conserve energy during nuclear breakup process

Secondary particles measurement

Yields study

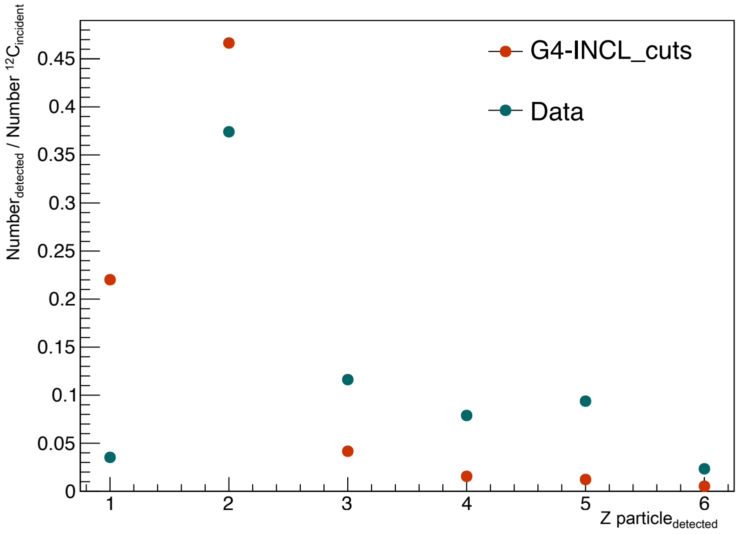

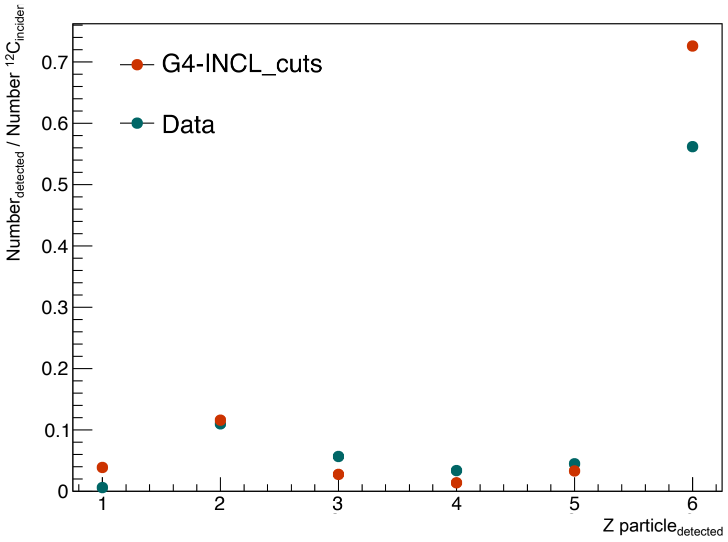

Secondary particles measurement

Yields study

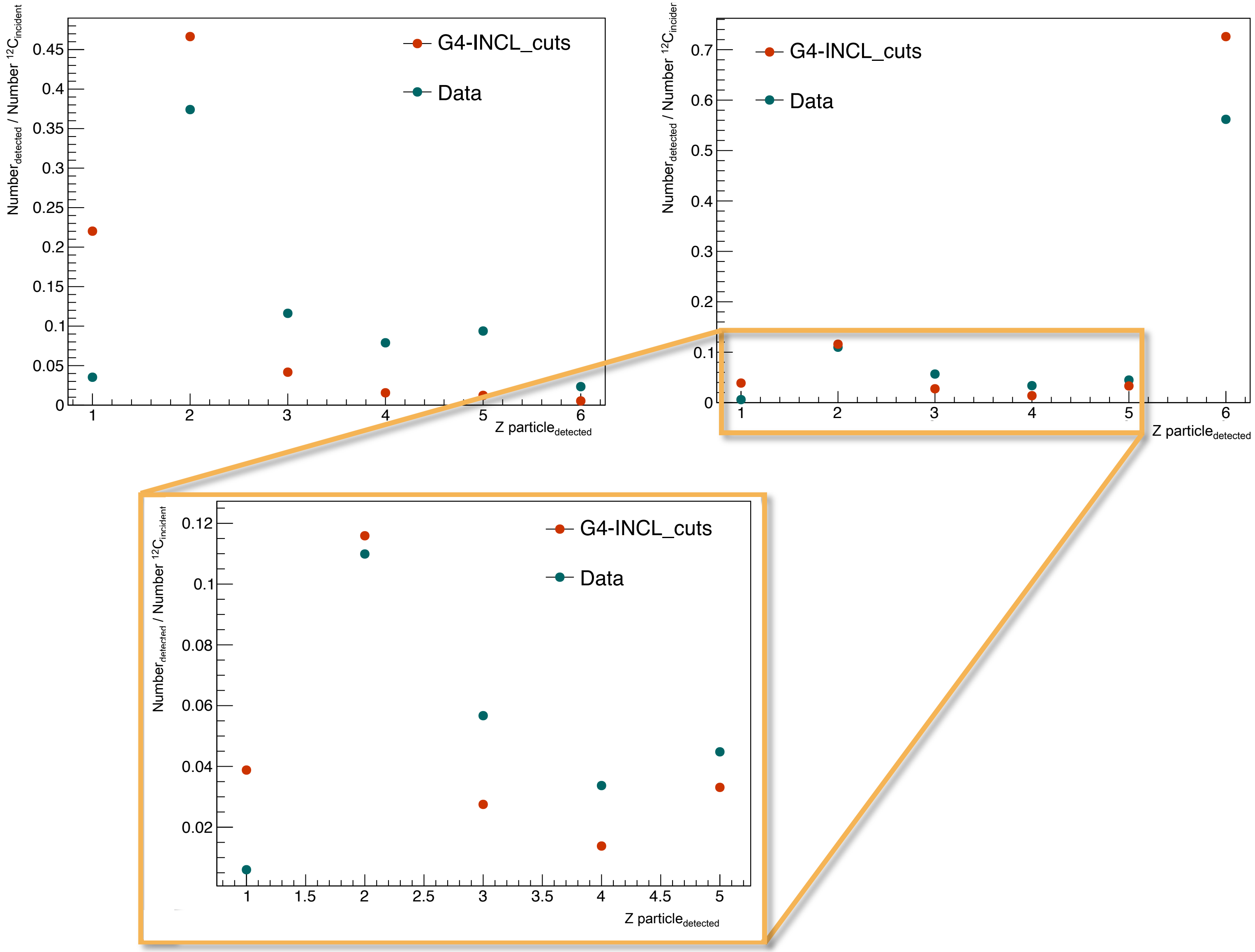

Secondary particles measurement

Yields study

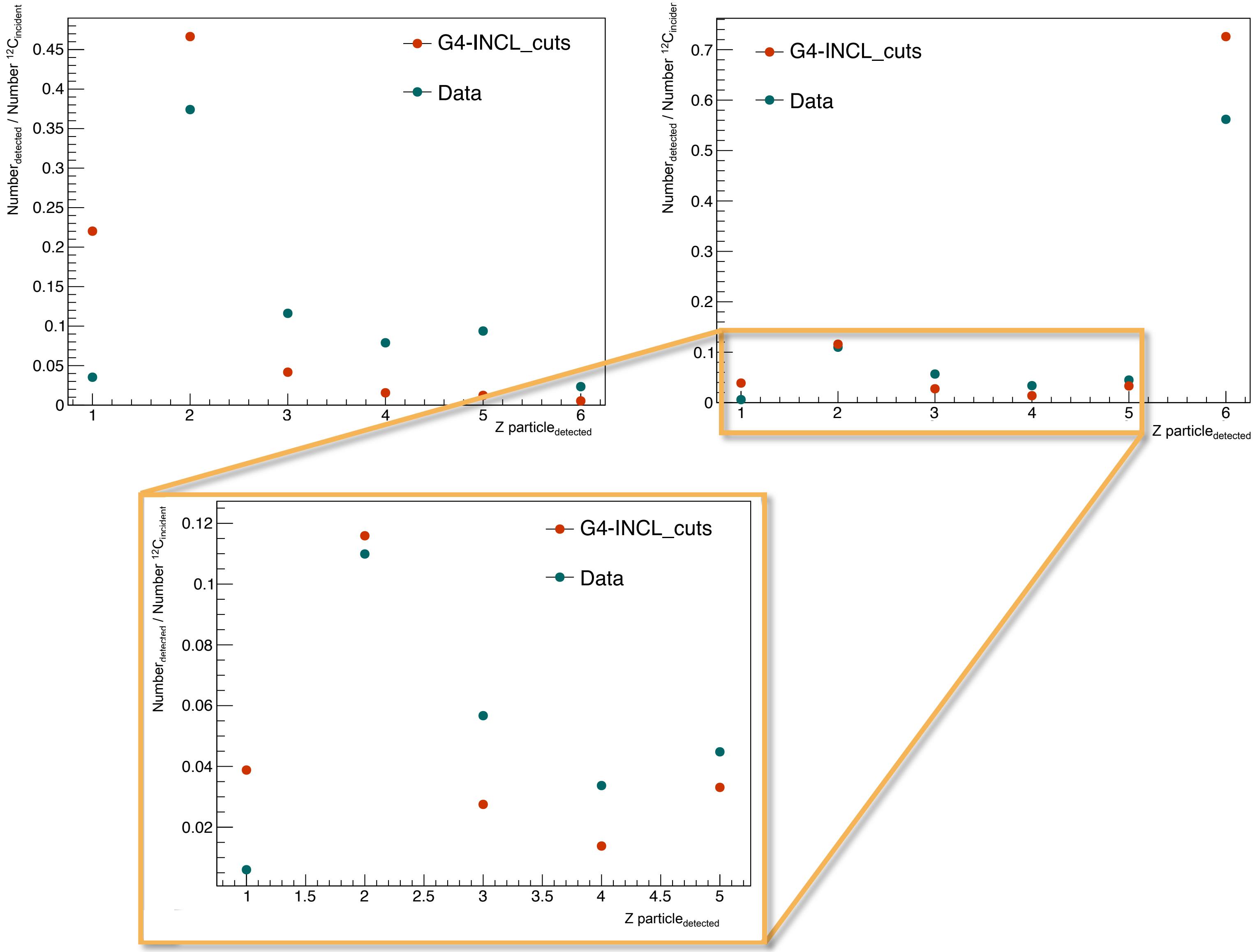

Relative yield

$$\Phi_Z = \frac{N_Z}{N_{events}}$$

Number of Z particle detected

Incident ^{12}C ions estimated

- Z=1 and Z=2
  → overestimation by Geant4 simulation
- Z=3, Z=4 and Z=5
  → underestimation by Geant4 simulation

Conclusion

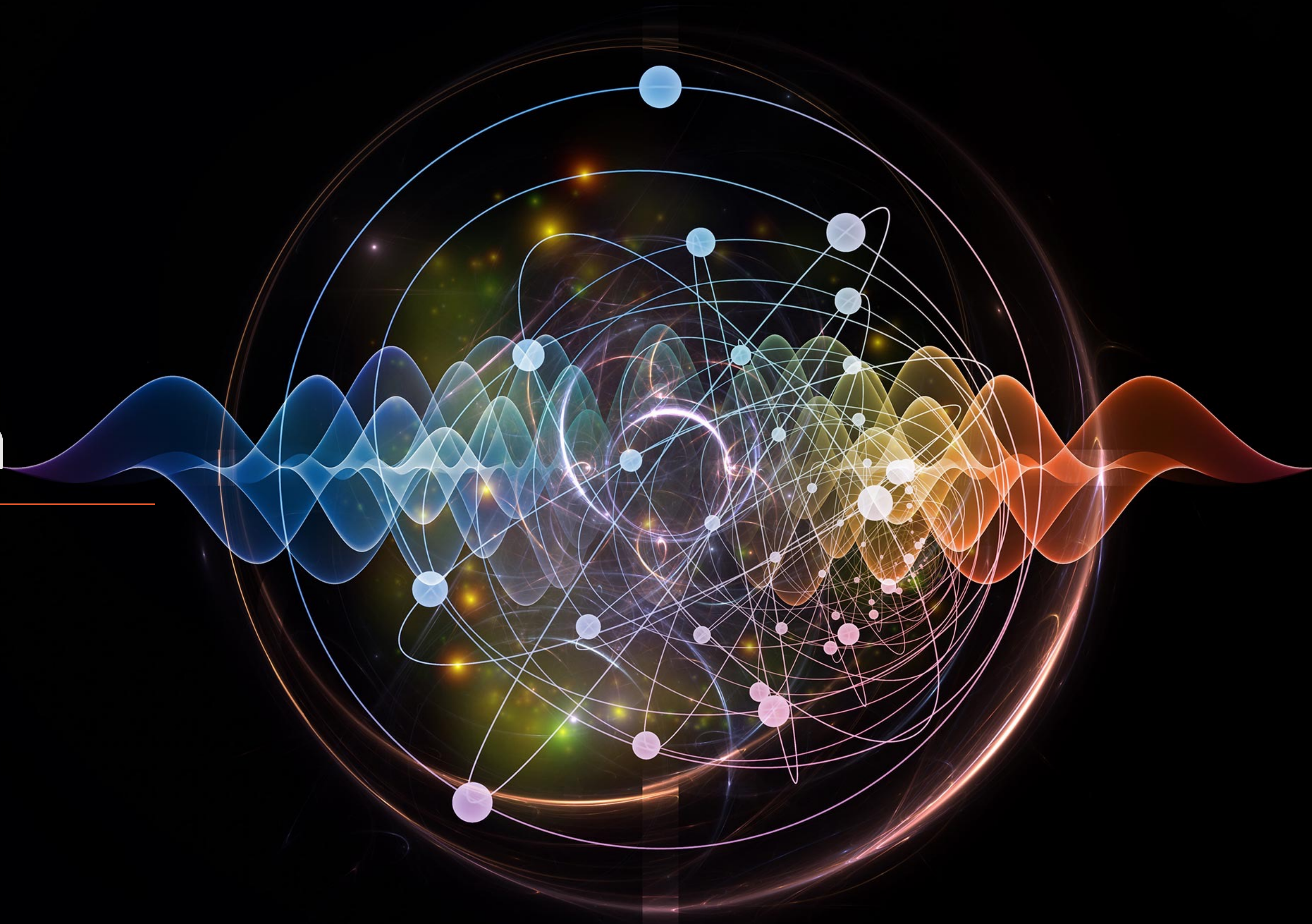

Conclusion

CNAO CLINM experiment

→ Significant discrepancies between experimental data and Geant4 simulation

↳ inaccuracies in simulation of the carbon break-up into alphas

↳ underestimated secondary particle yields

Perspectives

→ More experimental measurements with varying conditions

→ Implementation in Geant4 of experimental data to improve nuclear models accuracy

IPHC Institut Pluridisciplinaire Hubert CURIEN STRASBOURG

cnrs

Thank you for your attention

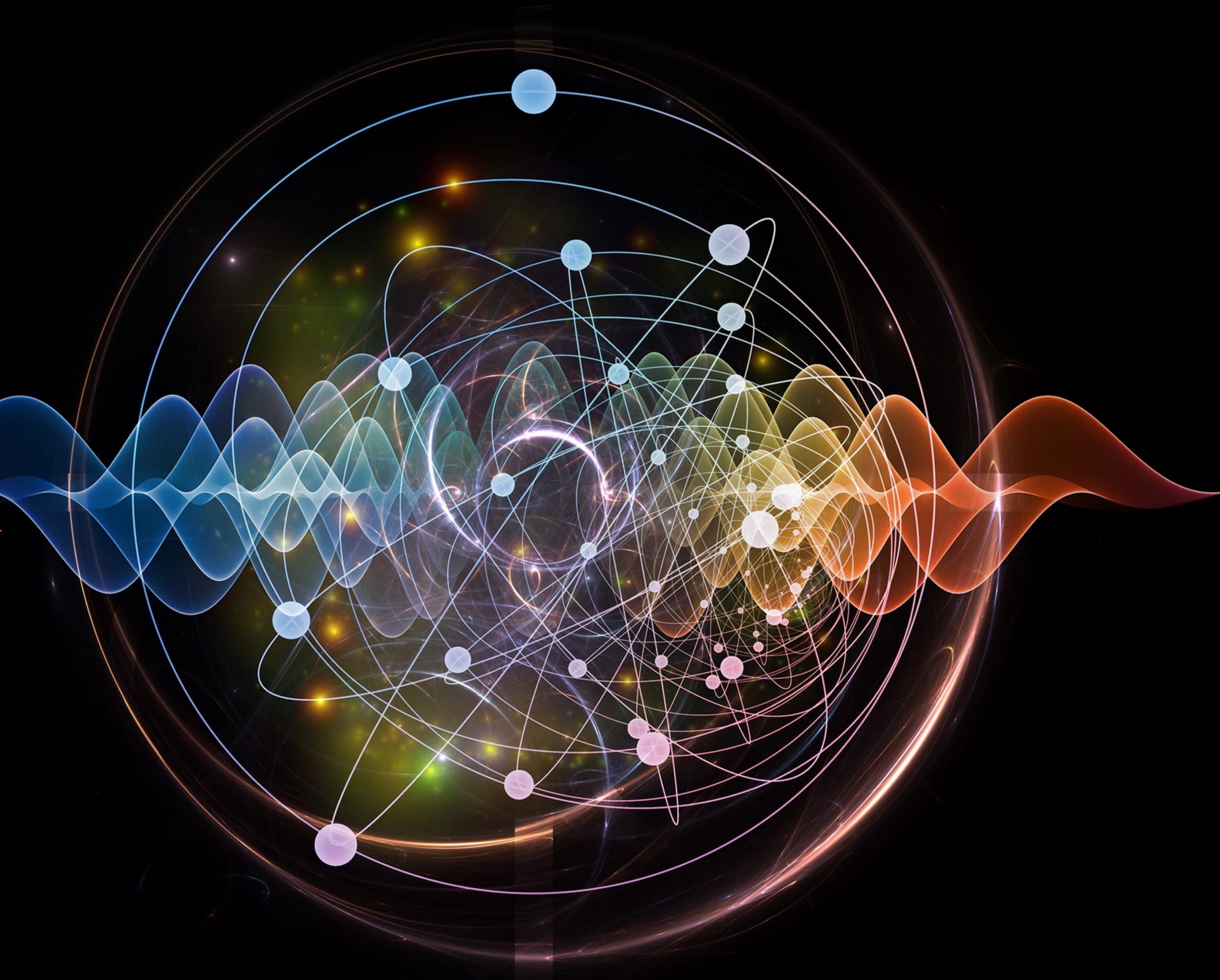

[1] K. Gunzert-Marx, H. Iwase, D. Schardt, R. S. Simon, Secondary beam fragments produced by 200 mev/u 12c ions in water and their dose contributions in carbon ion radiotherapy., New Journal of Physics (July 2008). doi:0.1088/1367-2630/10/7/075003.
URL http://stacks.iop.org/1367-2630/10/i=7/a=075003?key=crossref.d8c5fe2733dc0eb15571a822575b9130

[2] W.Tinganelli, M.Durante, Carbon ion radiobiology, Clinical Oncology (Oct. 2020).
URL https://tuprints.ulb.tu-darmstadt.de/16188/1/cancers-12-03022-v2.pdf

[3] U. Amaldi, G. Kraft, Radiotherapy with beams of carbon ions, Reports on Progress in Physics 68 (aug. 2005). doi:10.1088/0034-4885/68/8/R04.

[4] D. Cussol, Nuclear physics and hadrontherapy (2011).
URL https://hal.in2p3.fr/in2p3-00623351

[5] Y.Cao, D.Tang, Y.Xiang, L.Men, C.Liu, Q.Zhou, J.Wu, L.Huo, T.Song, Y.Wang, Z.Li, R.Wei, L.Shen, J. Z. Hong, Study on the appropriate timing of postoperative adaptive radiotherapy for high-grade glioma, Cancer Manag Res. (2021).
doi:https://doi.org/10.2147/CMAR.S300094.

[6] Nymus 3D animations – part of the Demcon group

[7] Dudouet, J. & Cussol, Daniel & Durand, D. & Labalme, M.. (2013). Benchmarking GEANT4 nuclear models for carbon-therapy at 95 MeV/A. Physical Review C. 89. doi: 10.1103/PhysRevC.89.054616.

[8] M. E. Wolf. Robust optimization in 4D treatment planning for carbon ion therapy of lung tumors. PhD thesis, Technische Universitä t, Darmstadt, November 2018. URL http://tuprints.ulb.tu-darmstadt.de/8354/

[9] University of Iowa health care - https://www.youtube.com/watch?v=nZ044EicYO4

[10] M. Kramer, et al., Treatment planning for heavy-ion radiotherapy: physical beam model and dose optimization., Phys. Med. Biol., 45(11): 528 3299 (2000). doi:10.1088/0031-9155/45/11/313.

[11] S.M. Valle, A. Alexandrov, G. Ambrosi, S. Argirò, G. Battistoni, et al.
FOOT: a new experiment to measure nuclear fragmentation at intermediate energies, Perspectives in Science, Volume 12, 2019, 100415, ISSN 2213-0209, https://doi.org/10.1016/j.pisc.2019.100415.

[12] A. Koning, D. Rochman, J.-C. Sublet, N. Dzysiuk, M. Fleming, S. van der Marck, Tendl: Complete nuclear data library for innovative nuclear science and technology, Nuclear Data Sheets 155 (2019) 1–55.
URL https://doi.org/10.1016/j.nds.2019.01.002

Back-up

General context

Secondary particles in heavy ion therapy
Physical aspects

Linear energy transfer (LET)

- Restricted local version of dE/dx
- Related to track length
- Dominated by ionization e⁻

$$LET = \frac{dE}{dx} - \sum E_c(e_\delta)$$

Total kinetic energy of electrons δ

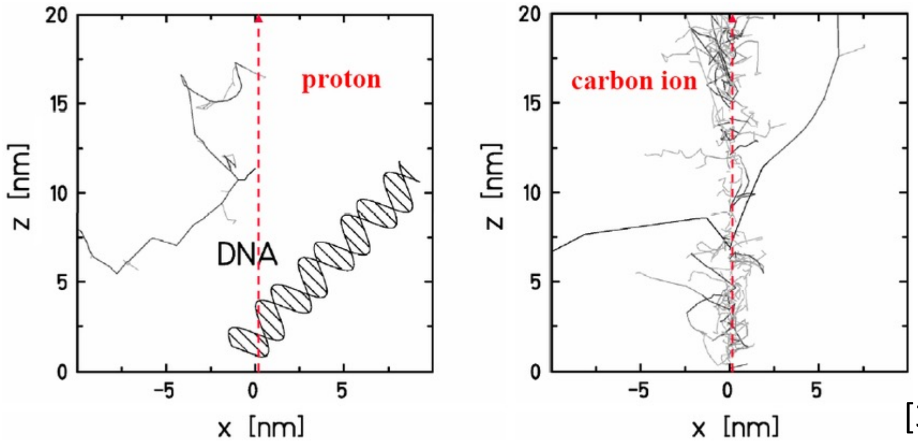

[3]

Secondary particles in heavy ion therapy

Biological aspects

Mean energy deposited

Dose → $D = \frac{dE}{dm} [Gy]$ J/kg

Mass element

Particle flux

→ $D = \frac{\Phi}{\rho} LET$ Linear energy transfer

Material density

Relative biological effectiveness

→ Take into account radiation type

→ Based on cellular survival curves

Reference dose with X-ray therapy

→ $RBE = \frac{D_{Xray}}{D_{ion}}$

Dose under investigation yielding equivalent cellular survival

Oxygen enhancement factor

→ Reduced oxygen concentration in cell (hypoxic cell) reduce radiation effectiveness

→ $OER = \frac{\text{radiation dose in hypoxia}}{\text{radiation dose in air}}$

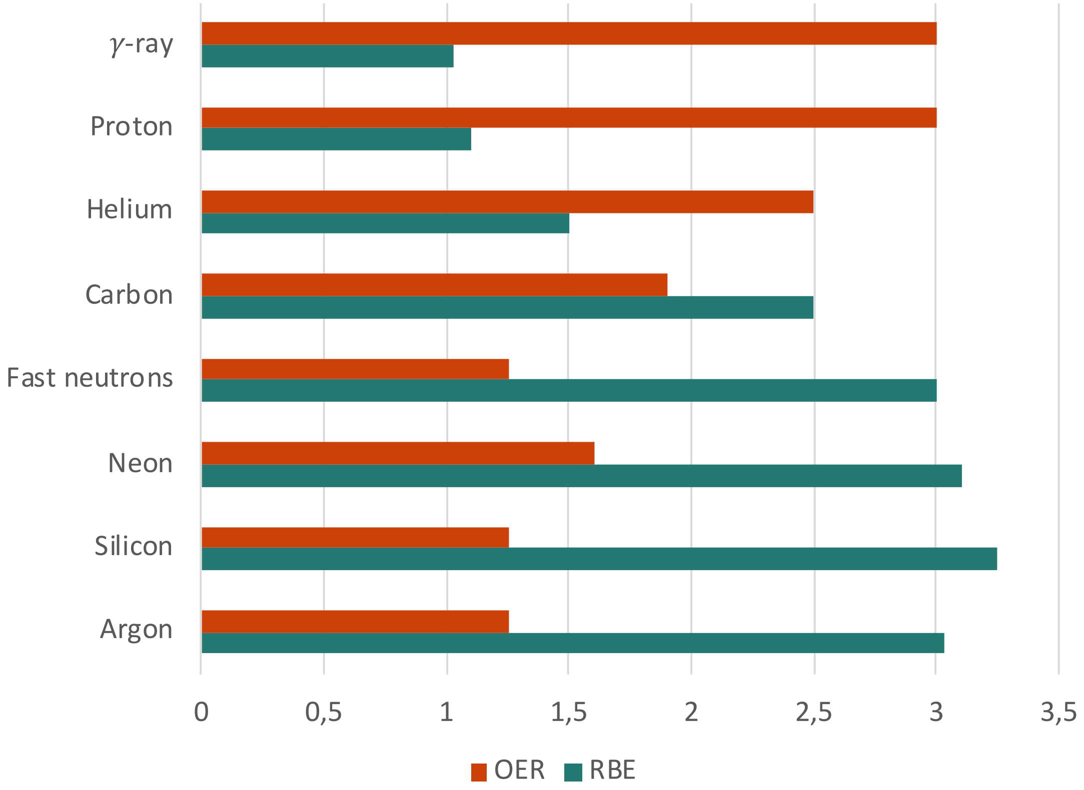

[4]

High RBE = Lot of damages

Low OER = Low resistance of hypoxic cells

Secondary particles in heavy ion therapy

Treatment plan

Imaging

Define tumoral/targeted volume

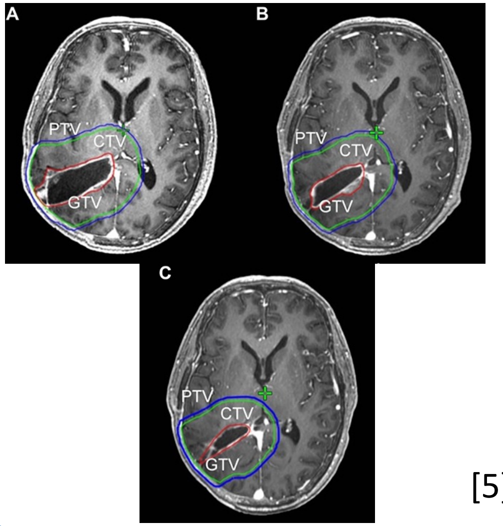

[5]

Treatment planning System (TPS)

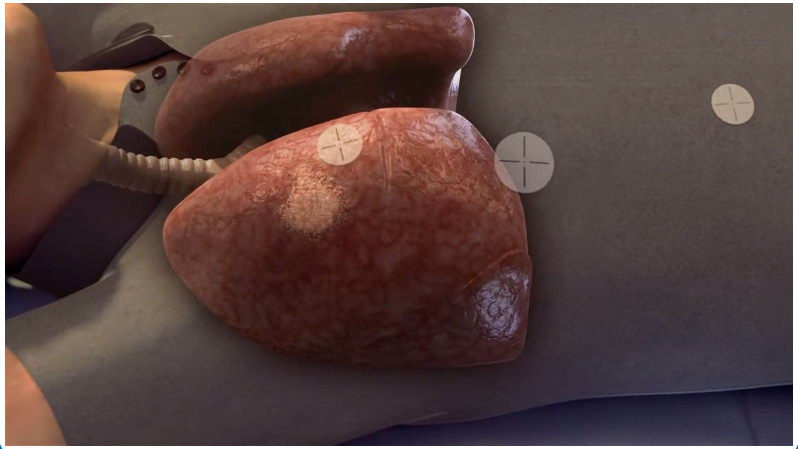

[6]

Treatment

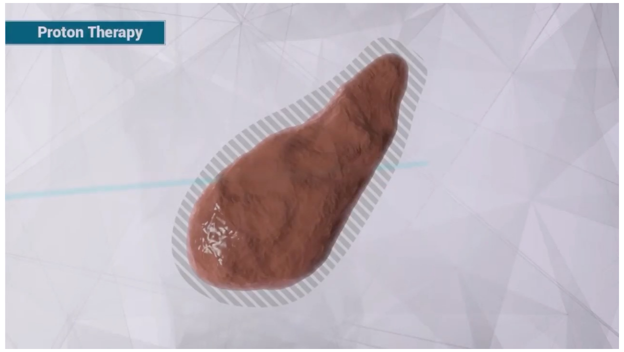

[6]

Irradiation Control (PET)

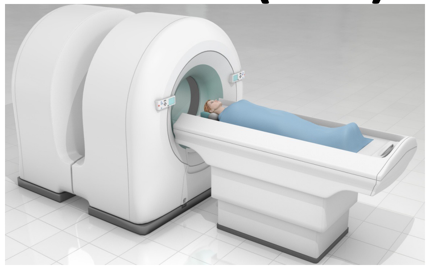

Corrections

Comparison between delivered dose and planned one

Margins

Dose calculation

Physical processes | Chemical processes | Biological processes

Uncertainties

Calibration

Secondary particles measurement

Calibration measurements

Amplitude (mV)

S ($V.MeV^{-1}$)
~ Scintillator material → conversion efficiency of energy deposited into detected signal
~ 10^{-2} to 10^{0} $g.MeV^{-1}.cm^{-2}$

Birks' law : $A = \frac{S*E+p}{1+k_B*E}$

Pedestal (mV)
Offset value added to measured signal to compensate background noise
~ few mV to 10^{1} mV

k_B (MeV^{-1})
~Quenching effect of light → High k_B ≡ high quenching
For organic scintillator ~ $10^{-2} – 10^{-3}$ $cm.MeV^{-1}$
For inorganic scintillator ~ $10^{-3} – 10^{-4}$ $cm.MeV^{-1}$

Secondary particles measurement

Plastic scintillator

Voltage applied : - 1200 V

Calibration in amplitude

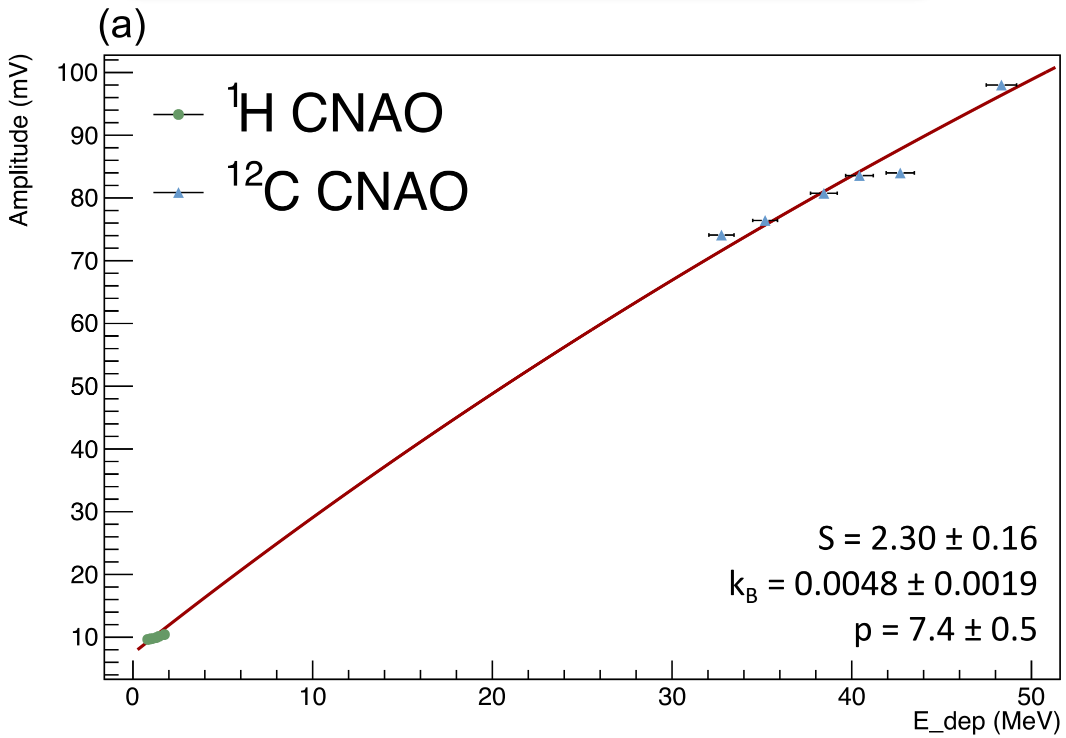

Birks' law : $A = \frac{S*E+p}{1+k_B*E}$

Energy resolution

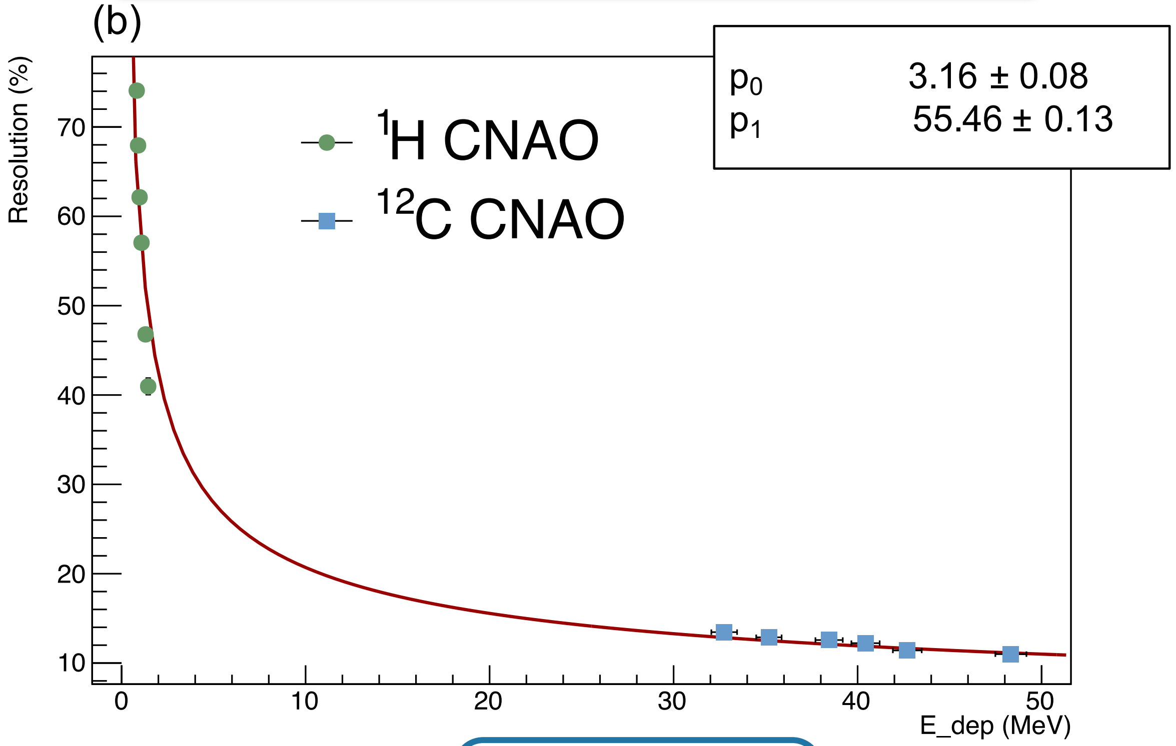

Energy resolution : $\frac{\sigma_E}{E} = p_o + \frac{p_1}{\sqrt{E}}$

- **Birk's law respected up to 50 MeV**
- **Energy resolution : beam straggling effects**

Secondary particles measurement

$CeBr_3$ scintillator

Voltage applied : + 350 V

Calibration in amplitude

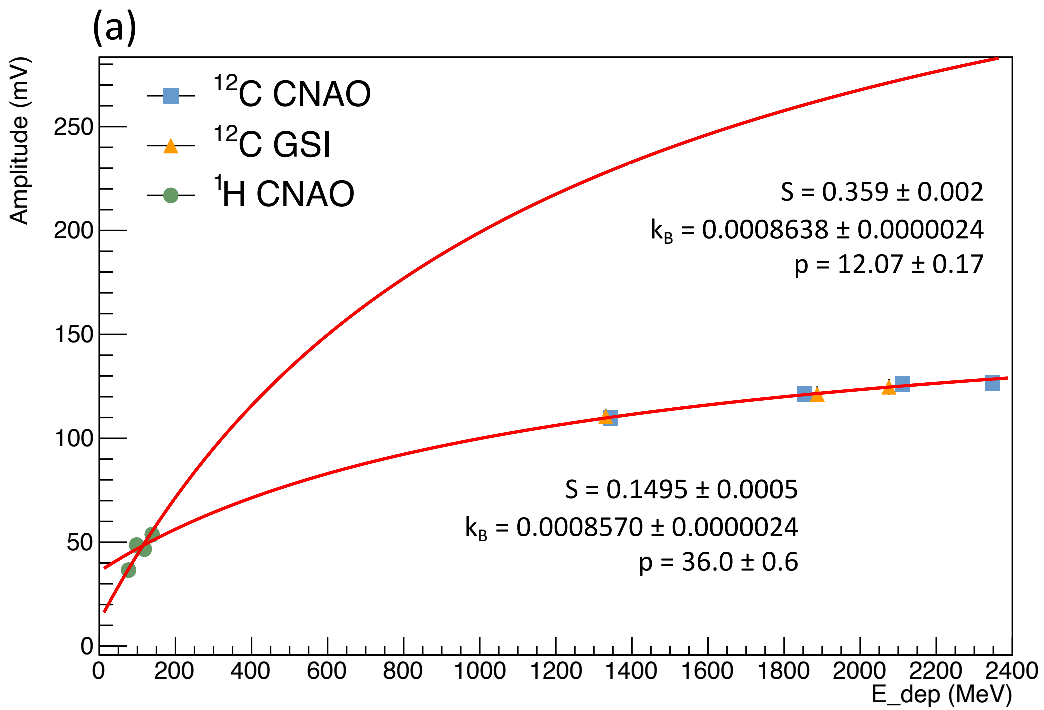

Birks' law : $A = \frac{S*E+p}{1+k_B*E}$

Energy resolution

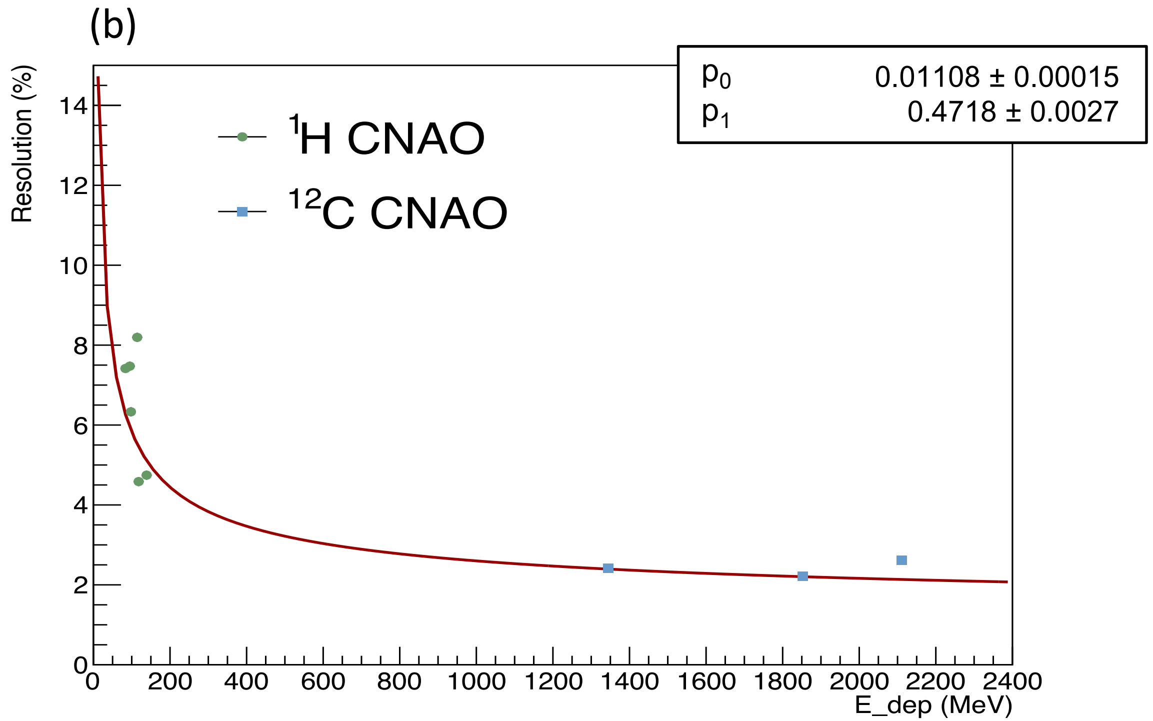

Energy resolution : $\frac{\sigma_E}{E} = p_o + \frac{p_1}{\sqrt{E}}$

Secondary particles measurement

$CeBr_3$ scintillator

Voltage applied : + 350 V

Calibration in amplitude

(a)

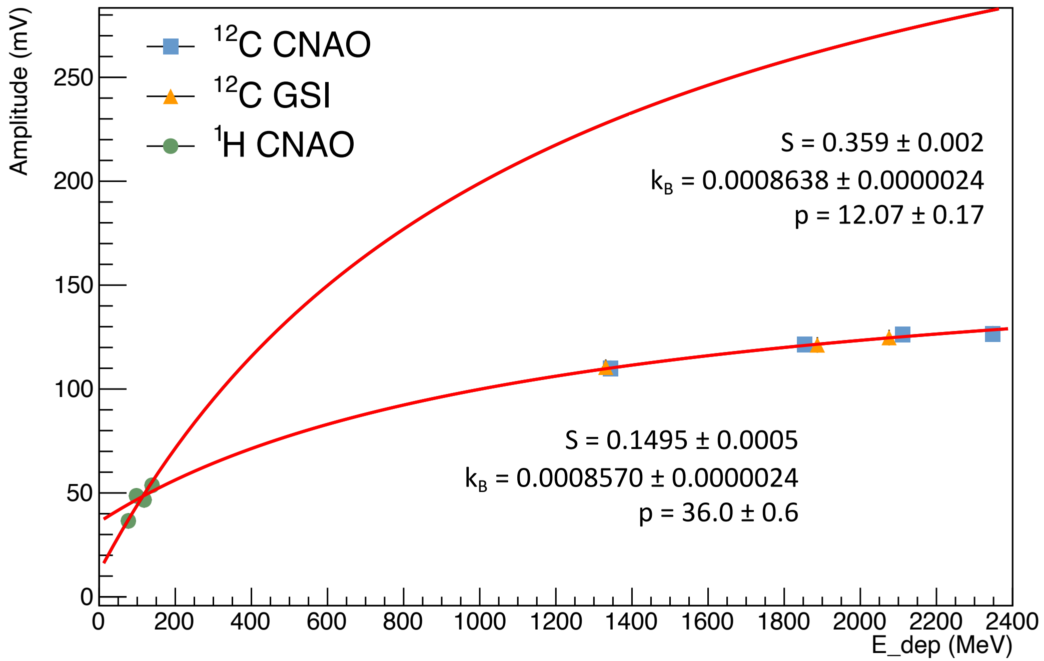

Birks' law : $A = \frac{S*E+p}{1+k_B*E}$

- **Distinct calibration functions for each ion type**
- **Birk constant similar for both ions**
- **Birk's law up to 2350 MeV**

Secondary particles measurement

$CeBr_3$ scintillator

Voltage applied : + 350 V

Energy resolution

- **~10 MeV energy resolution for both ion types**
- **Highlight scintillator precision for this ion energies**

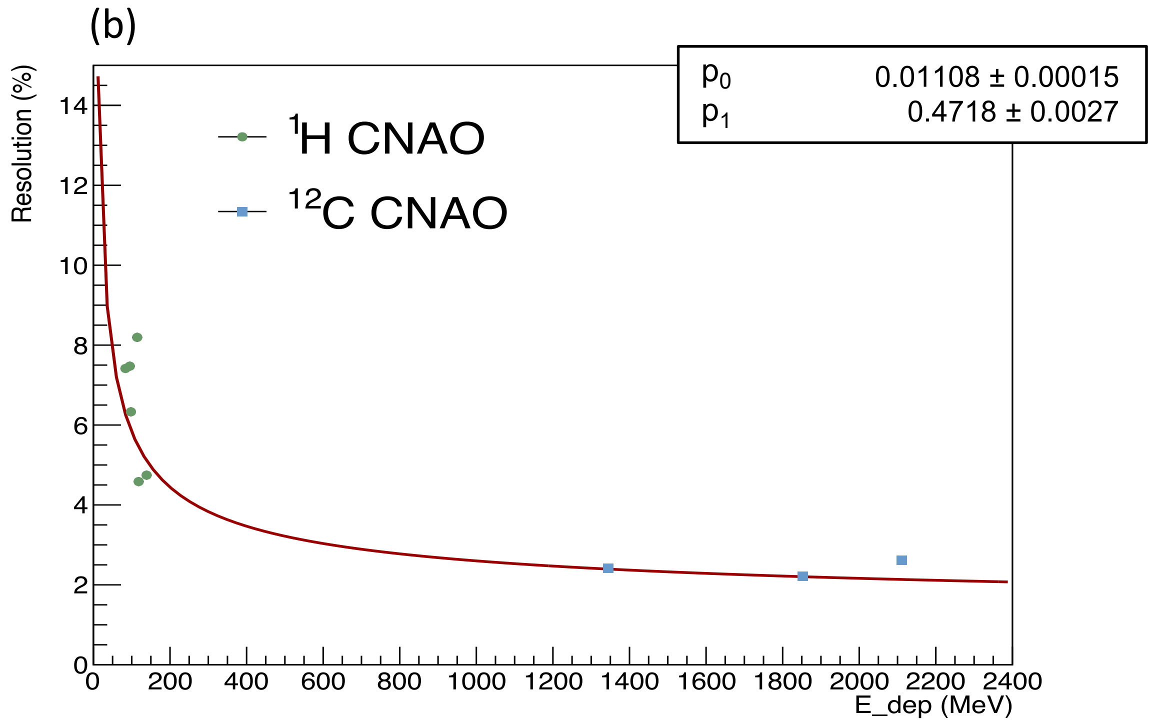

Energy resolution :

$$\frac{\sigma_E}{E} = p_o + \frac{p_1}{\sqrt{E}}$$

Secondary particles measurement

Calibration measurements

$CeBr_3$ +400V (a) and +600V (b)

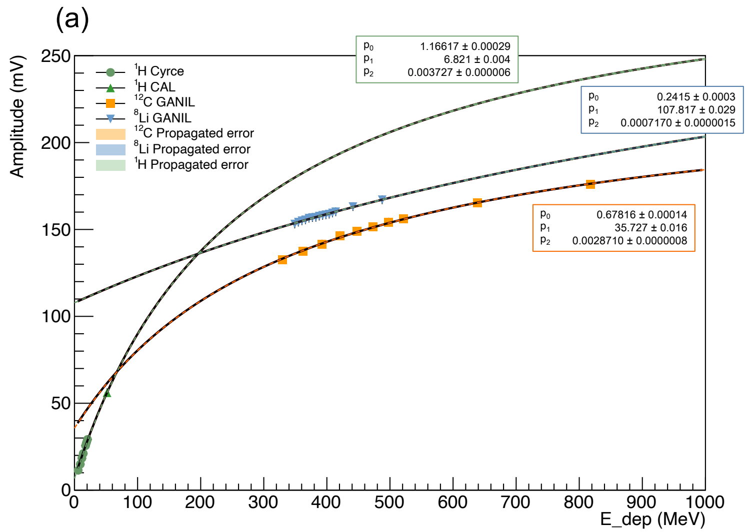

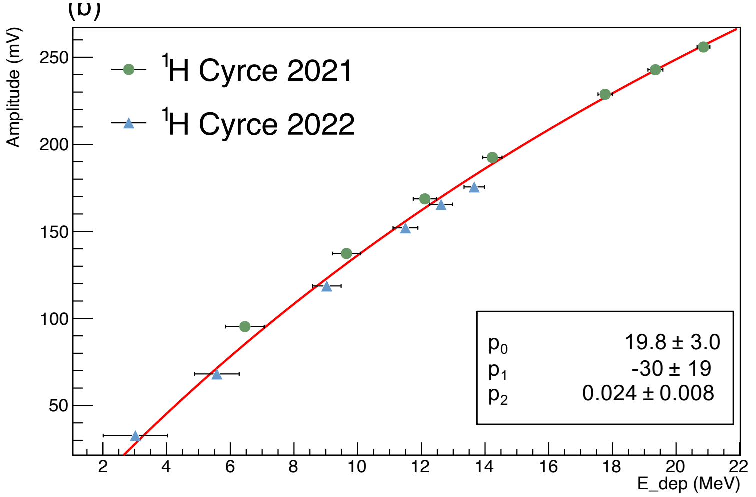

Time resolution

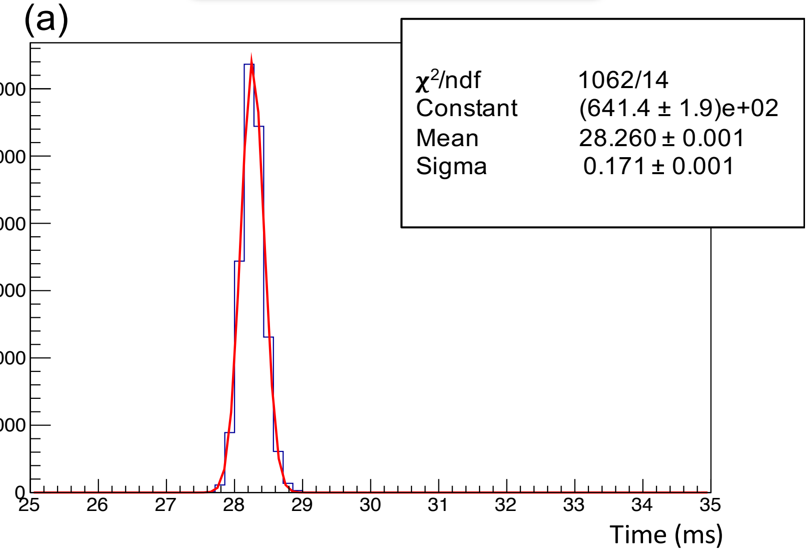

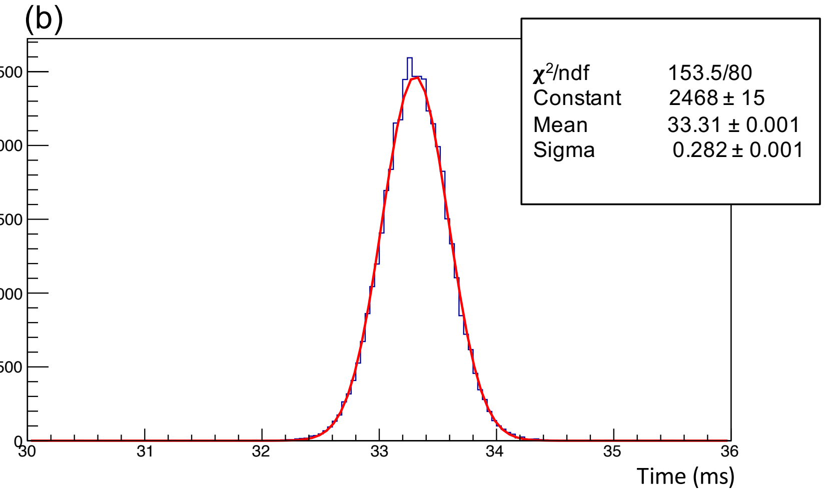

$CeBr_3$ deposited energy 120MeV/u ^{12}C (a) and 80MeV/u ^{1}H (b)

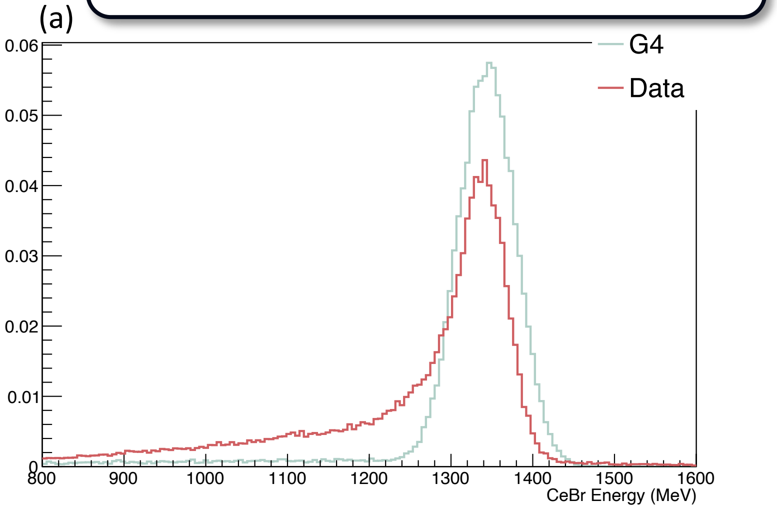

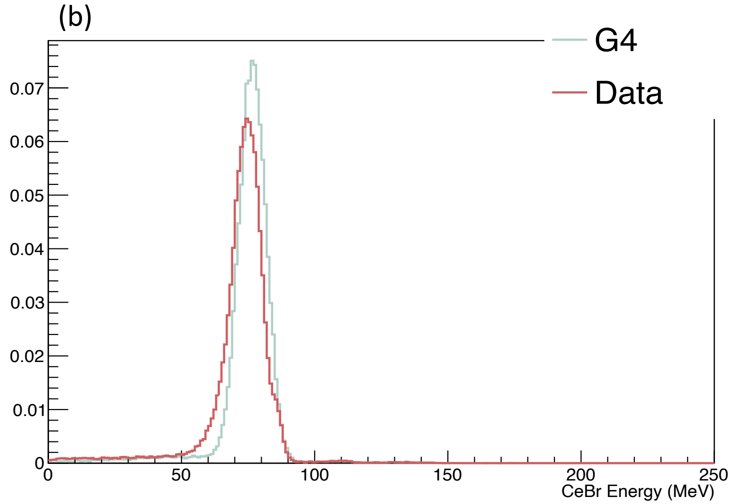

Secondary particles measurement

Calibration measurements

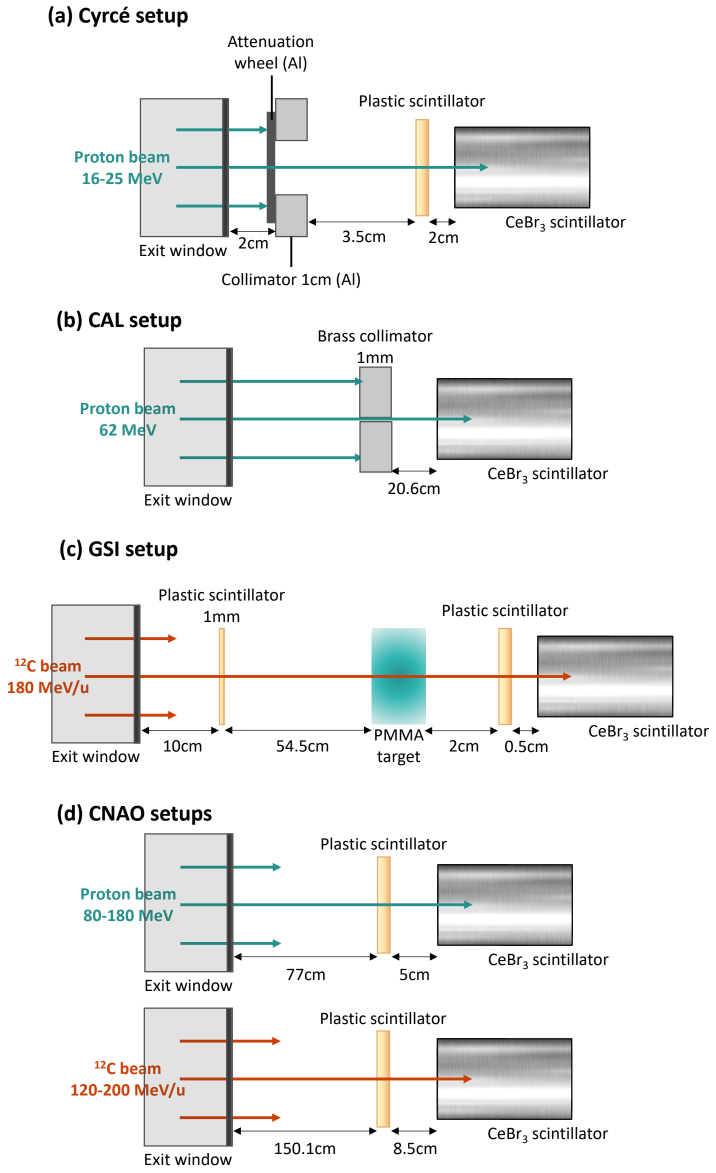

Resolution in time of the coincidence detection

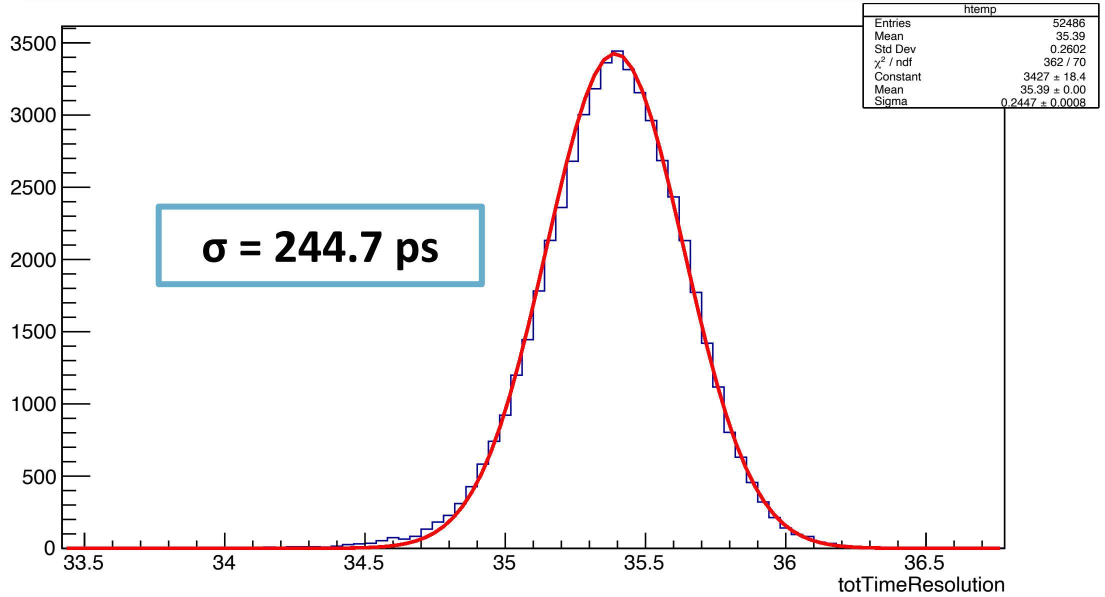

Facility	Ion type	Energy
Cyrcé - Strasbourg	^{1}H	16 - 25 MeV
CAL - Nice	^{1}H	60 MeV
GSI - Darmstadt	^{12}C	110 - 180 MeV/u
CNAO - Pavia	^{12}C	120 - 200 MeV/u

Secondary particles measurement

Detectors

Plastic scintillator
Photomultiplier (PMT) (- 1200 V)

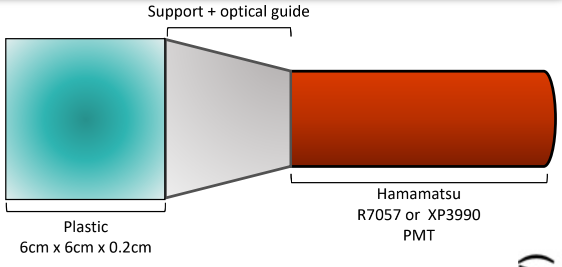

$CeBr_3$ crystal scintillator
PMT (usually + 1200 V)
+ 600 V for protons and high energy γ
+ 350 V / + 400 V for ^{12}C

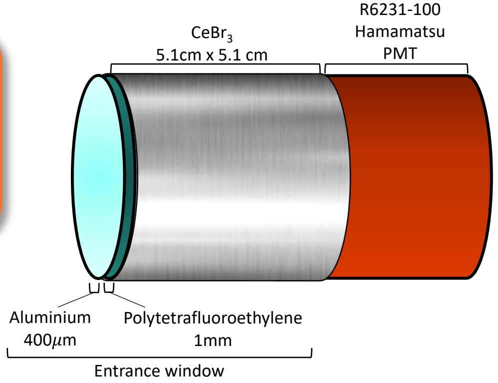

ΔE-E method :

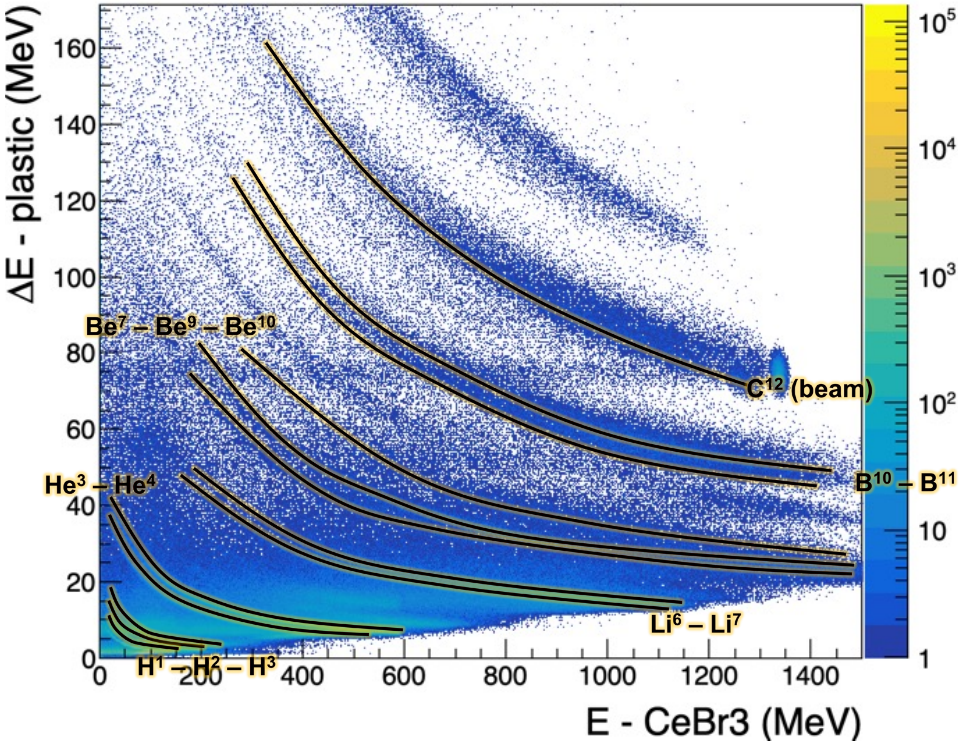

ΔE-E results from simulation with a carbon-ion beam of 200MeV, the detectors at 5° from the beam axis, and a PMMA target of 4 cm

Work done by M. Vanstalle

Analysis

Secondary particles measurement

Experiment at CNAO

Config.1

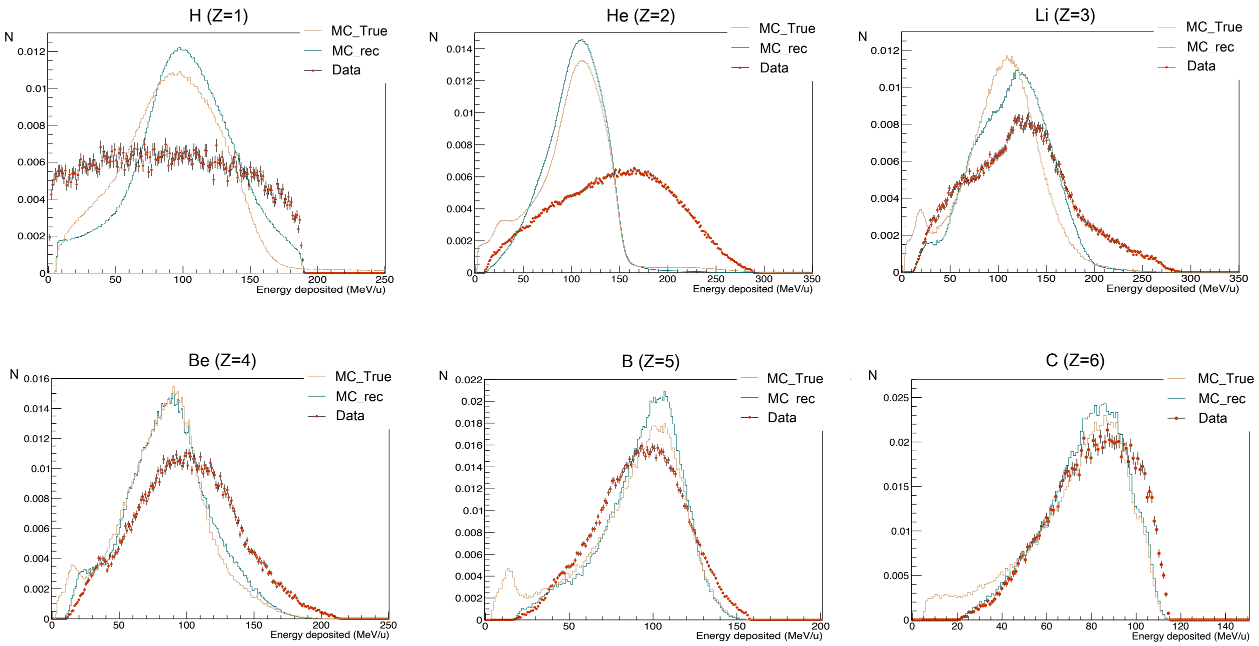

Config.2

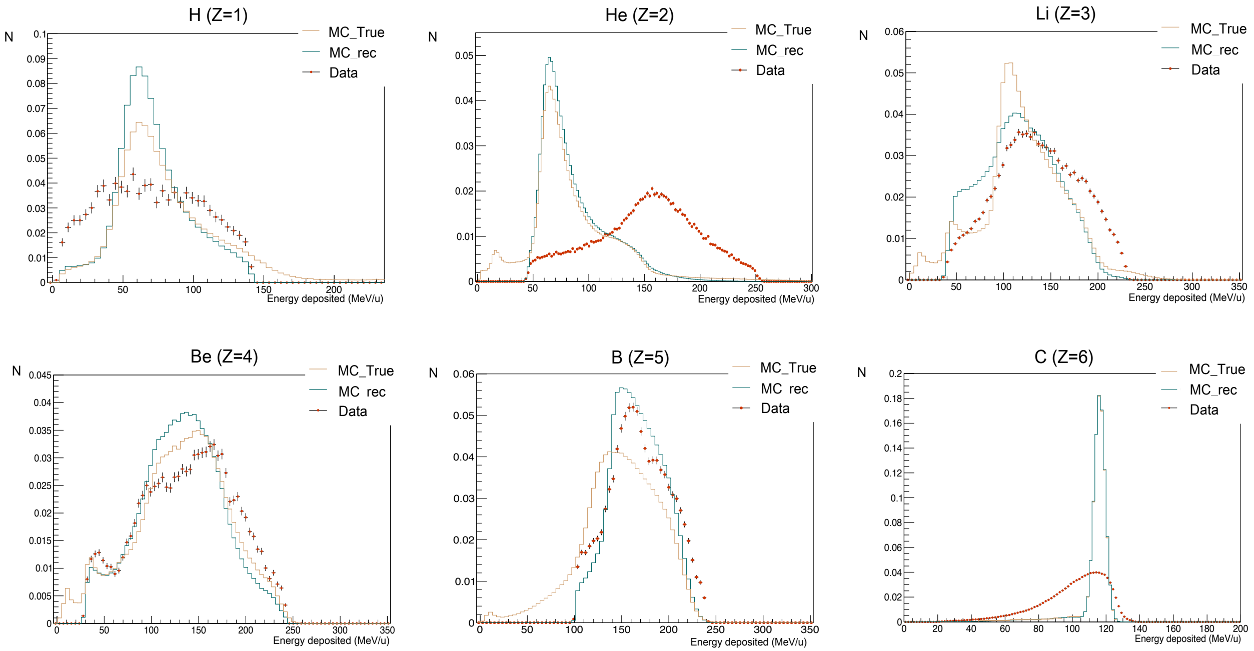

→ Centered around beam energy (after target)
- Fragments from projectile

→ Data broader than MC
- beam spread bigger than anticipated
- further refinement in beam control needed
- angular secondaries distributions non accurate

Secondary particles measurement
Experiment at CNAO

Config.1

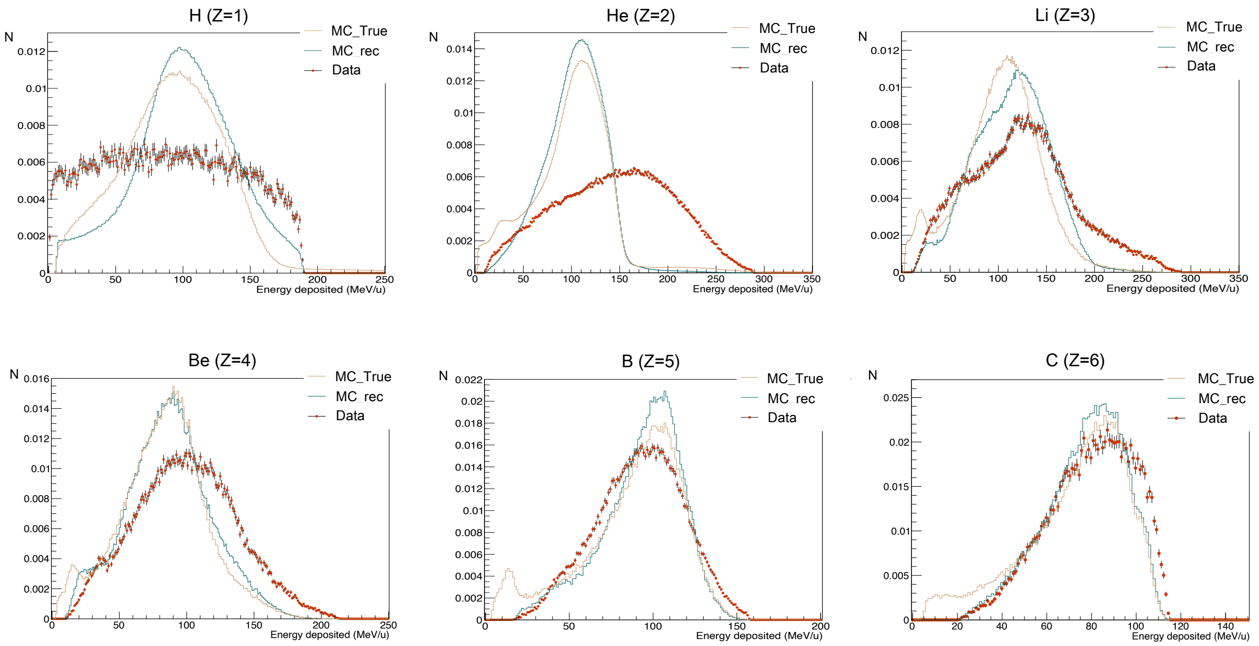

Config.2

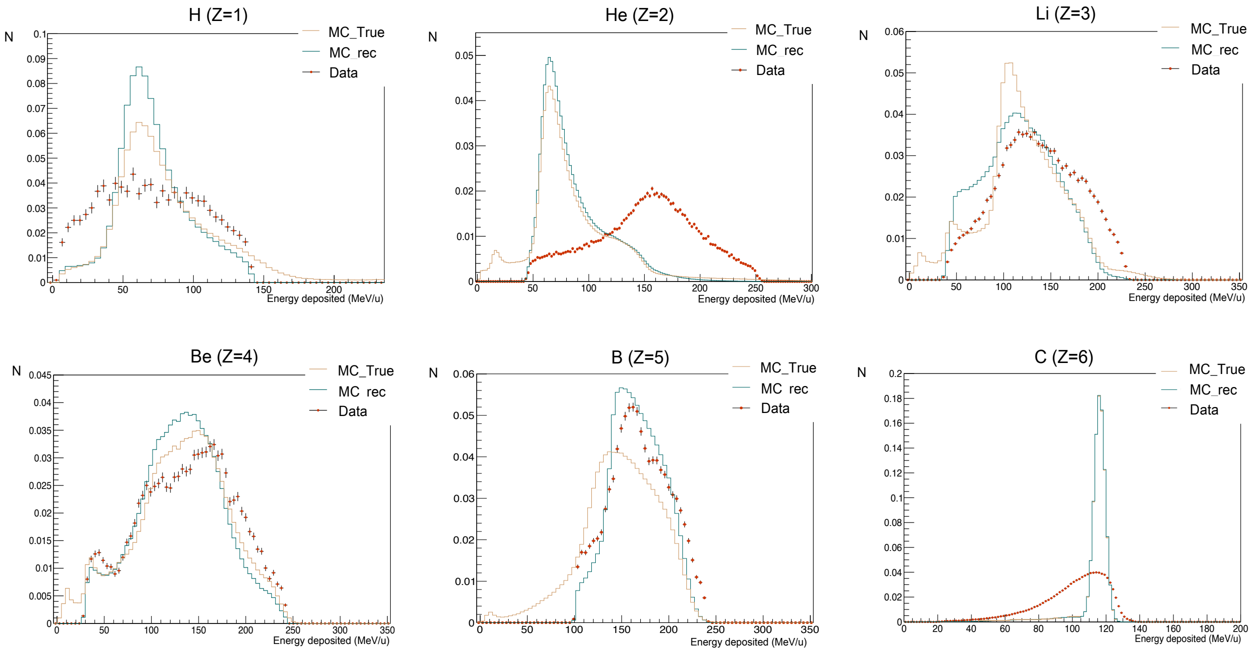

→ Centered around beam energy (after target)
- Fragments from projectile

→ Data broader than MC
- beam spread bigger than anticipated
- further refinement in beam control needed
- angular secondaries distributions non accurate

Purity → $\dfrac{\text{Z particles correctly attributed in a cut}}{\text{total number of particle in the cut}}$

Efficiency → $\dfrac{\text{Z particles correctly attributed in a cut}}{\text{total number of Z particle detected}}$

MC evaluated

Secondary particles measurement
Experiment at CNAO

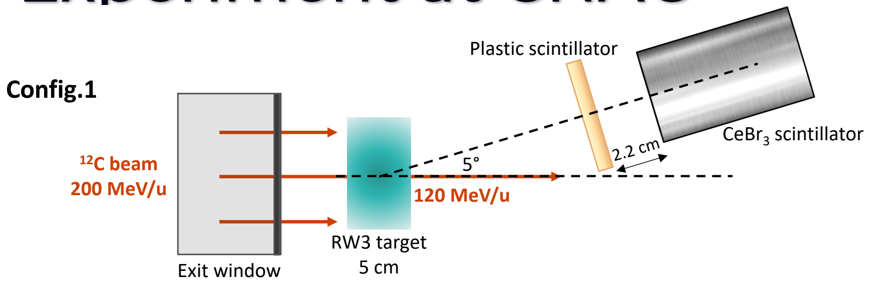

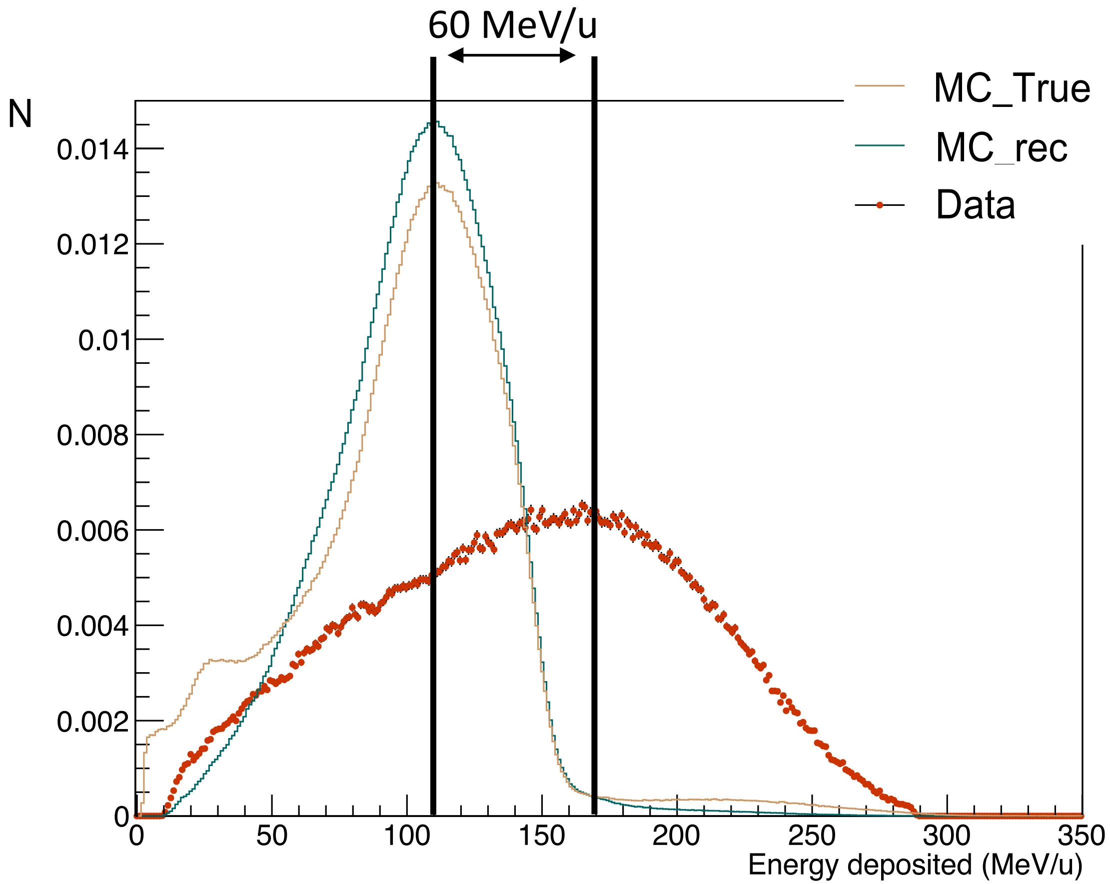

Z=2 Helium (MC_rec and MC_true)

- Good accordance in distribution and energy
- Underestimation of He by 6.02% in the cut

Z=2 Helium (purity and efficiency)

- High cut purity 88.01%
  - → high production rate of He during C fragmentation
  - → low contamination rate
- High cut efficiency 83.01%
  - → include most He particles in analysis

Secondary particles measurement

Experiment at CNAO

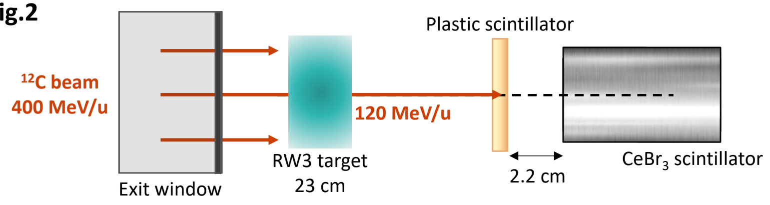

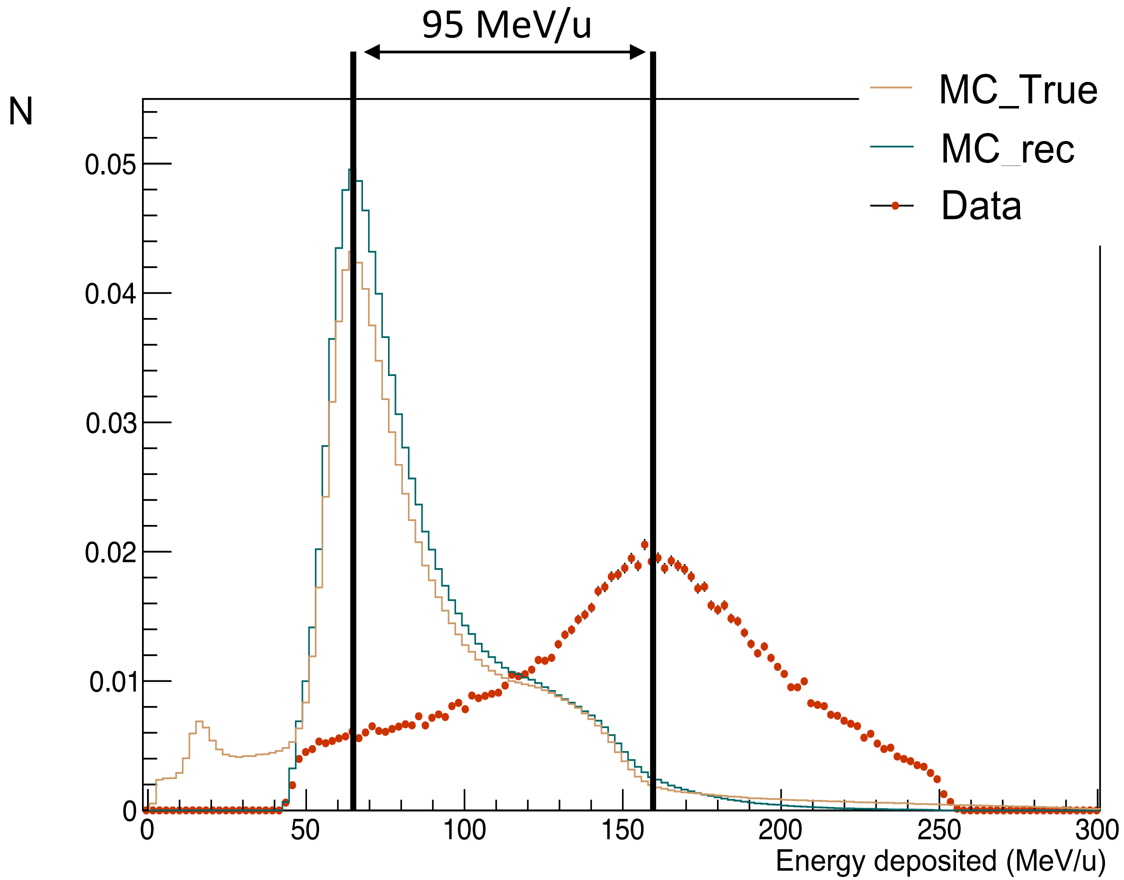

Z=2 Helium (MC_rec and MC_true)

- Good accordance in distribution and energy
- Underestimation of He by 7.25% in the cut

Z=2 Helium (purity and efficiency)

- High cut purity 85.11 %
  - → high production rate of He during C fragmentation
  - → low contamination rate
- High cut efficiency 79.36 %
  - → include most He particles in analysis

Secondary particles measurement

Experiment at CNAO

Config.1

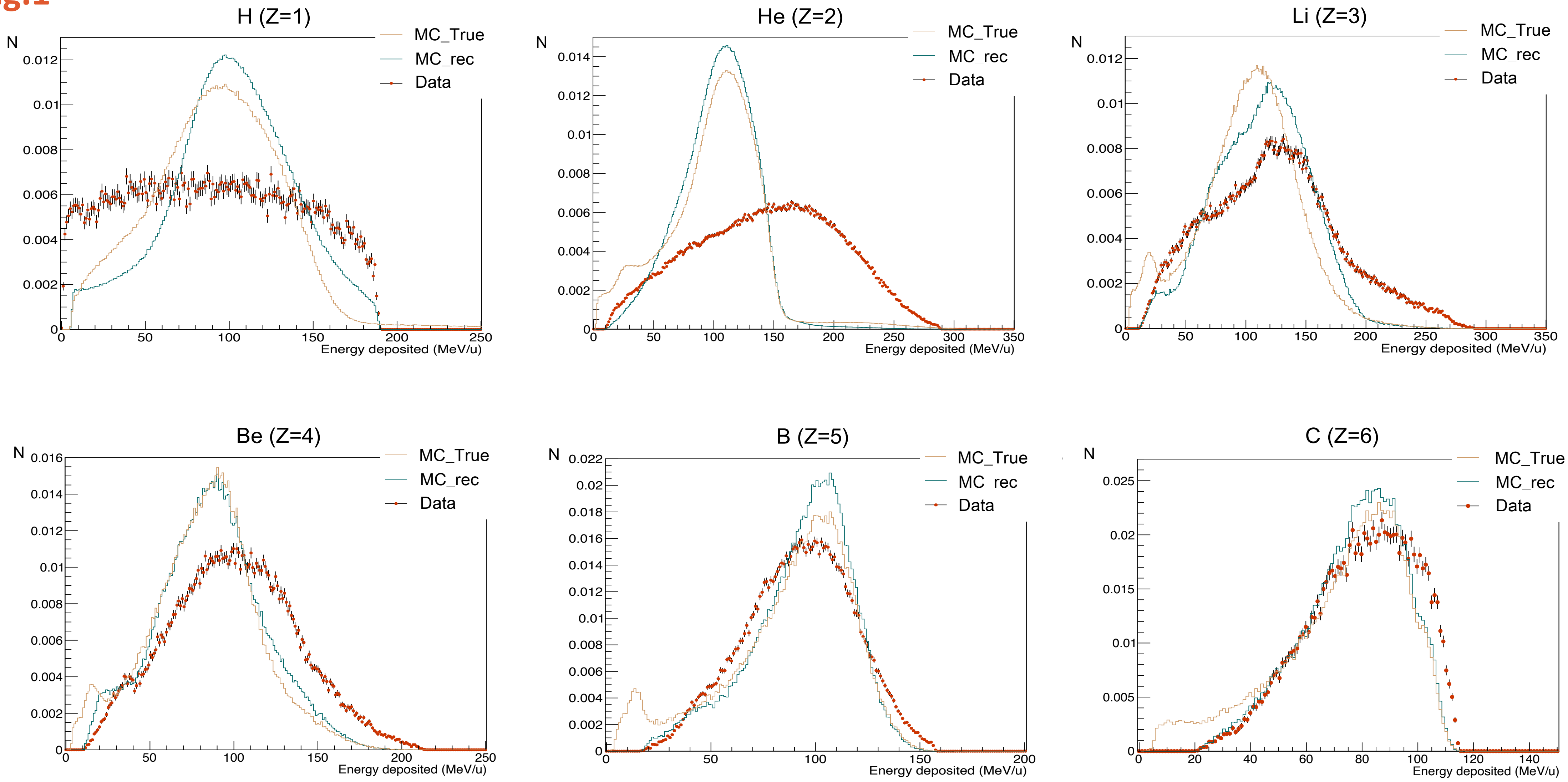

Secondary particles measurement

Experiment at CNAO

Config.2

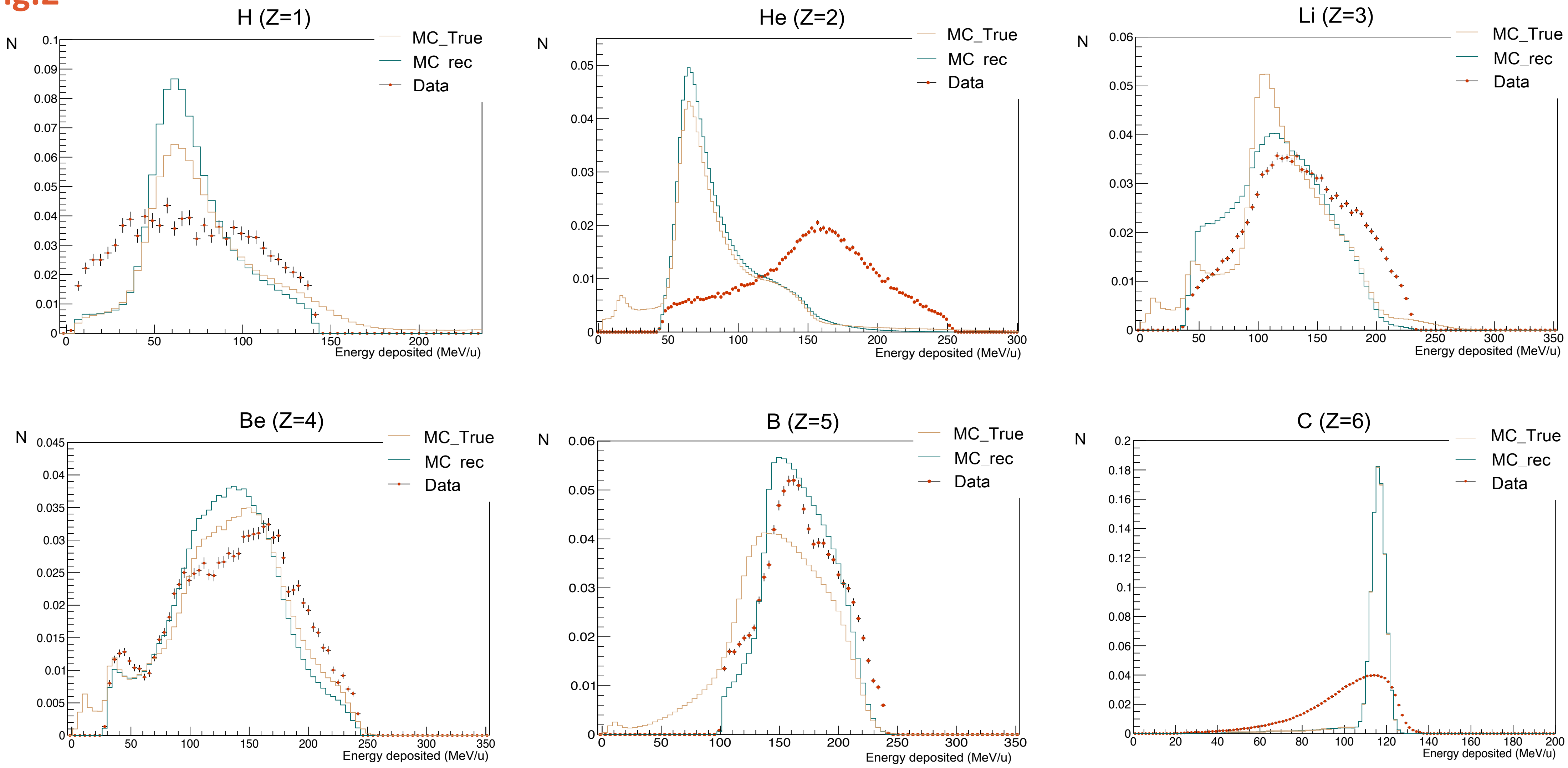

Secondary particles measurement

Experiment at CNAO

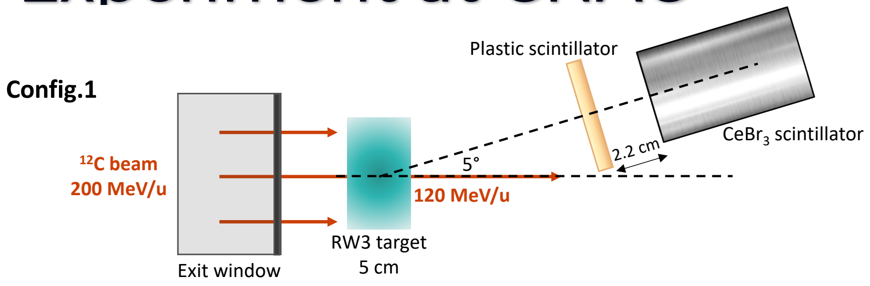

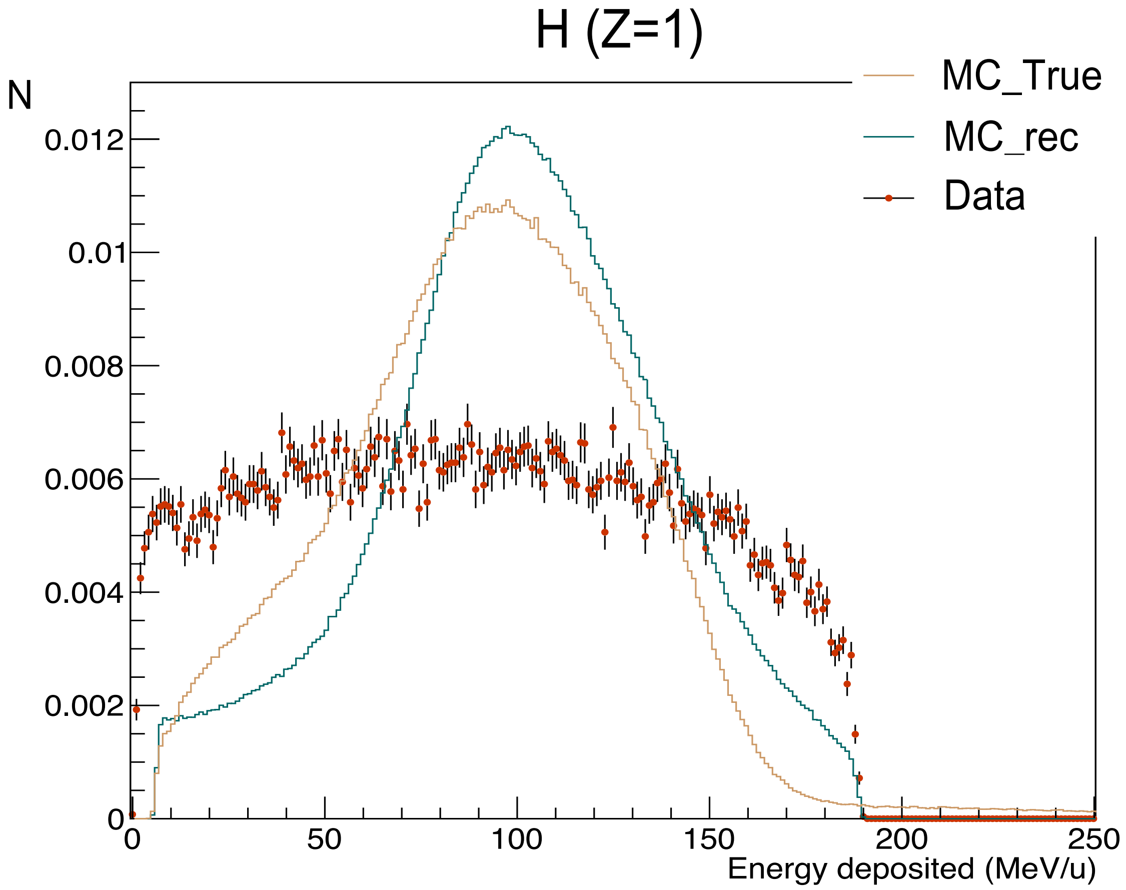

Z=1 Hydrogen (MC_rec and exp data)

- Strong correspondance in energy between
- Resolution constraint at low energy
- Proton scattering and beam spread

Z=1 Hydrogen (MC_rec and MC_true)

- Overall agreement
- Minor distribution and energy shift 5MeV/u
- Overestimation of H by 39.31% in the cut

Z=1 Hydrogen (purity and efficiency)

- Cut purity 45.52%
  - → mostly He mistakenly classified as H
  - → protons isolation challenging with this setup
- Cut efficiency 75.01%
  - → most H included in the analysis

Secondary particles measurement

Experiment at CNAO

Config.2

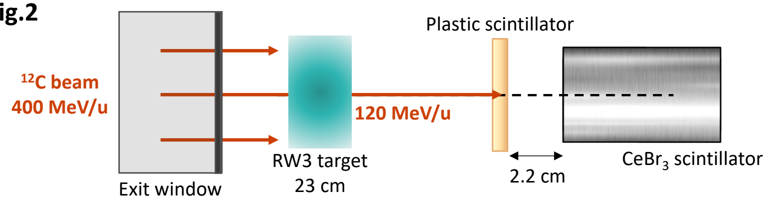

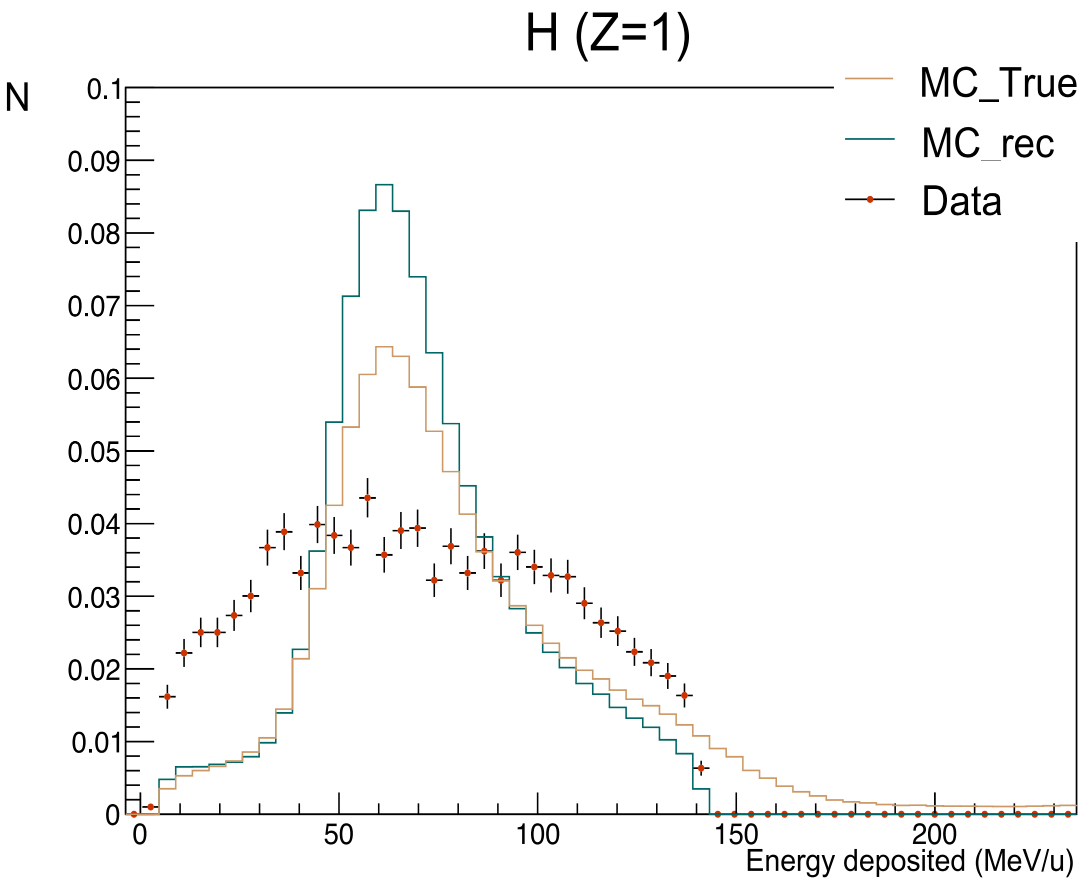

Z=1 Hydrogen (MC_rec and exp data)

- Both centered at 70MeV/u
- Resolution constraint at low energy
- Proton scattering and beam spread

Z=1 Hydrogen (MC_rec and MC_true)

- Overall agreement
- Overestimation of H by 55.09% in the cut

Z=1 Hydrogen (purity and efficiency)

- Cut purity 36.54%
  - → mostly He mistakenly classified as H
  - → protons isolation challenging with this setup
- Cut efficiency 78.88%
  - → most H included in the analysis

Secondary particles measurement

Experiment at CNAO

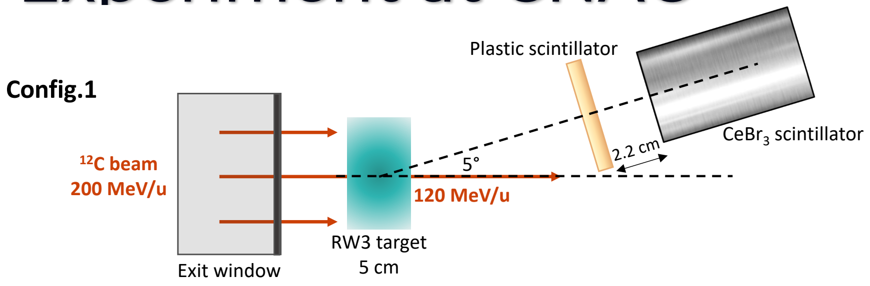

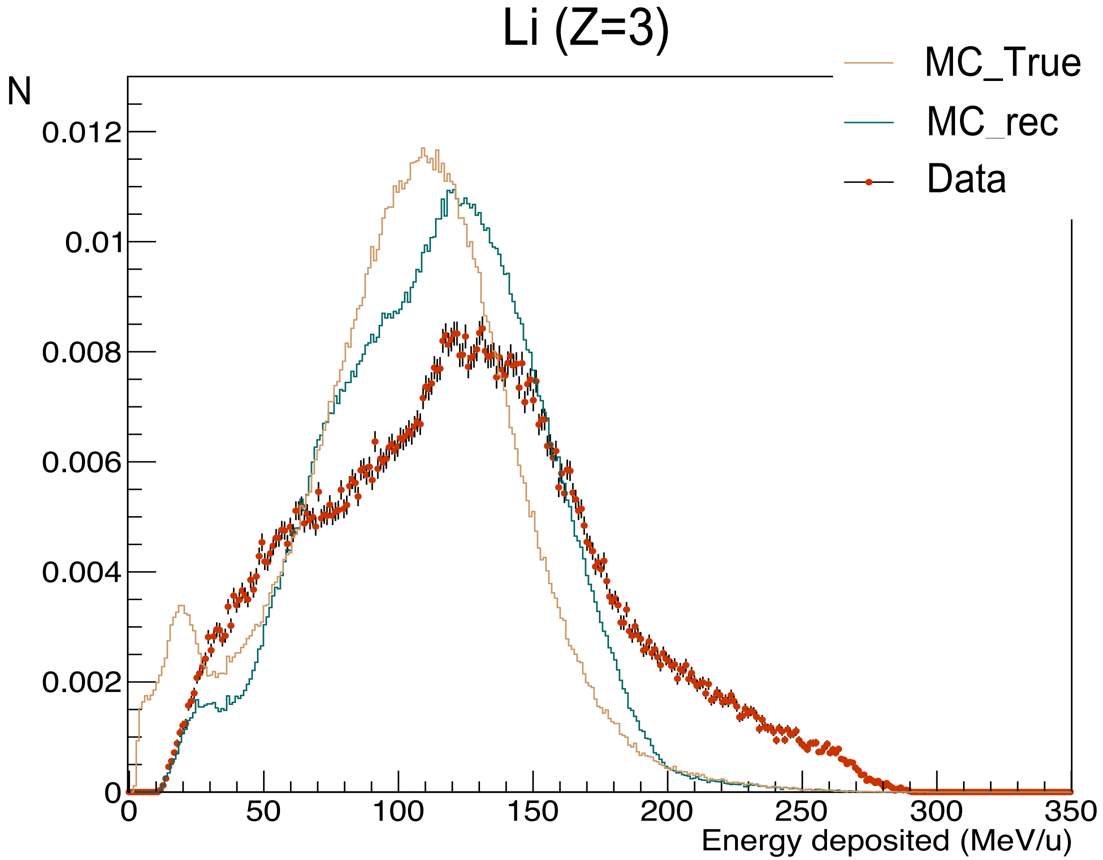

Z=3 Lithium (MC_rec and exp data)

- Isolation and identification difficult (statistical presence of He)
- Agreement in energy apart resolution

Z=3 Lithium (MC_rec and MC_true)

- Overall agreement
- Minor distribution and energy shift 10MeV/u
- Overestimation of Li by 15.31% in the cut

Z=3 Lithium (purity and efficiency)

- Cut purity 53.27%
  - → overlap in the energy loss with He and Be
- Cut efficiency 62.90%
  - → significant fraction of Li excluded
  - → confirm overlap

Secondary particles measurement

Experiment at CNAO

Config.2

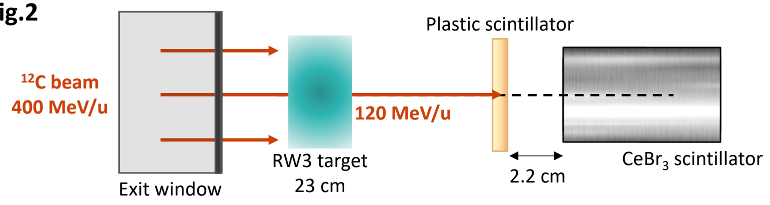

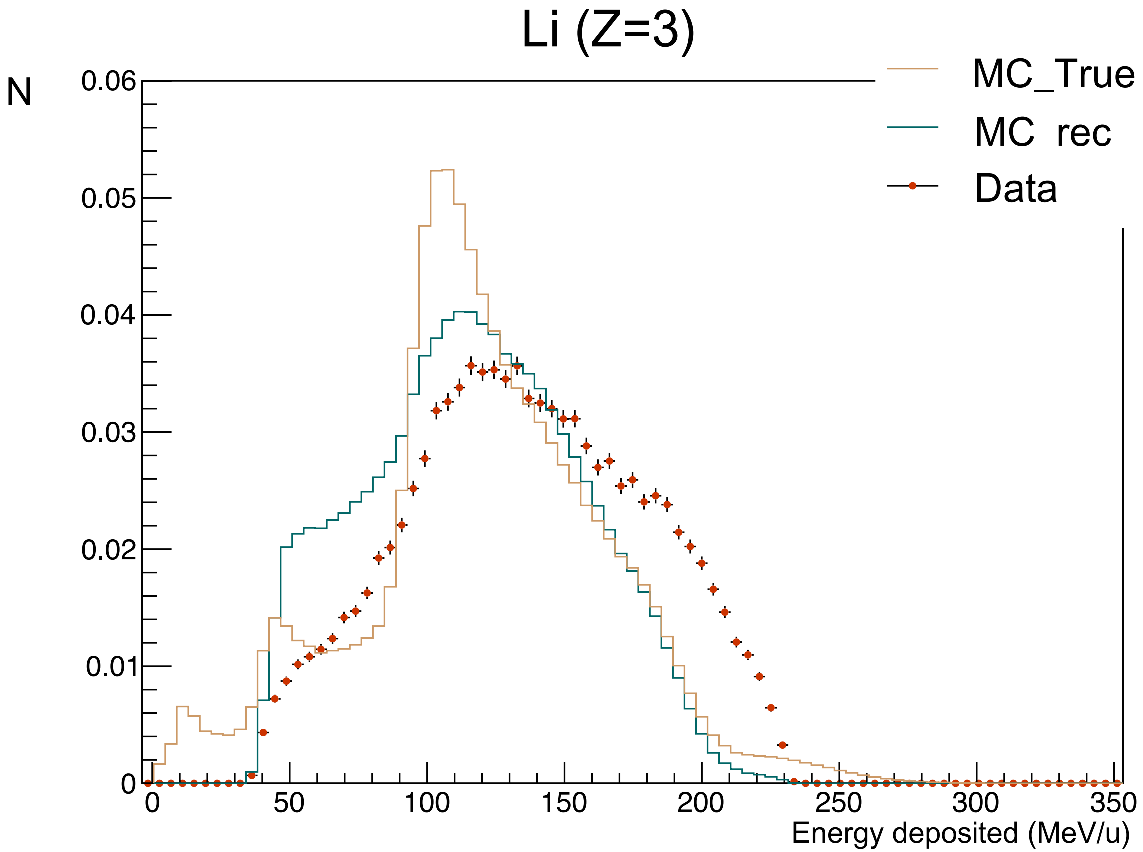

Z=3 Lithium (MC_rec and exp data)

- Isolation and identification difficult (statistical presence of He even more important)
- Small shift in energy of 10MeV/u

Z=3 Lithium (MC_rec and MC_true)

- Overall agreement
- Minor distribution and energy shift 10MeV/u
- Overestimation of Li by 6.75% in the cut

Z=3 Lithium (purity and efficiency)

- Cut purity 58.18%
  - → overlap in the energy loss with He and Be
- Cut efficiency 62.39%
  - → significant fraction of Li excluded
  - → confirm overlap

Secondary particles measurement

Experiment at CNAO

Config.1

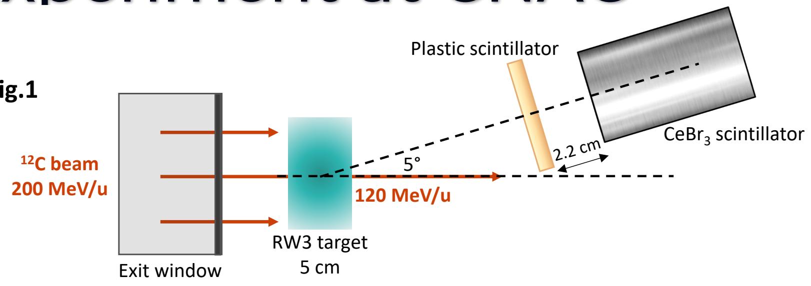

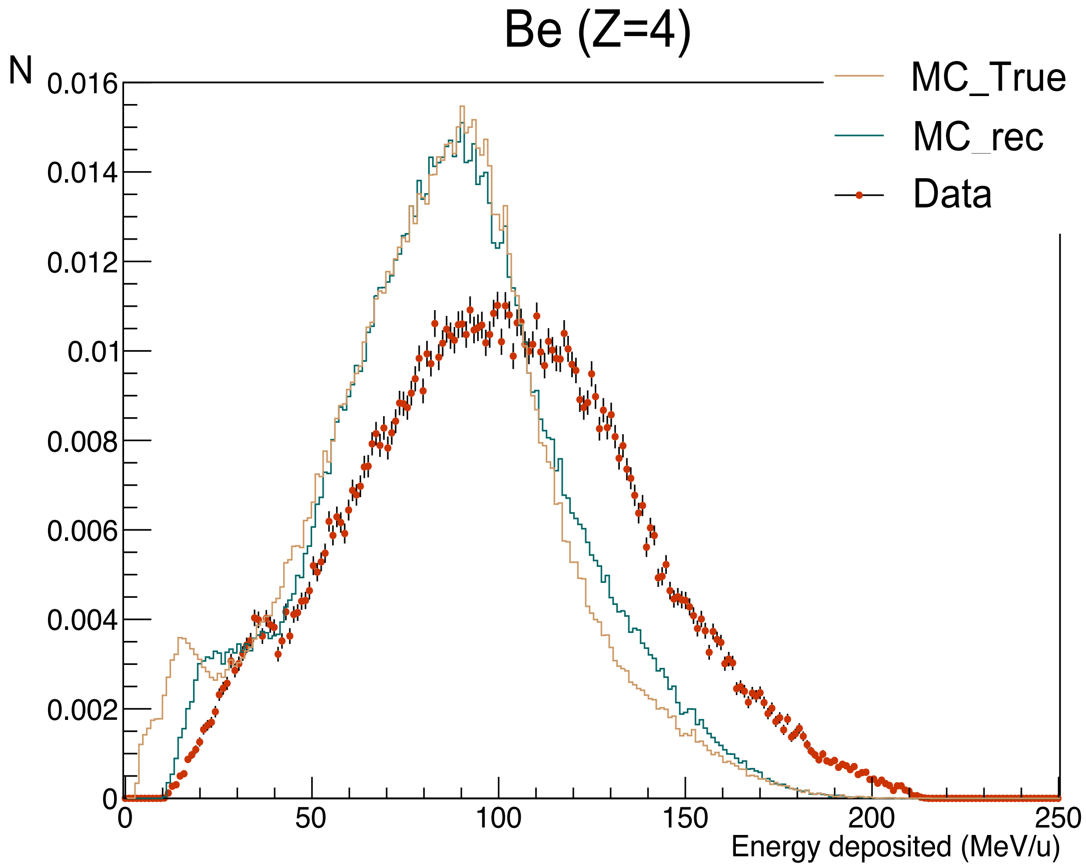

Z=4 Beryllium (MC_rec and exp data)

- Energy shift of 10MeV/u
- Better accurate resolution reproduction

Z=4 Beryllium (MC_rec and MC_true)

- Good agreement in distribution and energy
- Slight underestimation of Be of 4.65% in the cut

Z=4 Beryllium (purity and efficiency)

- High cut purity 77.92%
  → effective discrimination criteria
- Cut efficiency of 74.46%
  → reasonable balance between capturing most particles and maintaining purity

Secondary particles measurement

Experiment at CNAO

Config.2

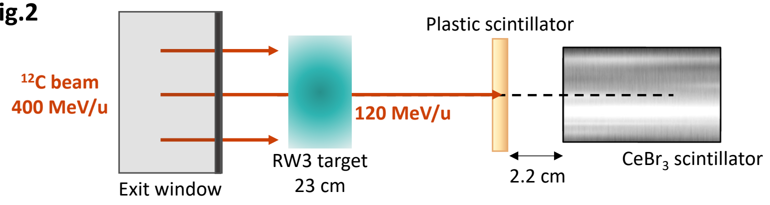

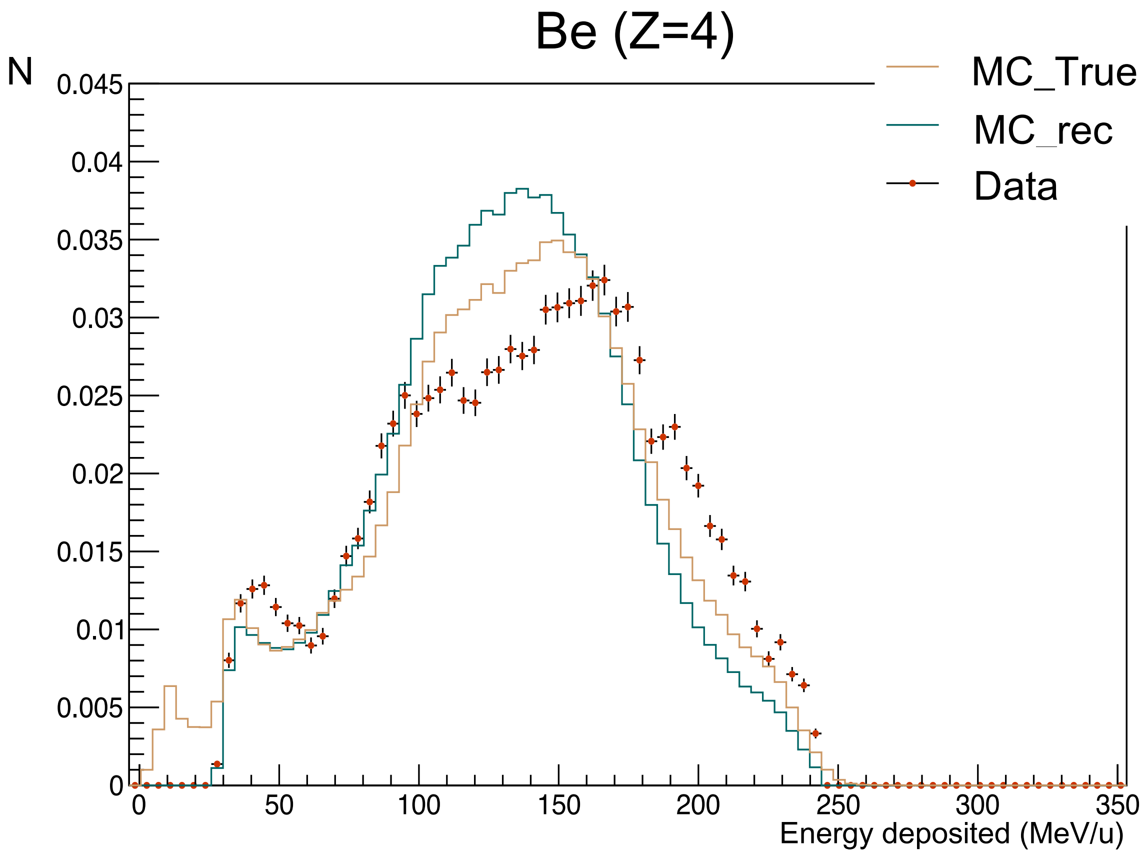

Z=4 Beryllium (MC_rec and exp data)

- Energy shift of 25MeV/u
- Better accurate resolution reproduction

Z=4 Beryllium (MC_rec and MC_true)

- Good agreement in distribution and energy
- Slight underestimation of Be of 13.09% in the cut

Z=4 Beryllium (purity and efficiency)

- High cut purity 69.96%
  → effective discrimination criteria
- Cut efficiency of 61.86%
  → reasonable balance between capturing most particles and maintaining purity

Secondary particles measurement

Experiment at CNAO

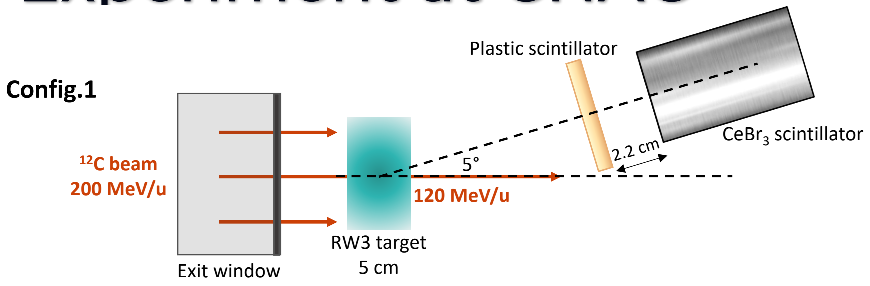

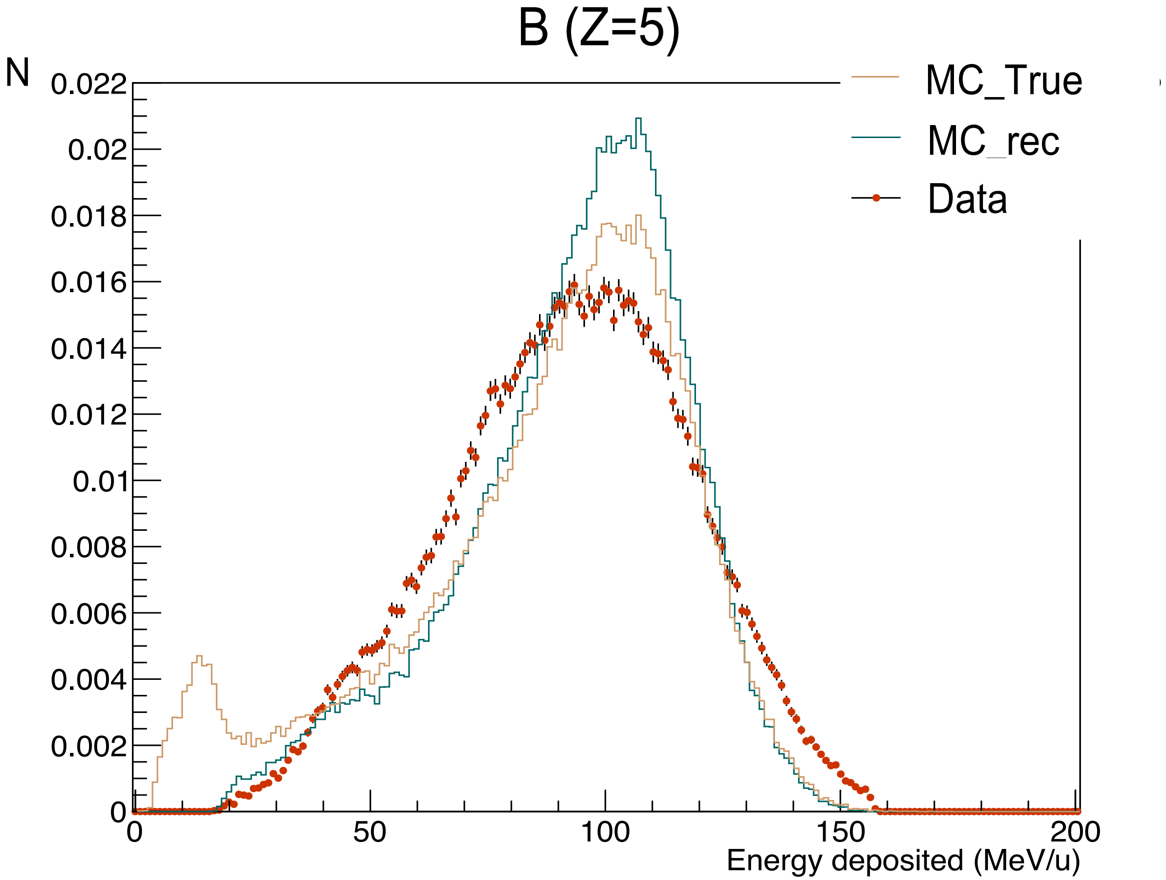

Z=5 Boron (MC_rec and exp data)
- Slight energy deviation less than 10MeV/u
- Improved reproduction of calculated resolution

Z=5 Boron (MC_rec and MC_true)
- Consistent agreement in distribution and energy
- Marginal underestimation of 0.67% in the cut

Z=5 Boron (purity and efficiency)
- High cut purity 80.05%
  → high purity at the higher energy setting
  → effective discrimination criteria
- Cut efficiency of 79.66%
  → reasonable balance between capturing most particles and maintaining purity

Secondary particles measurement

Experiment at CNAO

Config.2

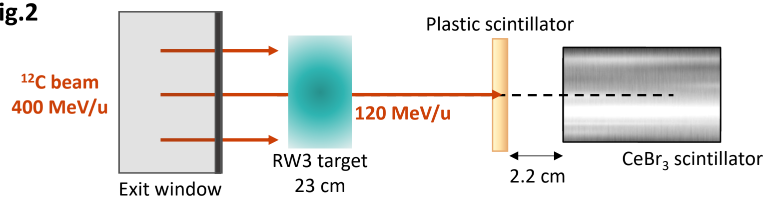

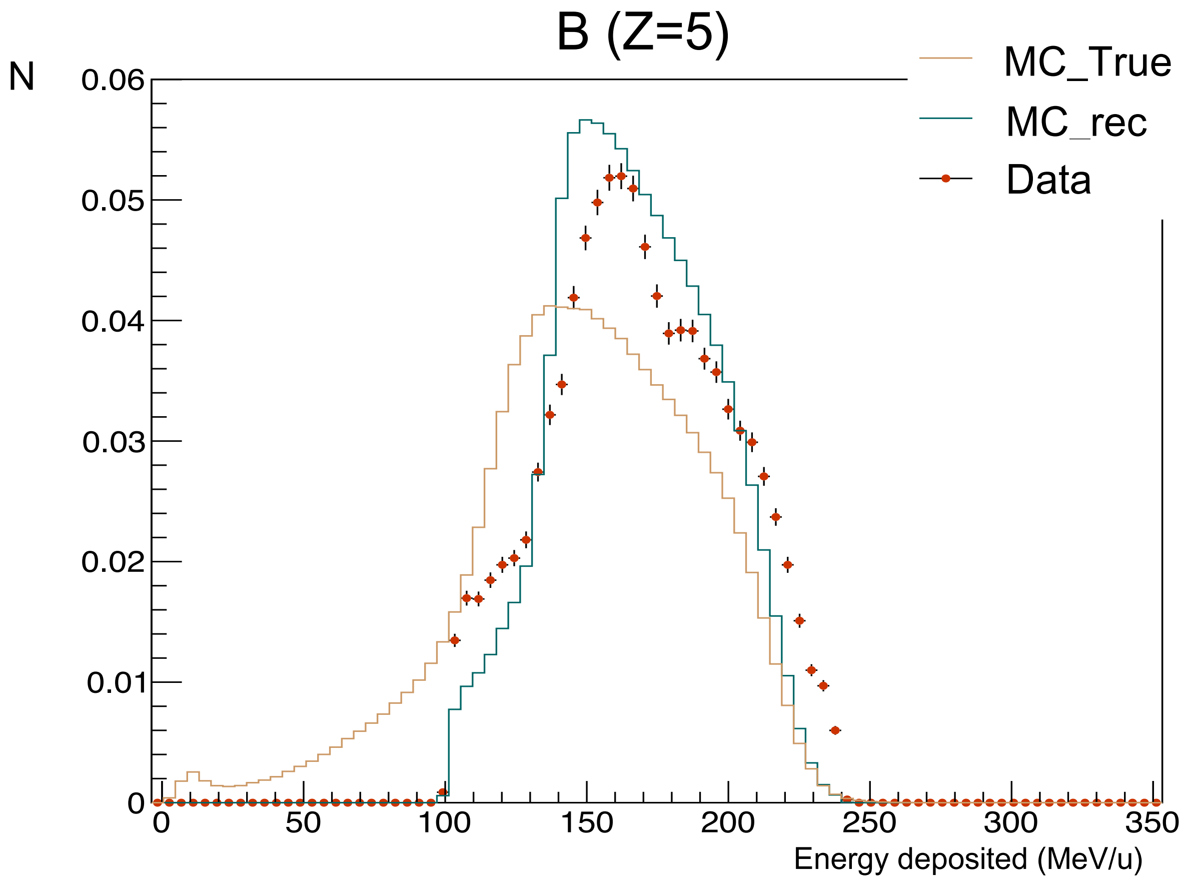

Z=5 Boron (MC_rec and exp data)

- Slight energy deviation of 10MeV/u
- Improved reproduction of calculated resolution

Z=5 Boron (MC_rec and MC_true)

- Consistent agreement in distribution and energy
- Small energy shift of 10MeV/u
- Marginal underestimation of 4.05% in the cut

Z=5 Boron (purity and efficiency)

- High cut purity 92.16%
  - → high purity at the higher energy setting
  - → effective discrimination criteria
- Cut efficiency of 65.58%
  - → reasonable balance between capturing most particles and maintaining purity

Secondary particles measurement

Experiment at CNAO

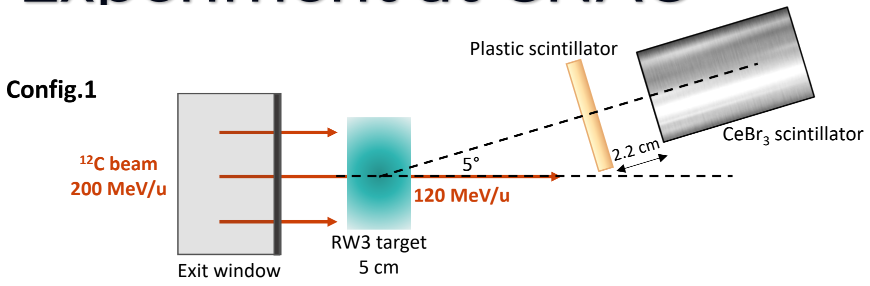

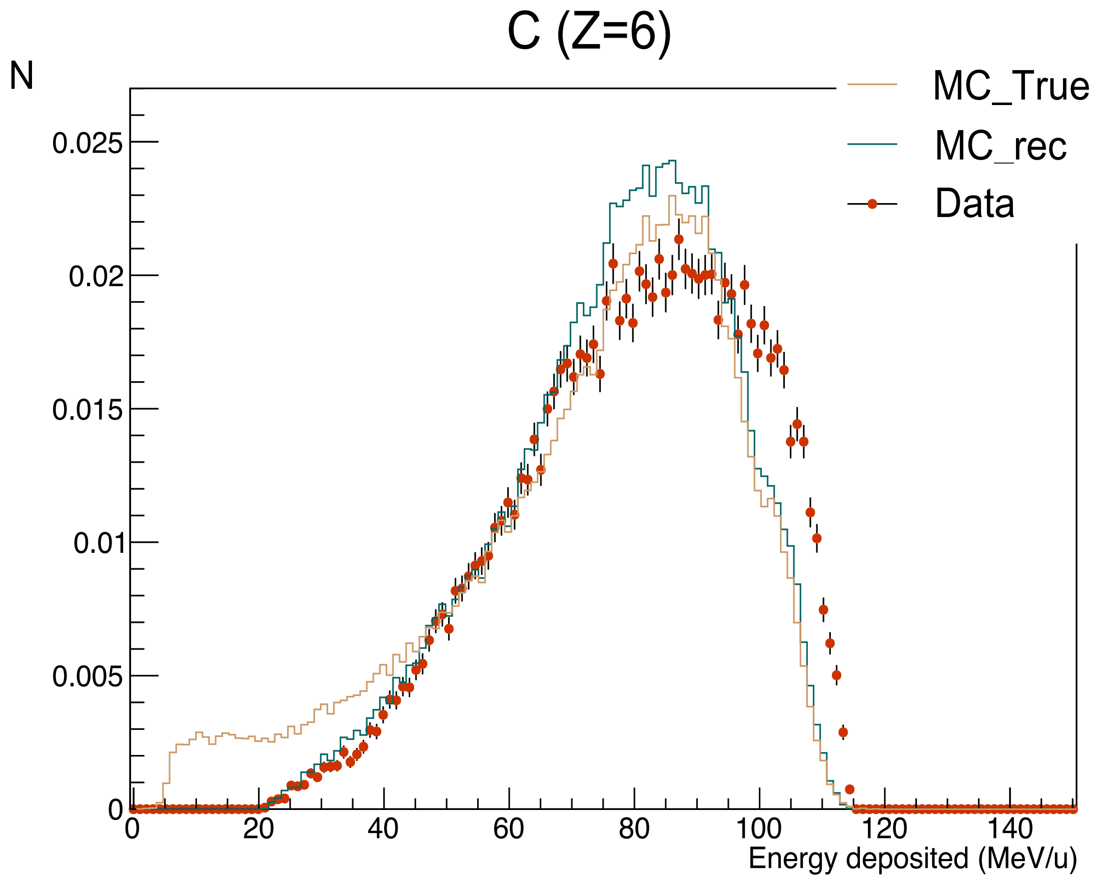

Z=6 Carbon (MC_rec and exp data)
- Slight energy shift less than 5MeV/u
- Close reproduction of calculated resolution

Z=6 Carbon (MC_rec and MC_true)
- Consistent agreement in distribution and energy
- Significant underestimation of 59.84% in the cut

Z=6 Carbon (purity and efficiency)
- Highest cut purity 94.56%
  → good identification fidelity
- Cut efficiency 59.16%

Secondary particles measurement
Experiment at CNAO

Config.2

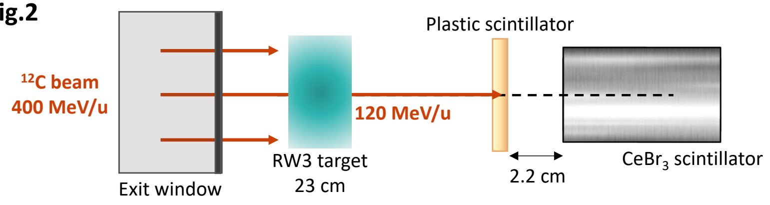

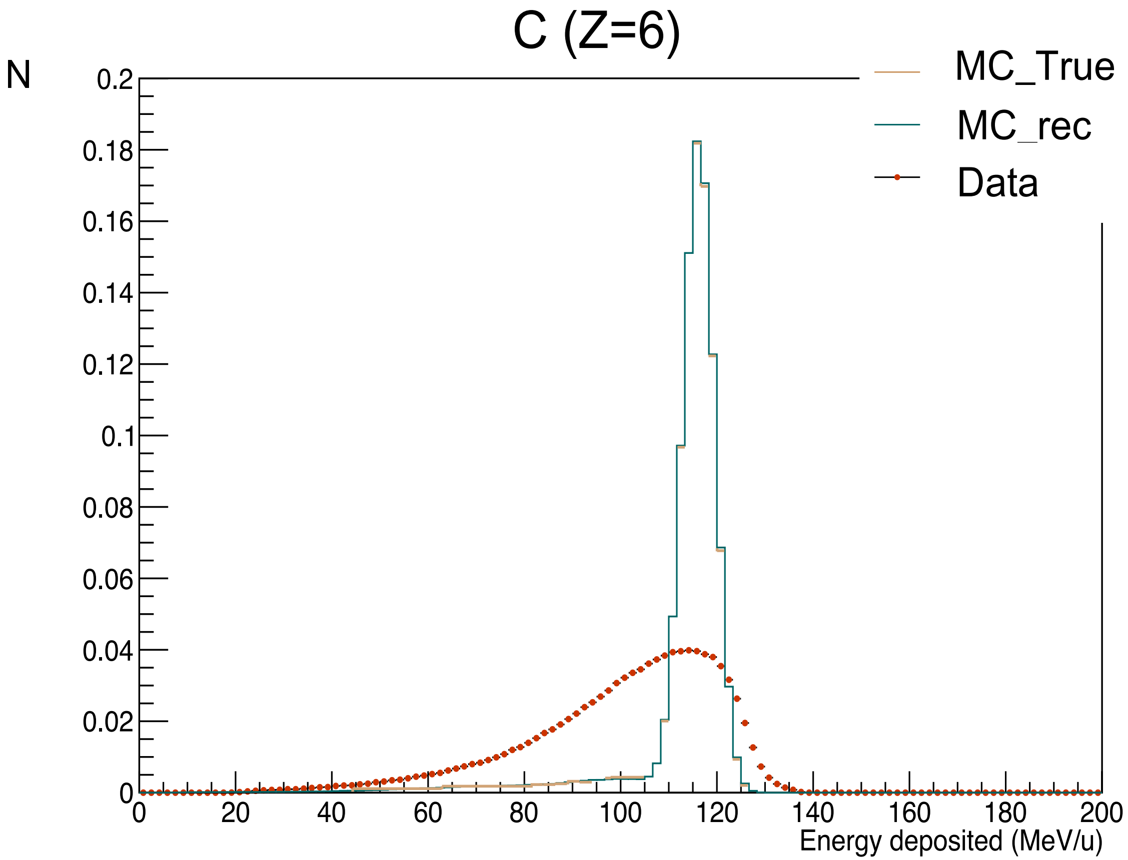

Z=6 Carbon (MC_rec and exp data)

- Slight energy shift less than 5MeV/u

Z=6 Carbon (MC_rec and MC_true)

- Consistent agreement in distribution and energy
- Insignificant underestimation of 0.24% in the cut

Z=6 Carbon (purity and efficiency)

- Highest cut purity 99.48%
  → good identification fidelity
  → isolation with great precision when aligned with the beam
- Cut efficiency 98.71%

Secondary particles measurement

Errors evaluation

Secondaries	200MeV/u on 5cm target, with detectors at 5°		400MeV/u on a 23cm target, with detectors at 0°	
	Cut purity	Cut efficiency	Cut purity	Cut efficiency
Z=1 (H)	45.52 ± 0.03 %	75.01 ± 0.03 %	36.54 ± 0.03 %	78.88 ± 0.04 %
Z=2 (He)	88.01 ± 0.01 %	83.01 ± 0.01 %	85.11 ± 0.01 %	79.36 ± 0.02 %
Z=3 (Li)	53.27 ± 0.06 %	62.90 ± 0.07 %	58.18 ± 0.04 %	62.39 ± 0.04 %
Z=4 (Be)	77.92 ± 0.09 %	74.46 ± 0.09 %	69.96 ± 0.05 %	61.86 ± 0.05 %
Z=5 (B)	80.05 ± 0.09 %	79.52 ± 0.10 %	92.16 ± 0.02 %	65.58 ± 0.03 %
Z=6 (C)	94.56± 0.08 %	59.16 ± 0.14 %	99.48 ± 0.01 %	98.71 ± 0.01 %

- Cut parameters highly effective for some Z (He and C)
- But variability in performance across different Z and experimental setups
- For H and Li further refinement of detectors resolution needed
  - → adjusting ΔE-E thresholds to reduce overlap
  - → adding detectors
  - → use better resolution detector than plastic like silicium